Preparation of Monocarbonyl Ruthenium Complexes Bearing Bidentate Nitrogen and Phosphine Ligands and their Catalytic Activity in the Carbonyl Compound Reduction.

Steven Giboulot,[a,b] Clara Comuzzi,[a] Alessandro Del Zotto,[a] Rosario Figliolia,[a] Giovanna Lippe,[a] Denise Lovison,[a] Paolo Strazzolini,[a] Sabina Susmel,[a] Ennio Zangrando,[c] Daniele Zuccaccia,[a] Salvatore Baldino,[a,d] Maurizio Ballico,[a,*] Walter Baratta[a,*]

Supporting Information

Table of Contents:

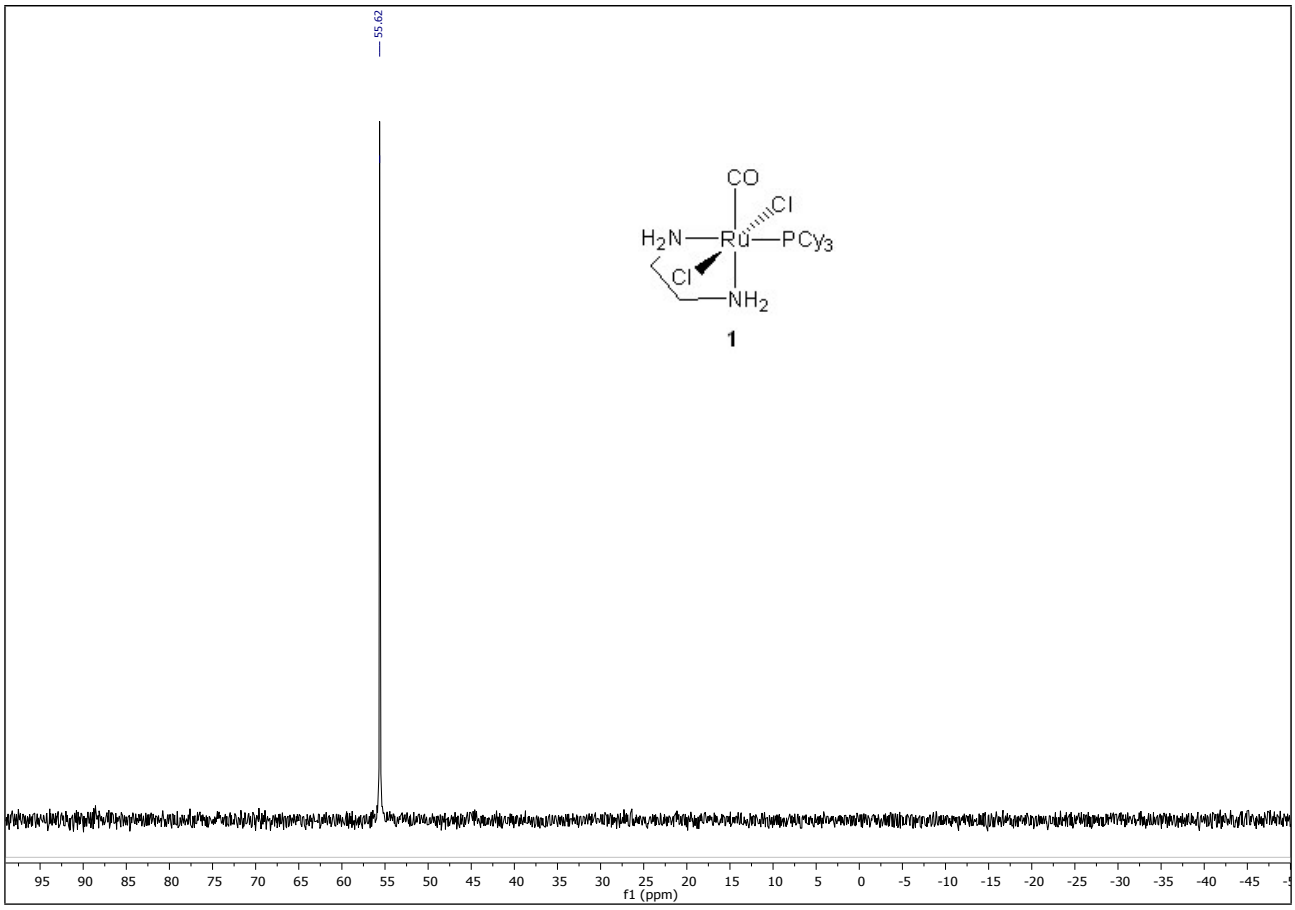

Figure S1. $^{31}P\{^{1}H\}$ NMR spectrum (81.0 MHz) of *trans*-[$RuCl_2(CO)(PCy_3)(en)$] (**1**) in CD_2Cl_2 at 20 °C.

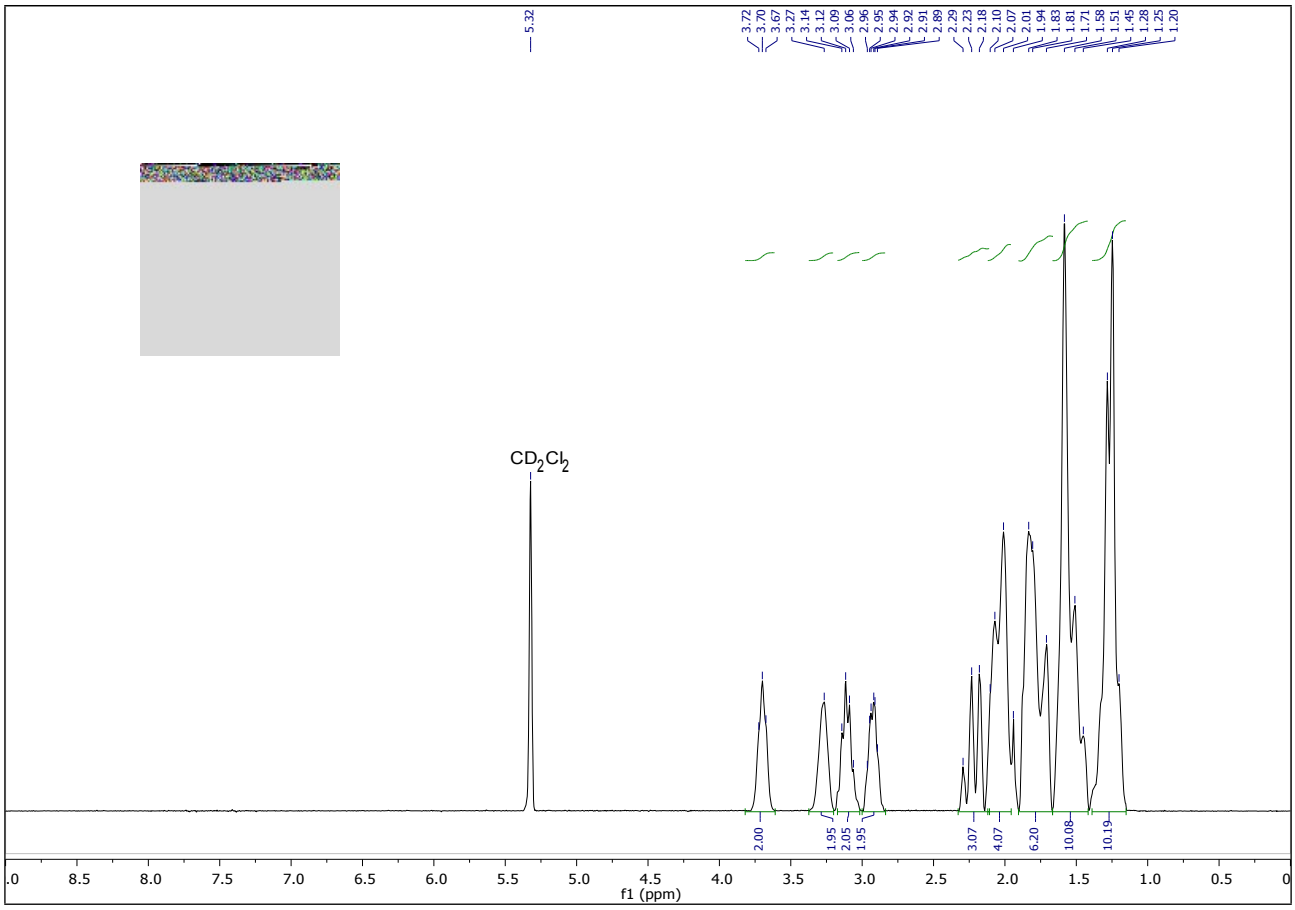

Figure S2. ^{1}H NMR spectrum (200.1 MHz) of *trans*-[$RuCl_2(CO)(PCy_3)(en)$] (**1**) in CD_2Cl_2 at 20 °C.

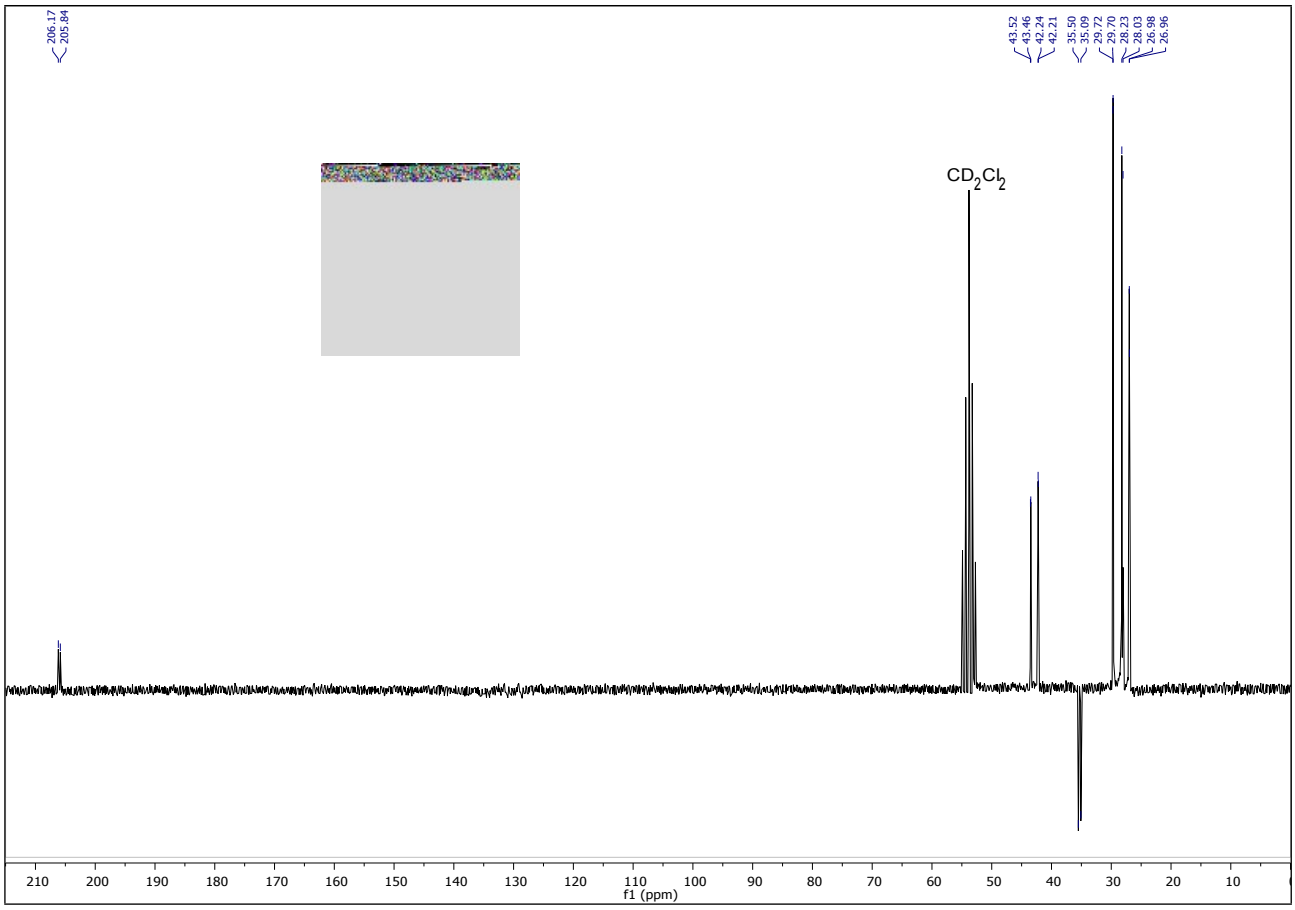

Figure S3. $^{13}C\{^{1}H\}$ PENDANT NMR spectrum (50.3 MHz) of *trans*-[$RuCl_2(CO)(PCy_3)(en)$] (**1**) in CD_2Cl_2 at 20 °C.

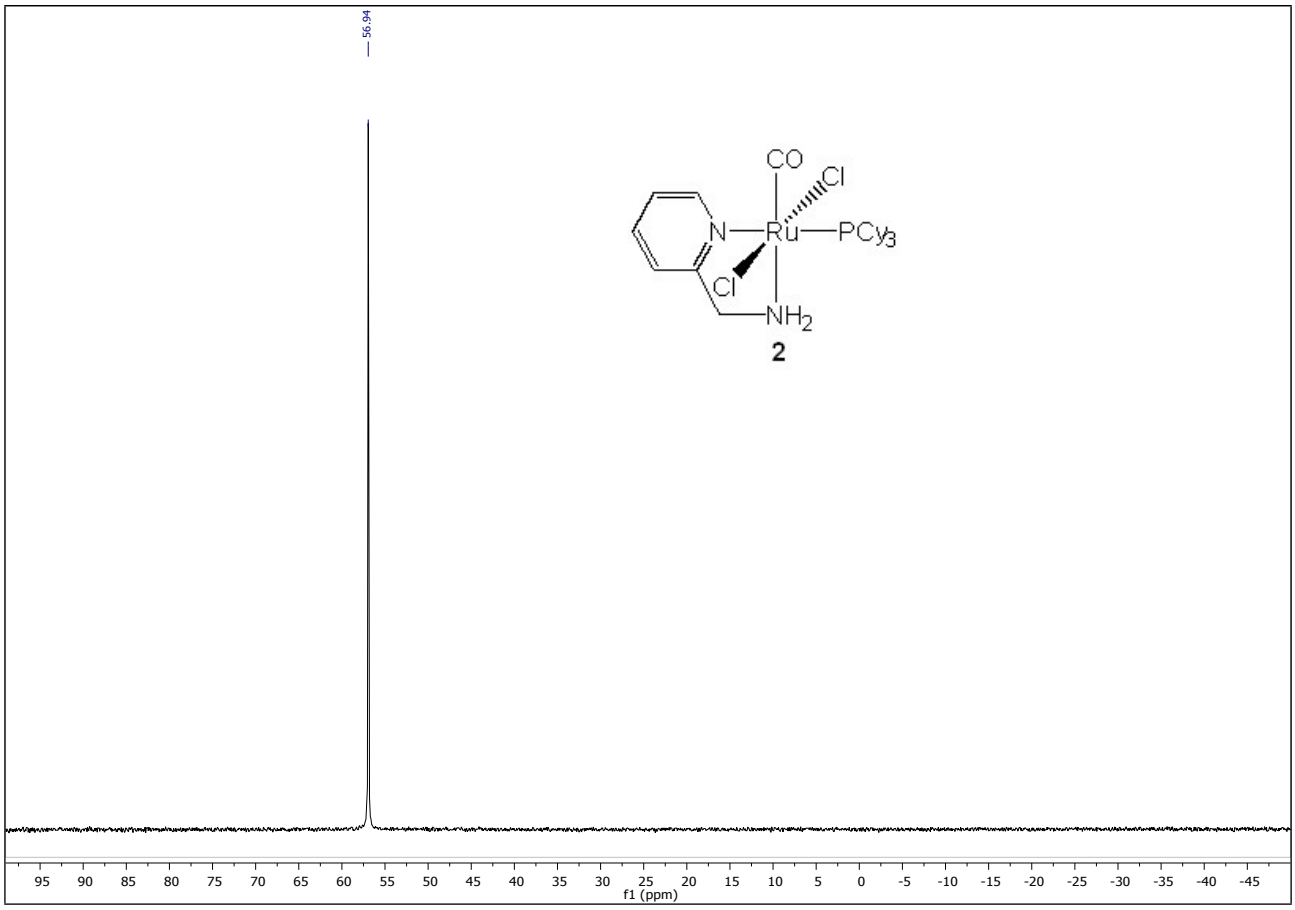

Figure S4. $^{31}P\{^{1}H\}$ NMR spectrum (81.0 MHz) of *trans*-[$RuCl_2(CO)(PCy_3)$(ampy)] (**2**) in CD_2Cl_2 at 20 °C.

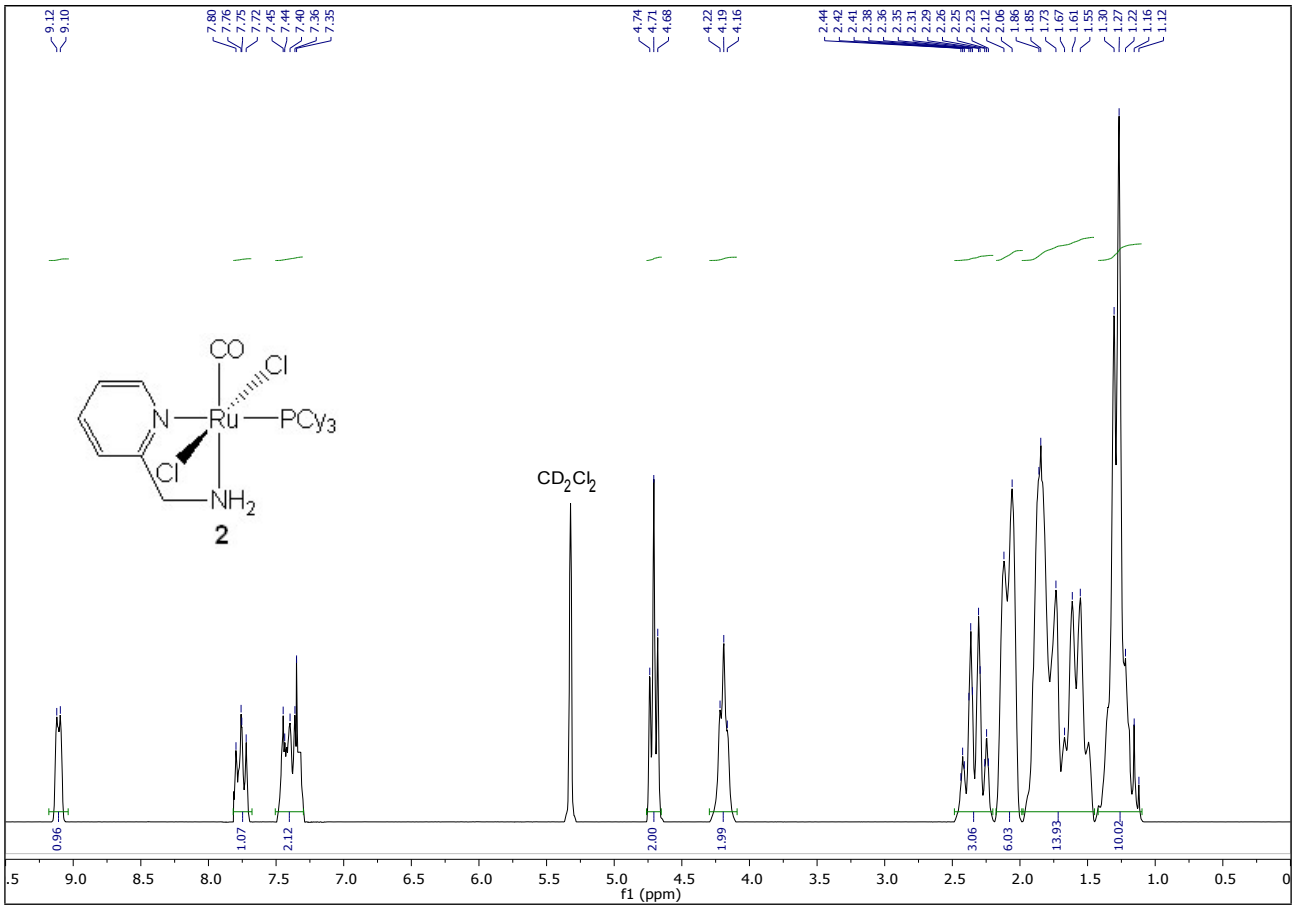

Figure S5. ^{1}H NMR spectrum (200.1 MHz) of *trans*-[$RuCl_2(CO)(PCy_3)$(ampy)] (**2**) in CD_2Cl_2 at 20 °C.

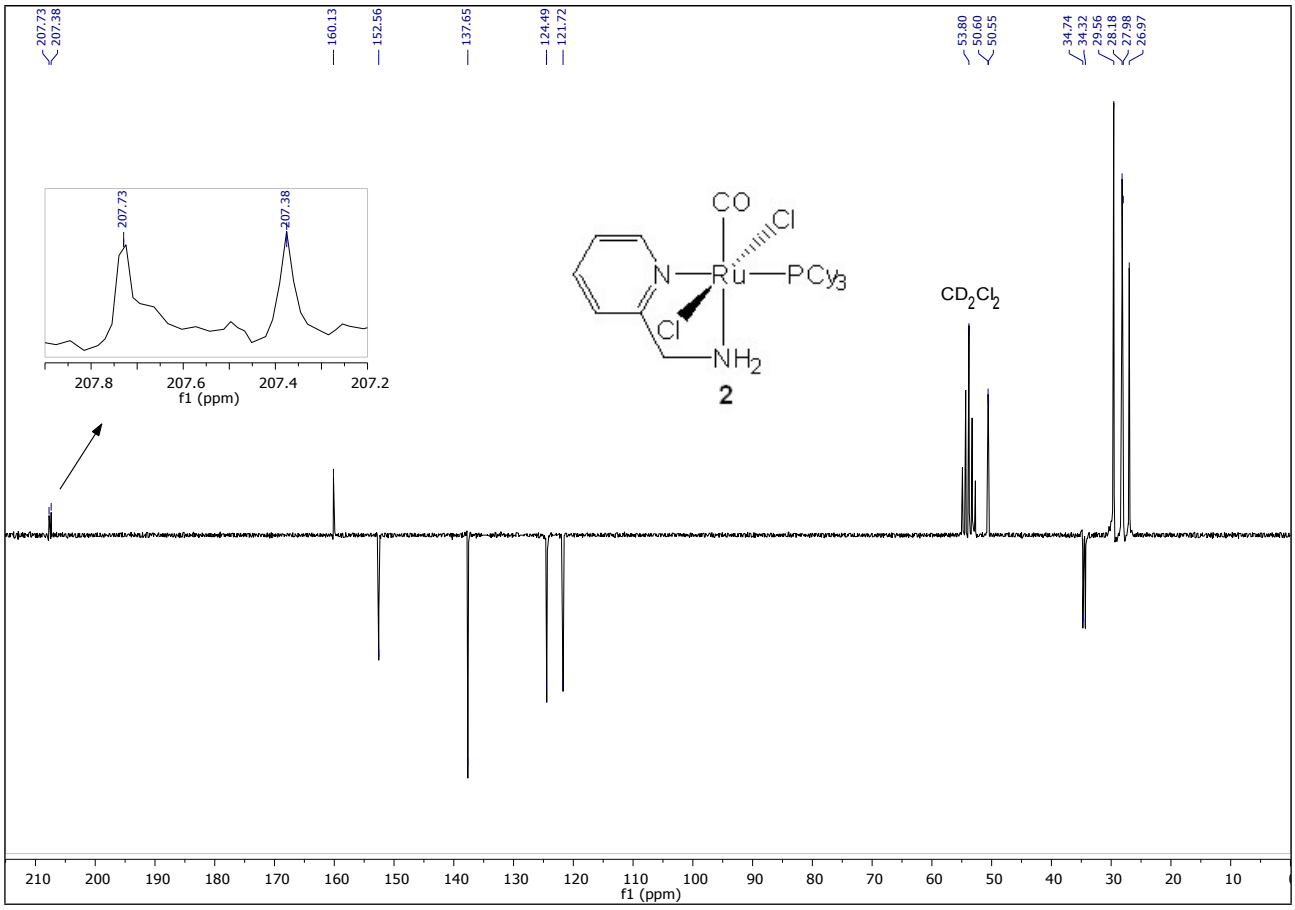

Figure S6. $^{13}C\{^{1}H\}$ PENDANT NMR spectrum (50.3 MHz) of *trans*-[$RuCl_2(CO)(PCy_3)$(ampy)] (**2**) in CD_2Cl_2 at 20 °C.

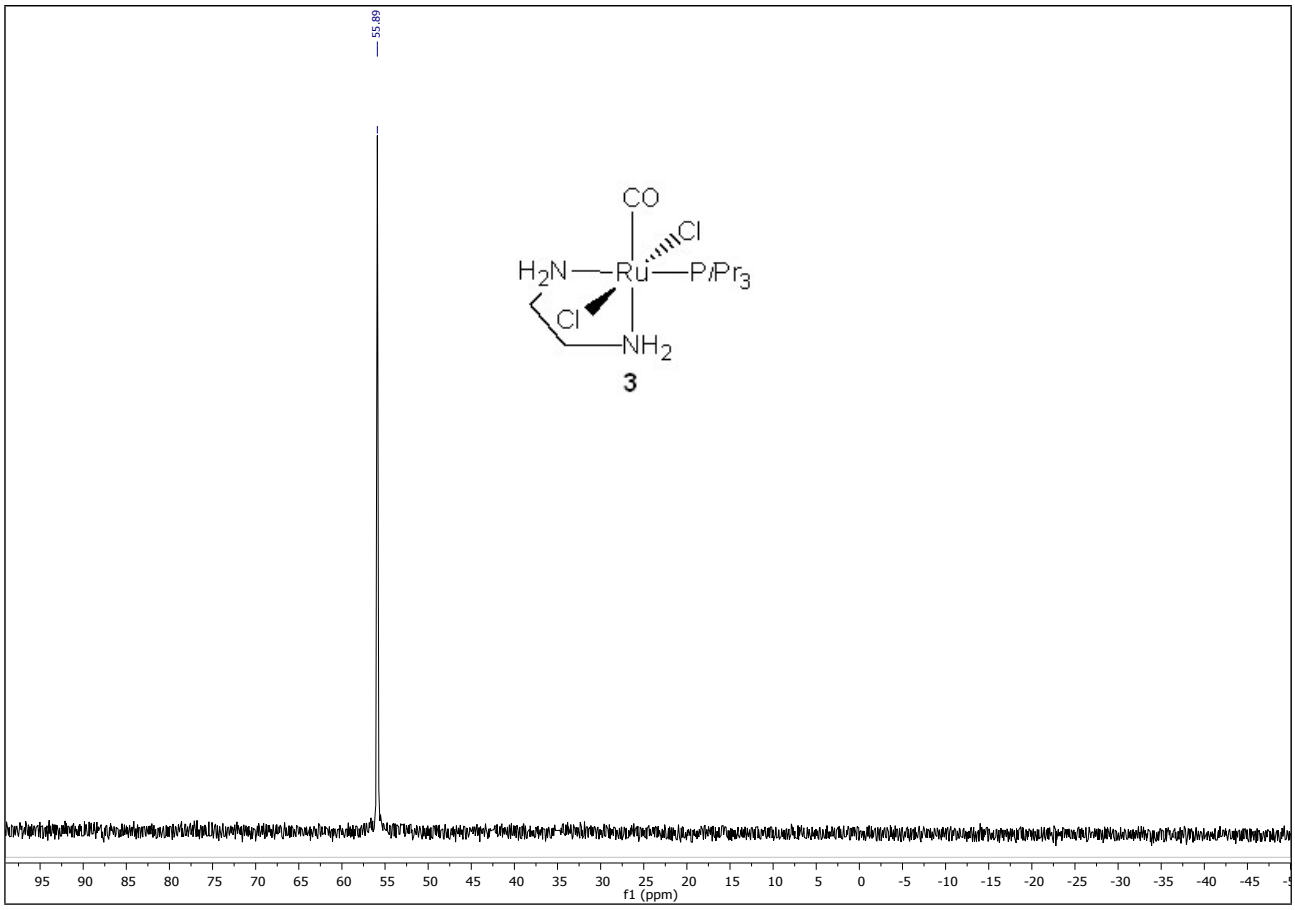

Figure S7. $^{31}P\{^{1}H\}$ NMR spectrum (81.0 MHz) of *trans*-[$RuCl_2(CO)(PiPr_3)(en)$] (**3**) in CD_2Cl_2 at 20 °C.

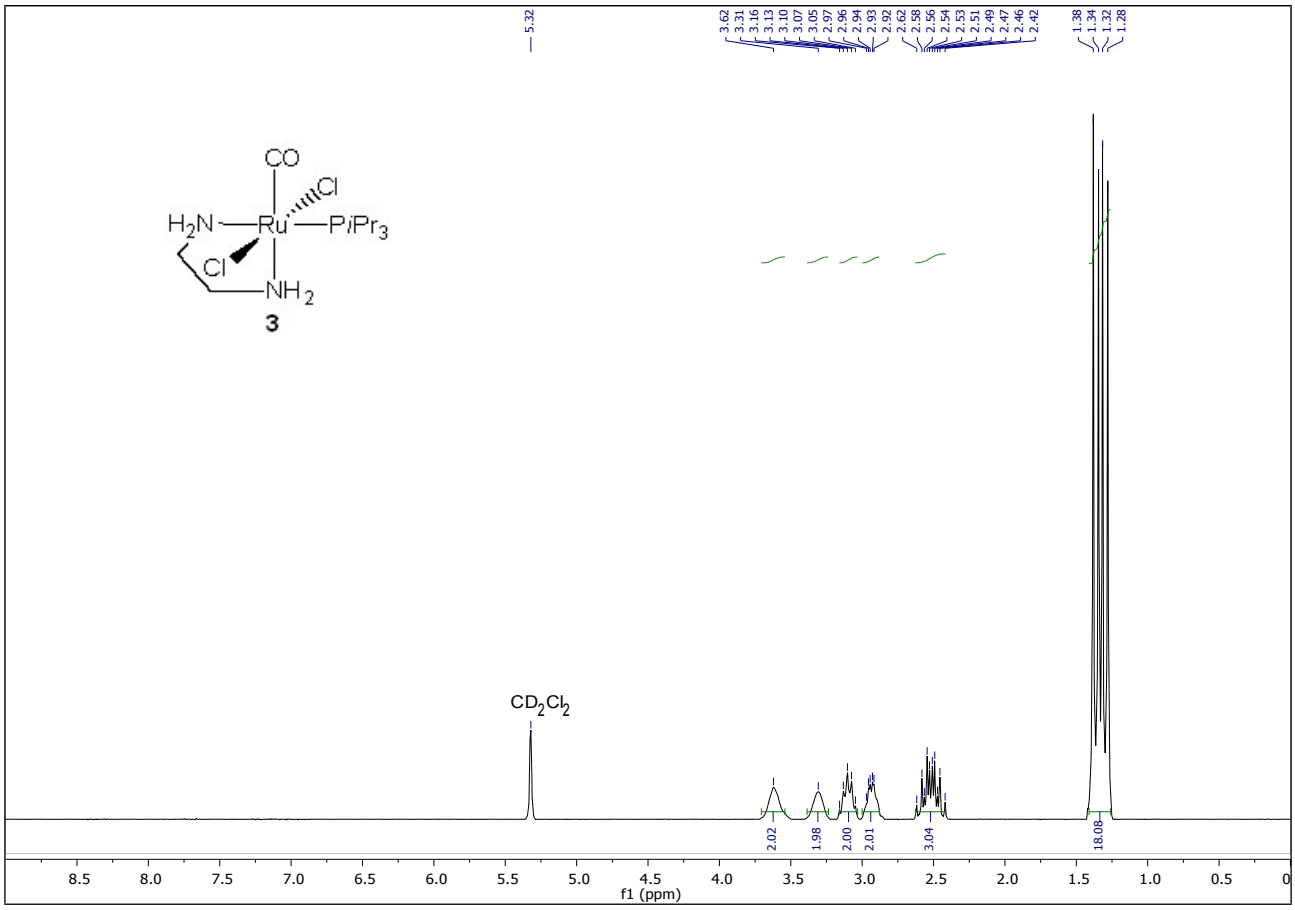

Figure S8. ^{1}H NMR spectrum (200.1 MHz) of *trans*-[$RuCl_2(CO)(PiPr_3)(en)$] (**3**) in CD_2Cl_2 at 20 °C.

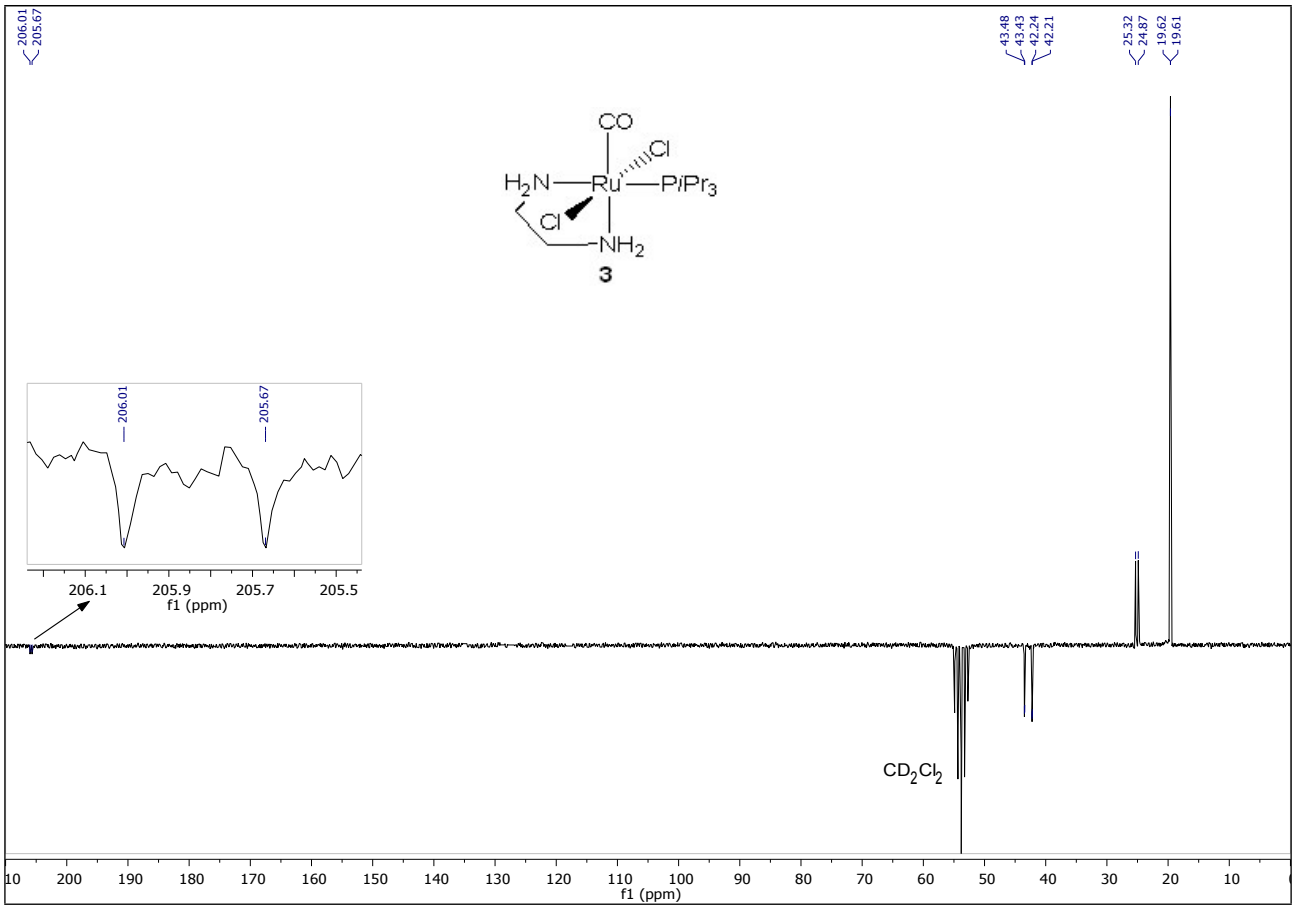

Figure S9. $^{13}C\{^{1}H\}$ PENDANT NMR spectrum (50.3 MHz) of *trans*-[$RuCl_2(CO)(PiPr_3)(en)$] (**3**) in CD_2Cl_2 at 20 °C.

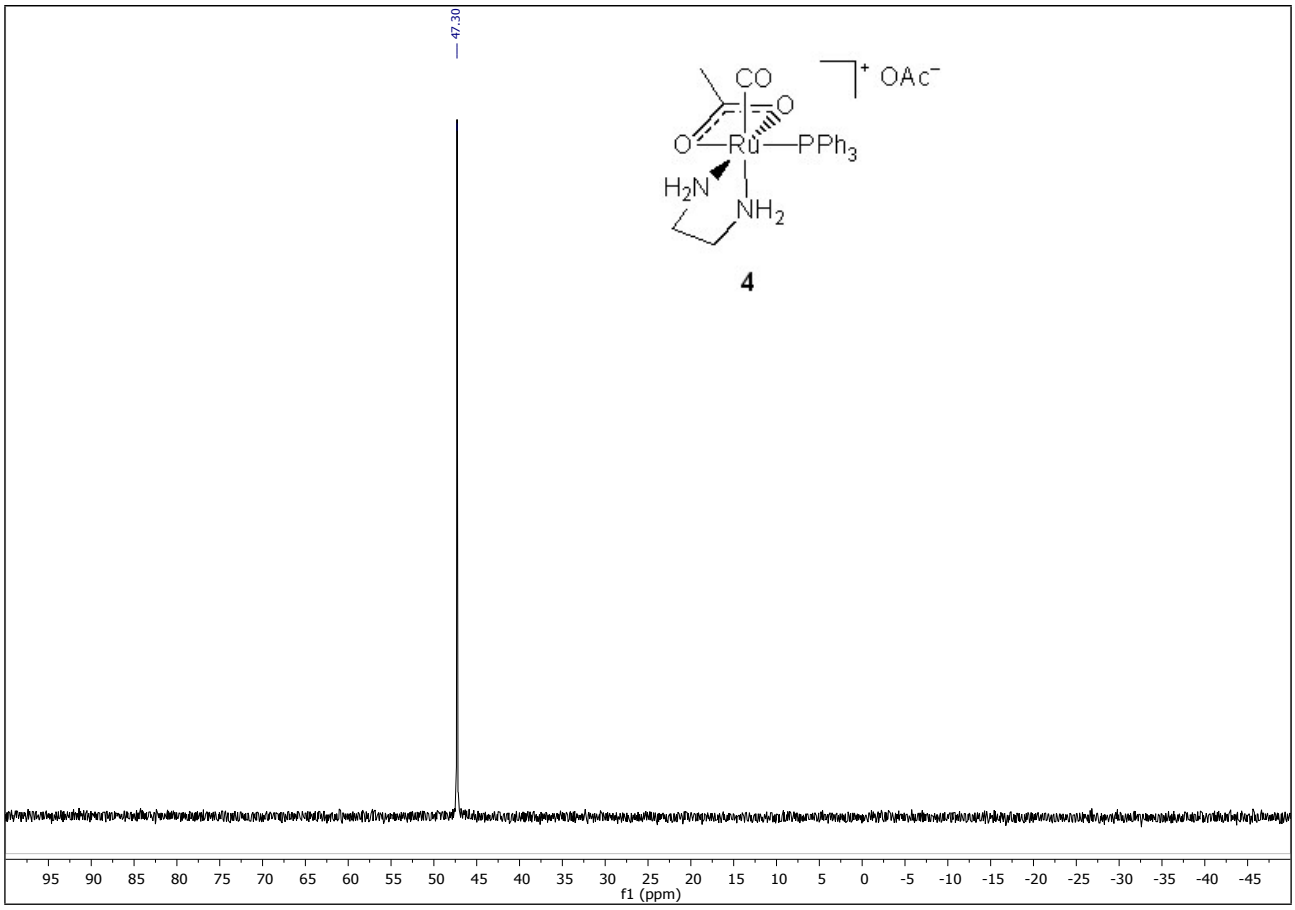

Figure S10. $^{31}P\{^{1}H\}$ NMR spectrum (162.0 MHz) of [Ru(OAc)(CO)(PPh_3)(en)]OAc (**4**) in CD_2Cl_2 at 20 °C.

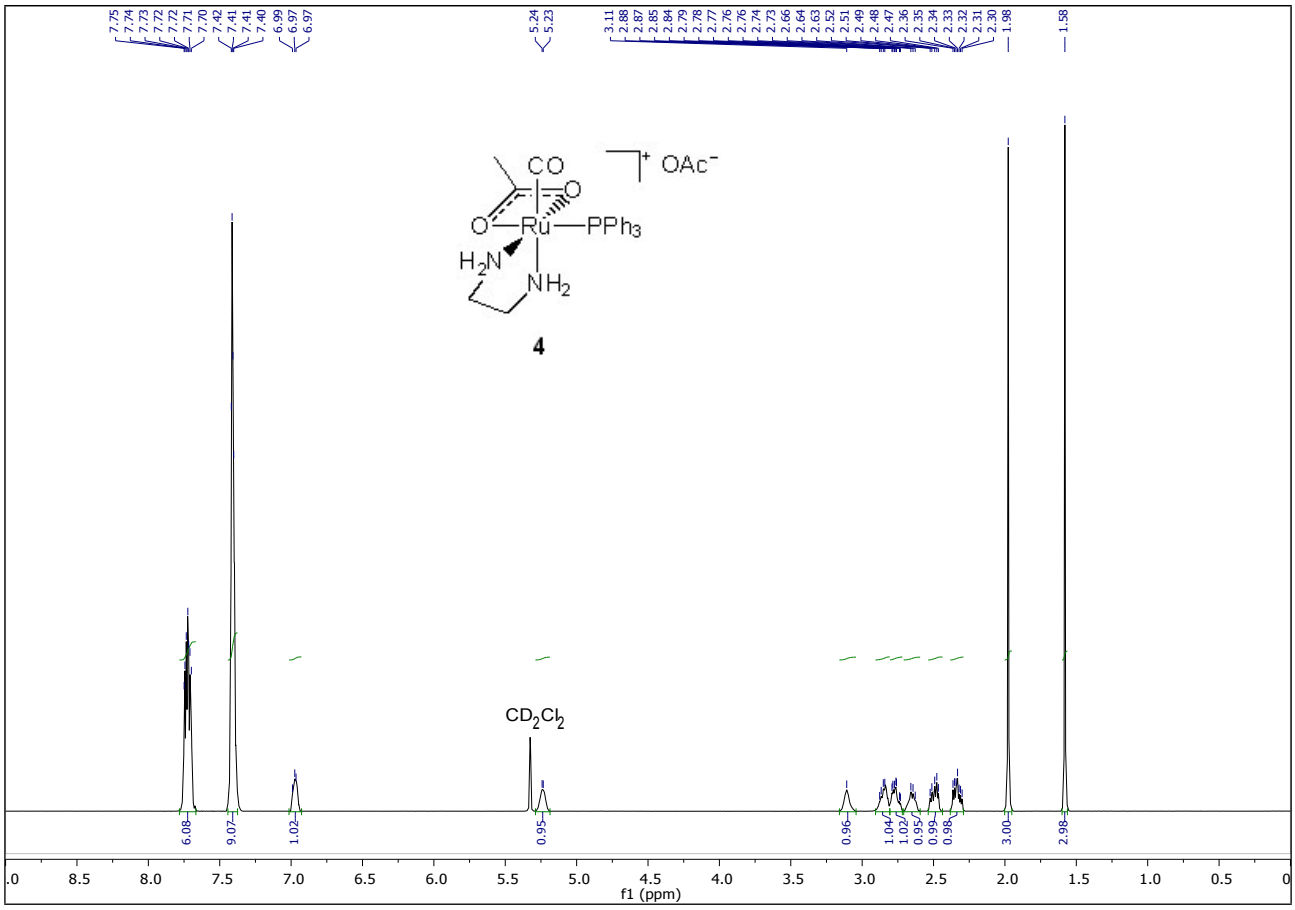

Figure S11. ^{1}H NMR spectrum (400.1 MHz) of [Ru(OAc)(CO)(PPh_3)(en)]OAc (**4**) in CD_2Cl_2 at 20 °C.

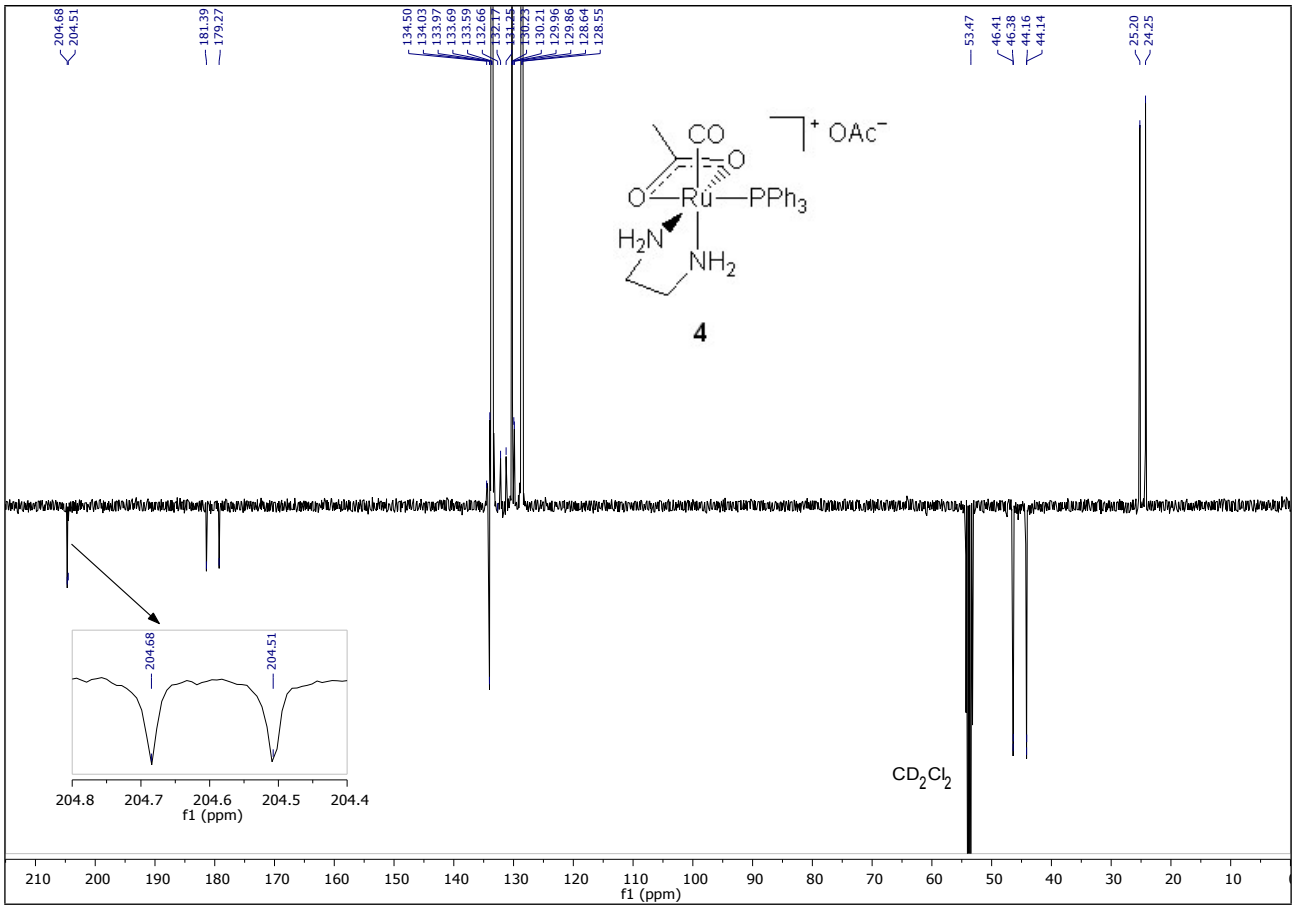

Figure S12. $^{13}C\{^{1}H\}$ DEPTQ NMR spectrum (100.6 MHz) of [Ru(OAc)(CO)(PPh_3)(en)]OAc (**4**) in CD_2Cl_2 at 20 °C.

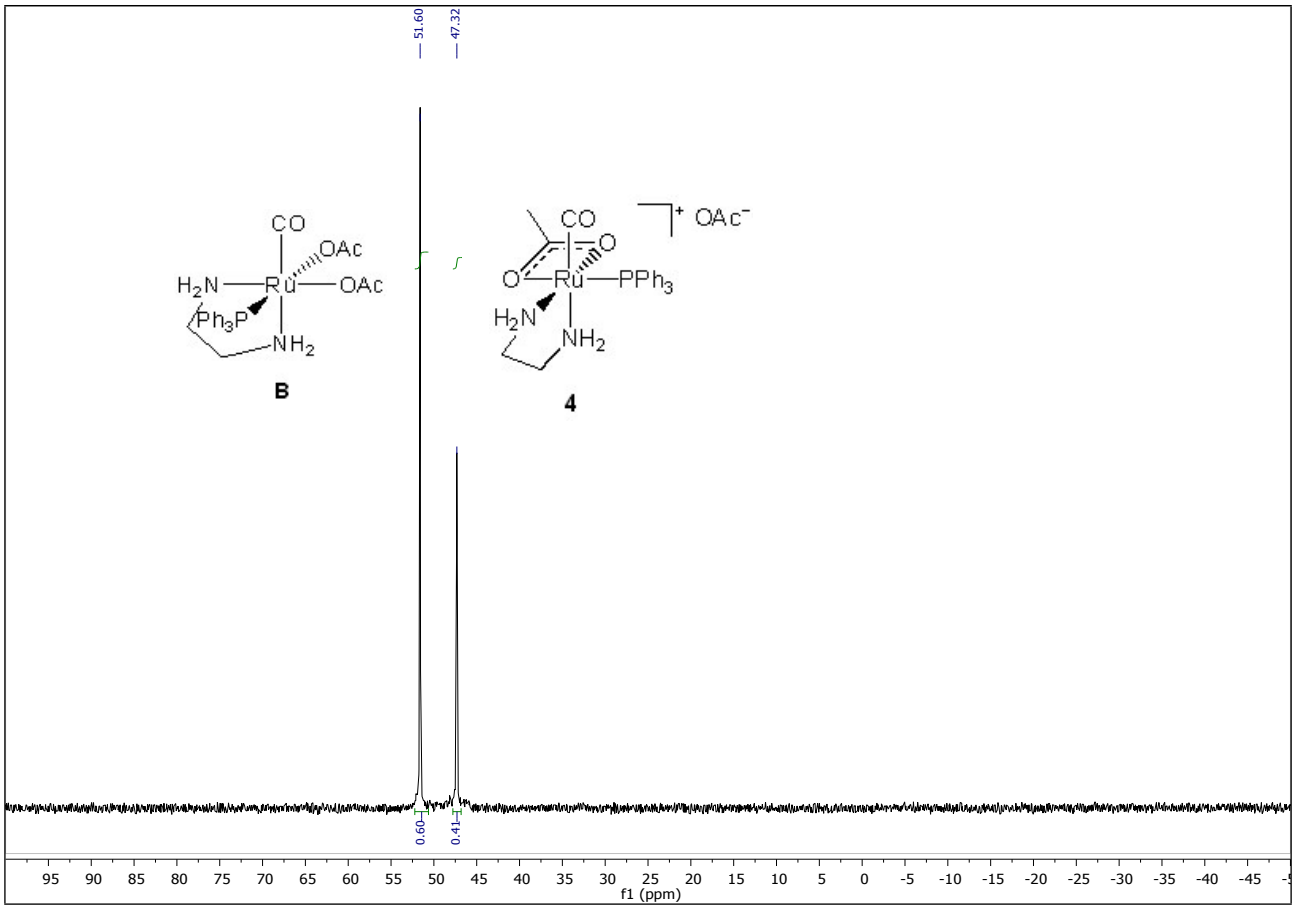

Figure S13. Control $^{31}P\{^{1}H\}$ NMR spectrum (81.0 MHz) of the mixture of [Ru(OAc)(CO)(PPh_3)(en)]OAc (**4**) and *trans*-[Ru(OAc)$_2$(CO)(PPh_3)(en)] (**B**) in CD_2Cl_2 at 20 °C.

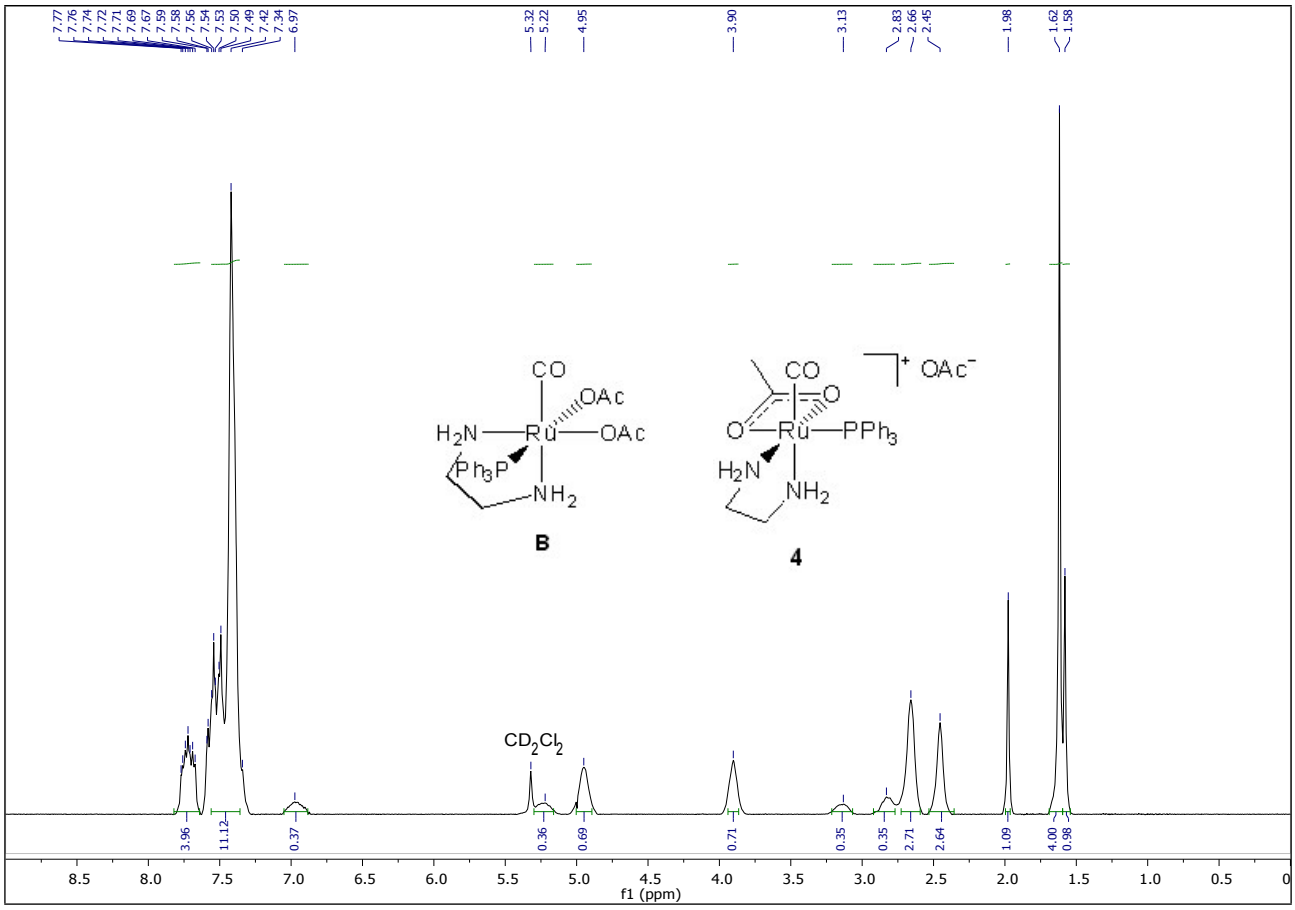

Figure S14. Control ^{1}H NMR spectrum (200.1 MHz) of the mixture of [Ru(OAc)(CO)(PPh_3)(en)]OAc (**4**) and *trans*-[Ru(OAc)$_2$(CO)(PPh_3)(en)] (**B**) in CD_2Cl_2 at 20 °C.

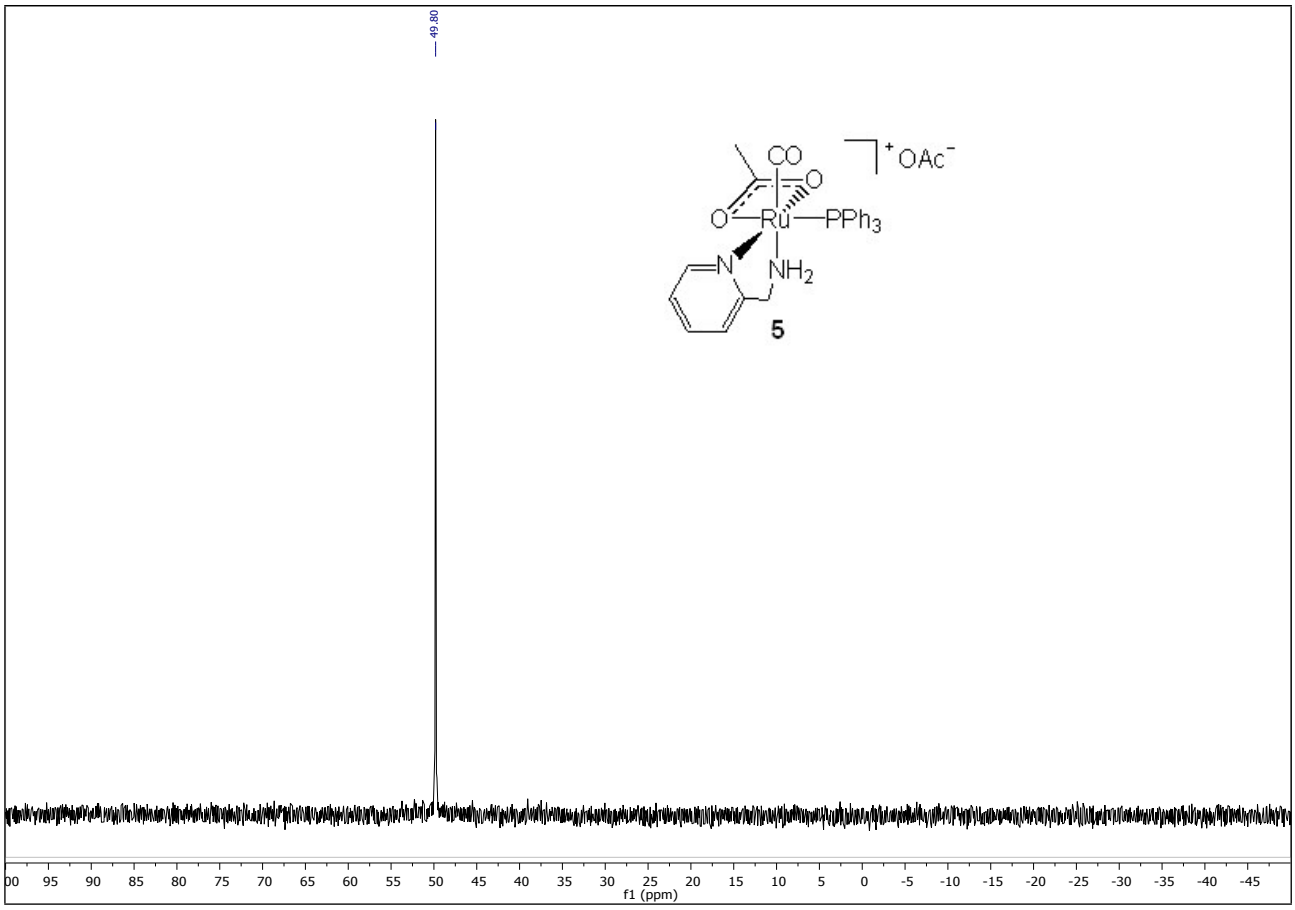

Figure S15. $^{31}P\{^{1}H\}$ NMR spectrum (162.0 MHz) of [Ru(OAc)(CO)(PPh_3)(ampy)]OAc (**5**) in CD_2Cl_2 at 20 °C.

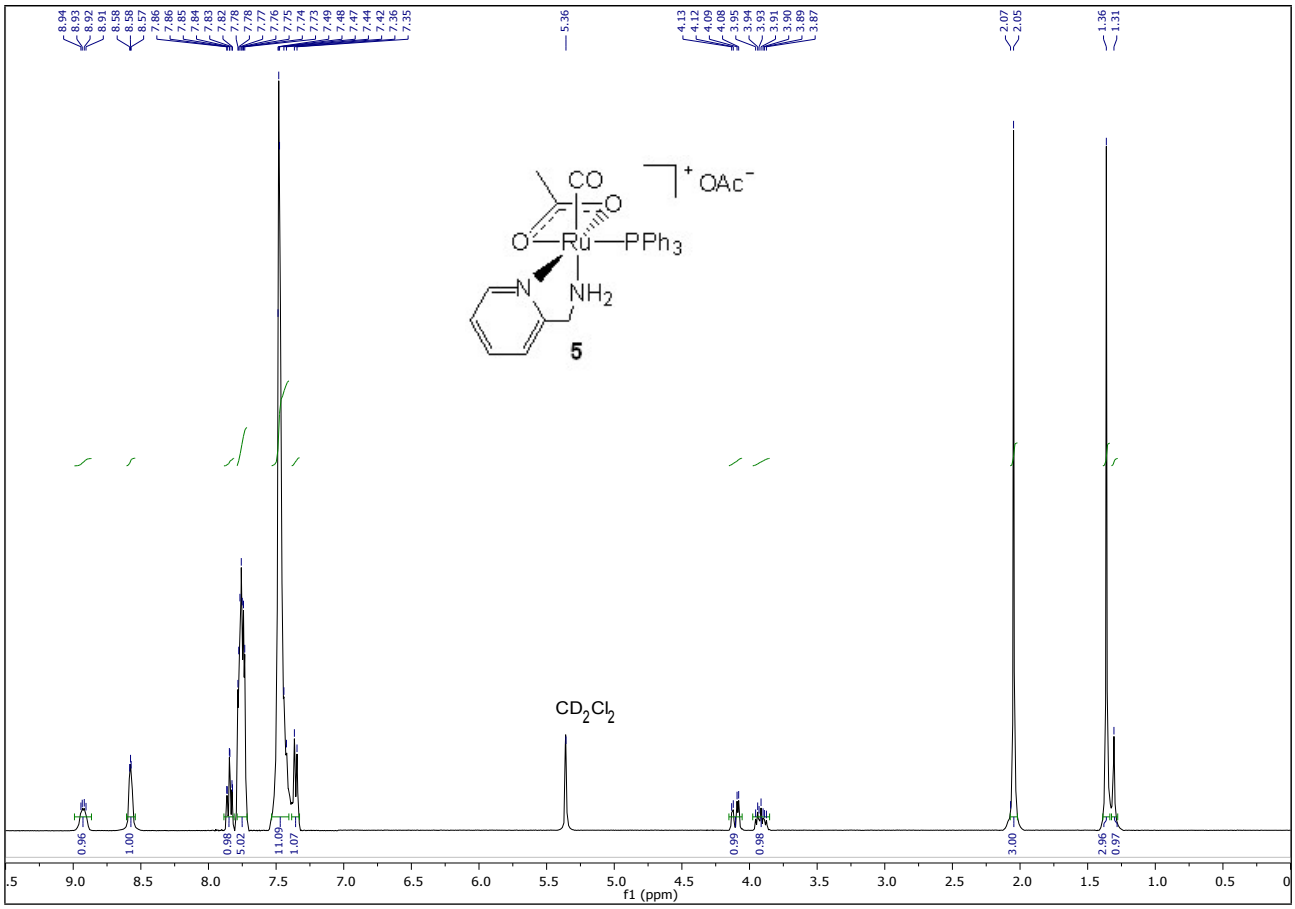

Figure S16. ^{1}H NMR spectrum (400.1 MHz) of [Ru(OAc)(CO)(PPh_3)(ampy)]OAc (**5**) in CD_2Cl_2 at 20 °C.

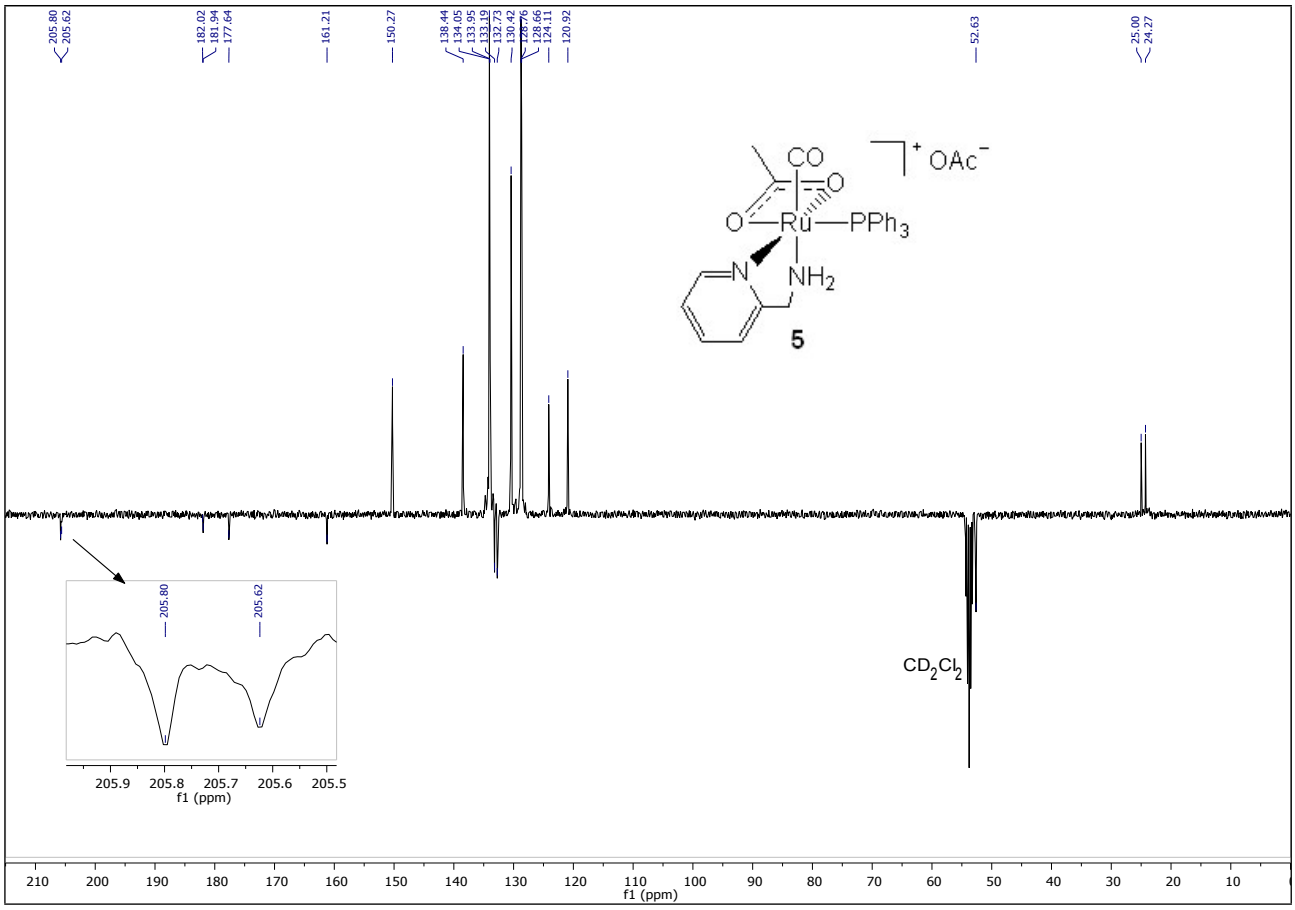

Figure S17. $^{13}C\{^{1}H\}$ DEPTQ NMR spectrum (100.6 MHz) of [Ru(OAc)(CO)(PPh_3)(ampy)]OAc (**5**) in CD_2Cl_2 at 20 °C.

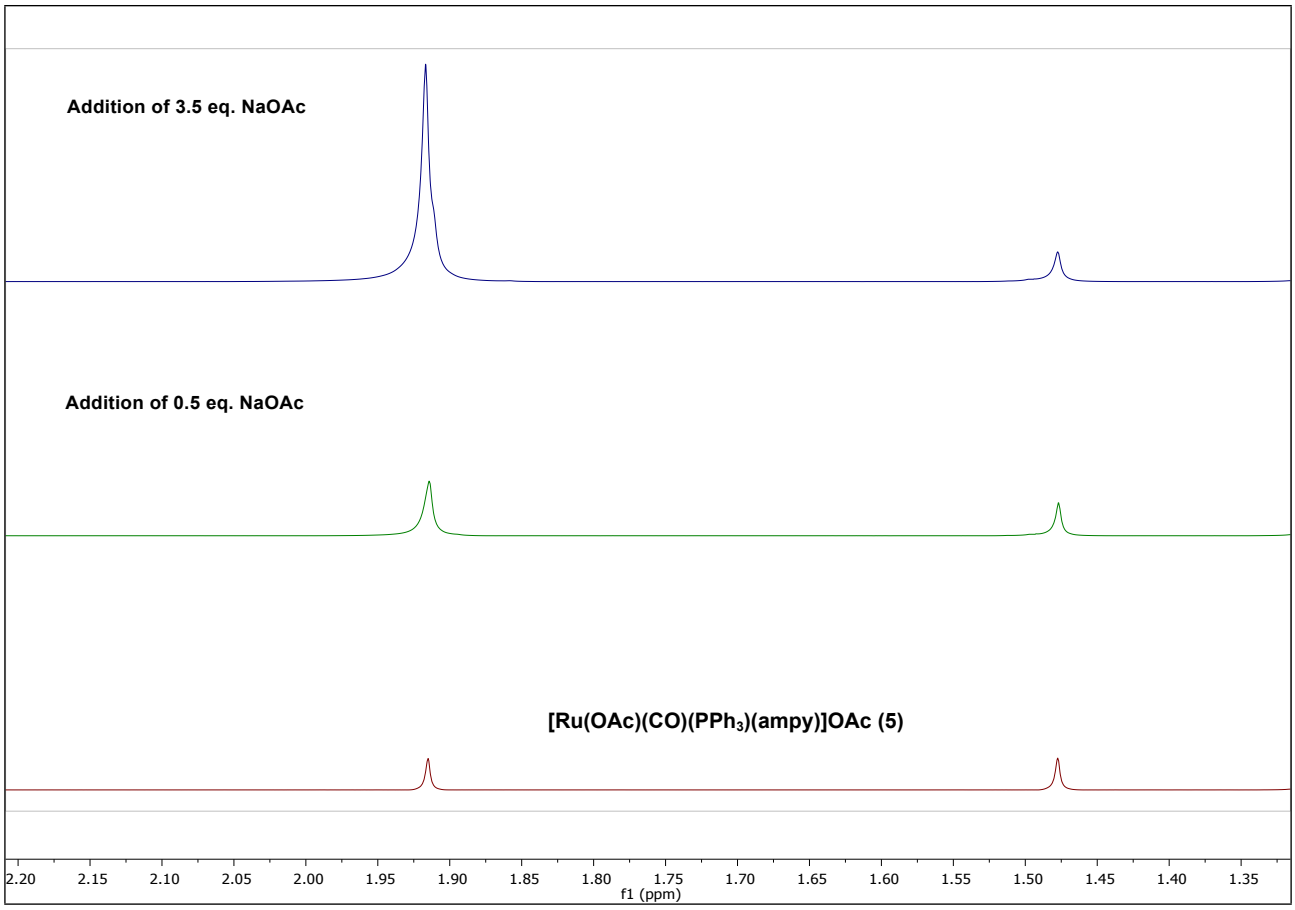

Figure S18. Effect of the addition of NaOAc to [Ru(OAc)(CO)(PPh_3)(ampy)]OAc (**5**) in the methyl acetate region of the ^{1}H NMR spectra in CD_3OD at 20 °C.

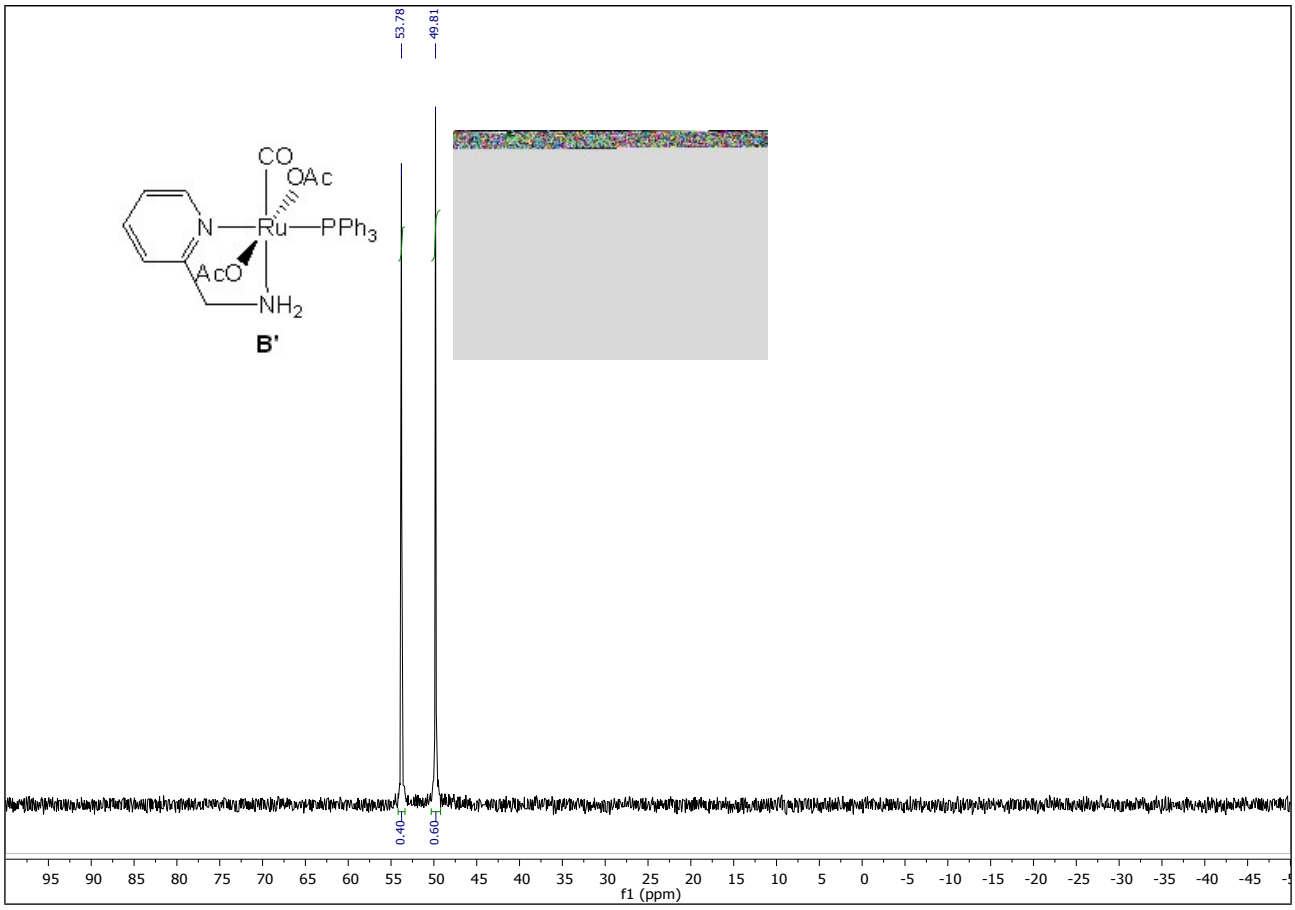

Figure S19. Control $^{31}P\{^{1}H\}$ NMR spectrum (81.0 MHz) of the mixture of [Ru(OAc)(CO)(PPh_3)(ampy)]OAc (**5**) and *trans*-[Ru$(OAc)_2$(CO)(PPh_3)(ampy)] (**B'**) in CD_2Cl_2 at 20 °C.

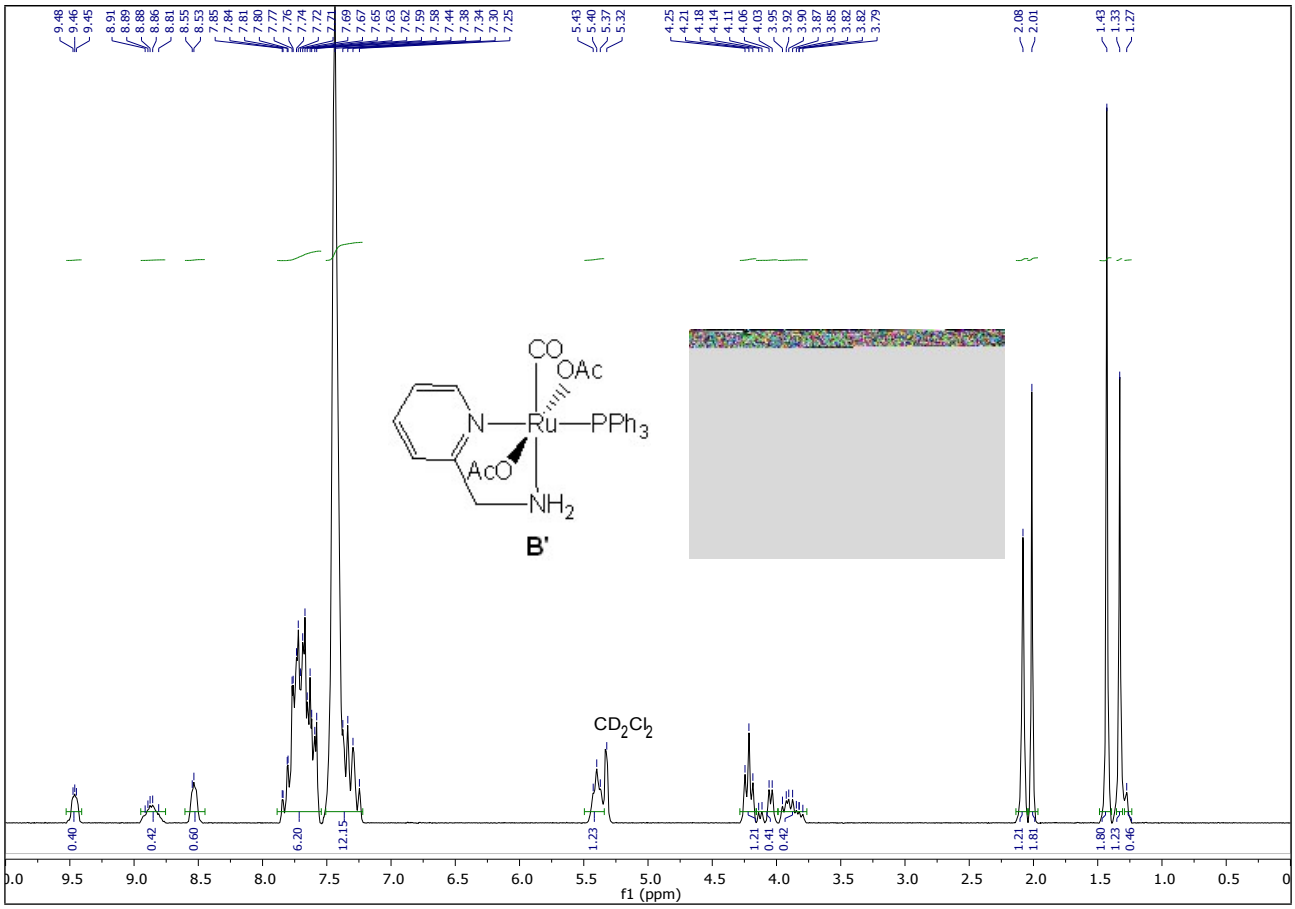

Figure S20. Control ^{1}H NMR spectrum (200.1 MHz) of the mixture of [Ru(OAc)(CO)(PPh_3)(ampy)]OAc (**5**) and *trans*-[Ru$(OAc)_2$(CO)(PPh_3)(ampy)] (**B'**) in CD_2Cl_2 at 20 °C.

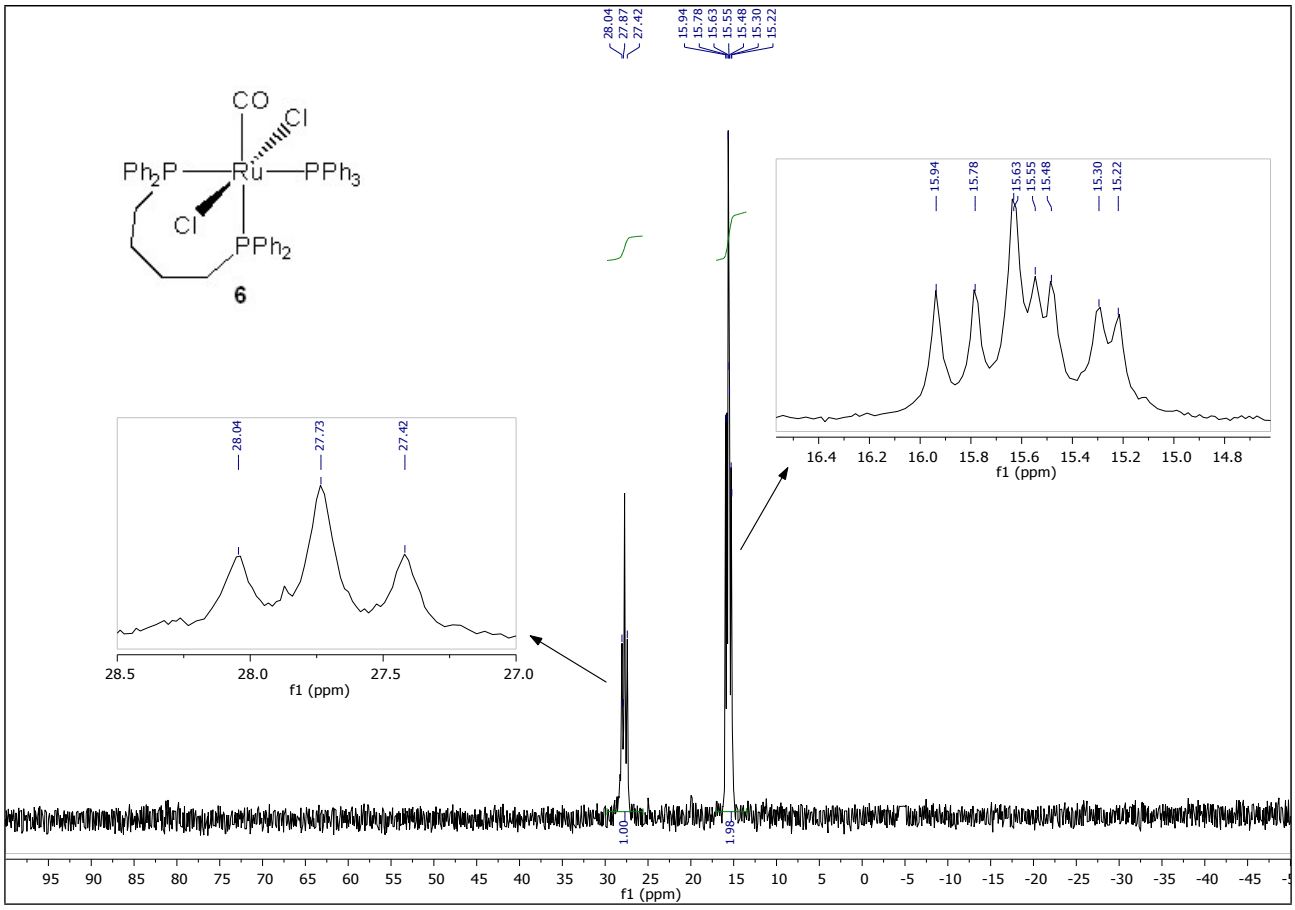

Figure S21. $^{31}P\{^{1}H\}$ NMR spectrum (81.0 MHz) of *trans*-[$RuCl_2(CO)(dppb)(PPh_3)$] (**6**) in CD_2Cl_2 at 20 °C.

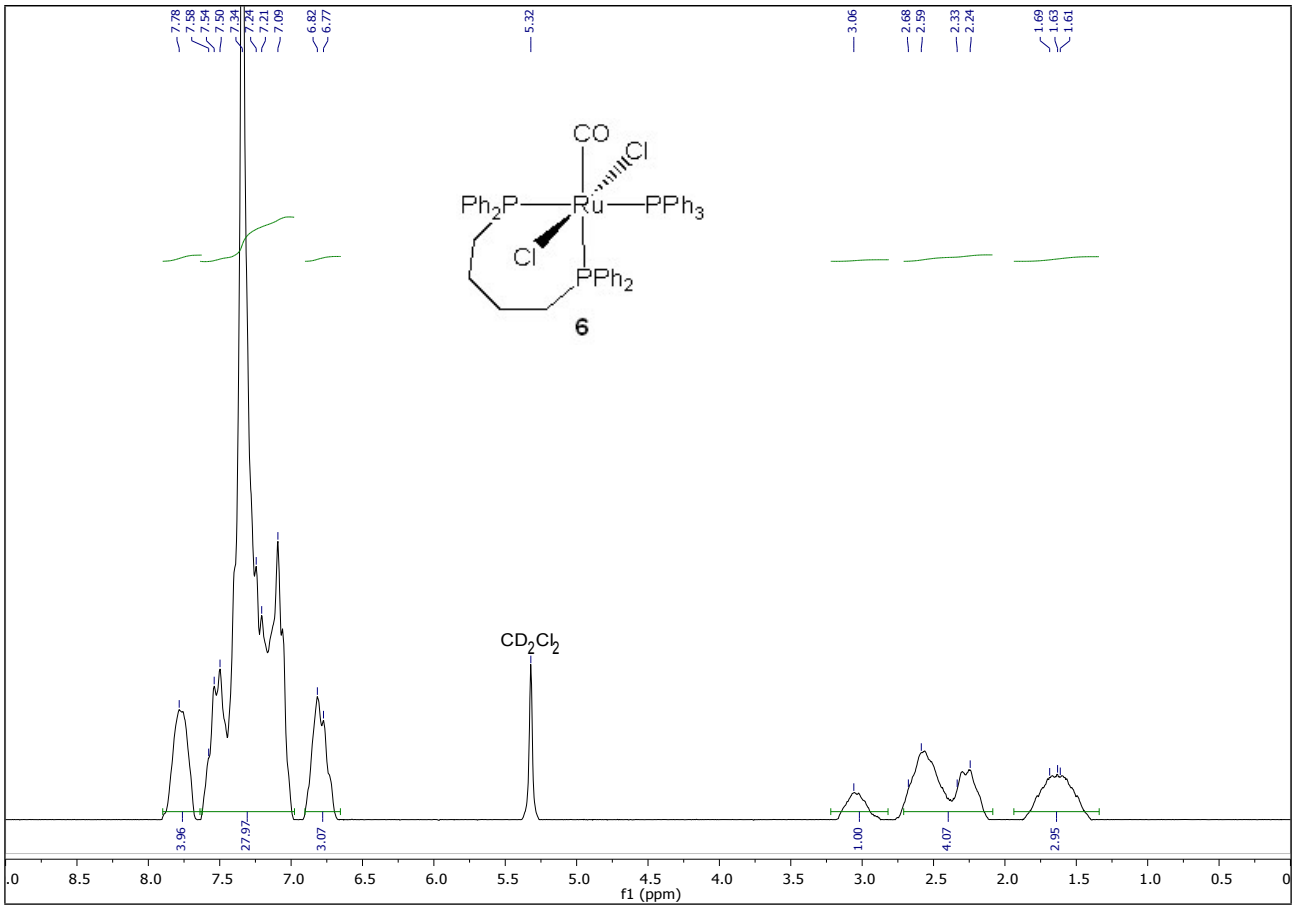

Figure S22. ^{1}H NMR spectrum (200.1 MHz) of *trans*-[$RuCl_2(CO)(dppb)(PPh_3)$] (**6**) in CD_2Cl_2 at 20 °C.

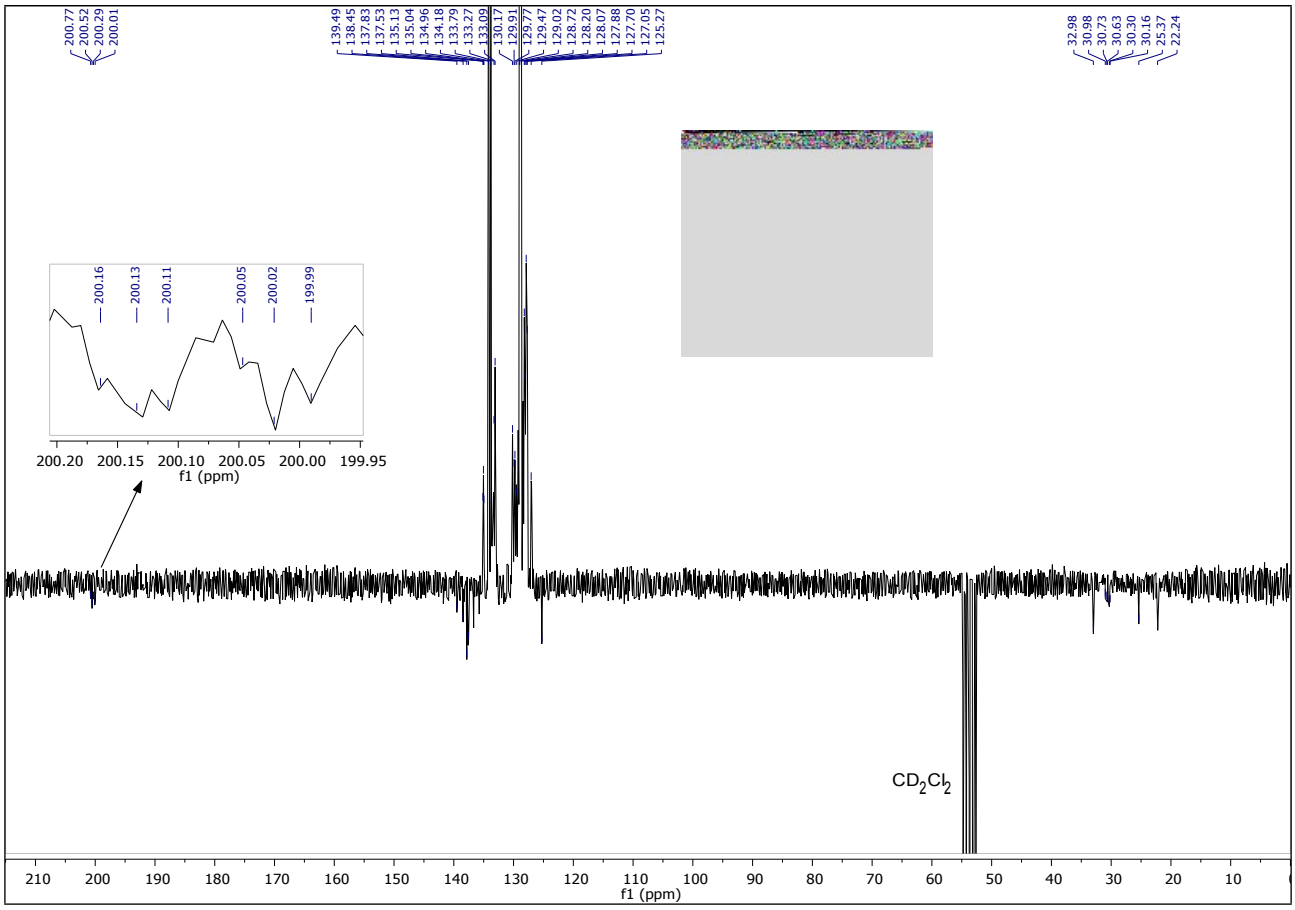

Figure S23. $^{13}C\{^{1}H\}$ DEPTQ NMR spectrum (100.6 MHz) of *trans*-[$RuCl_2(CO)(dppb)(PPh_3)$] (**6**) in CD_2Cl_2 at 20 °C.

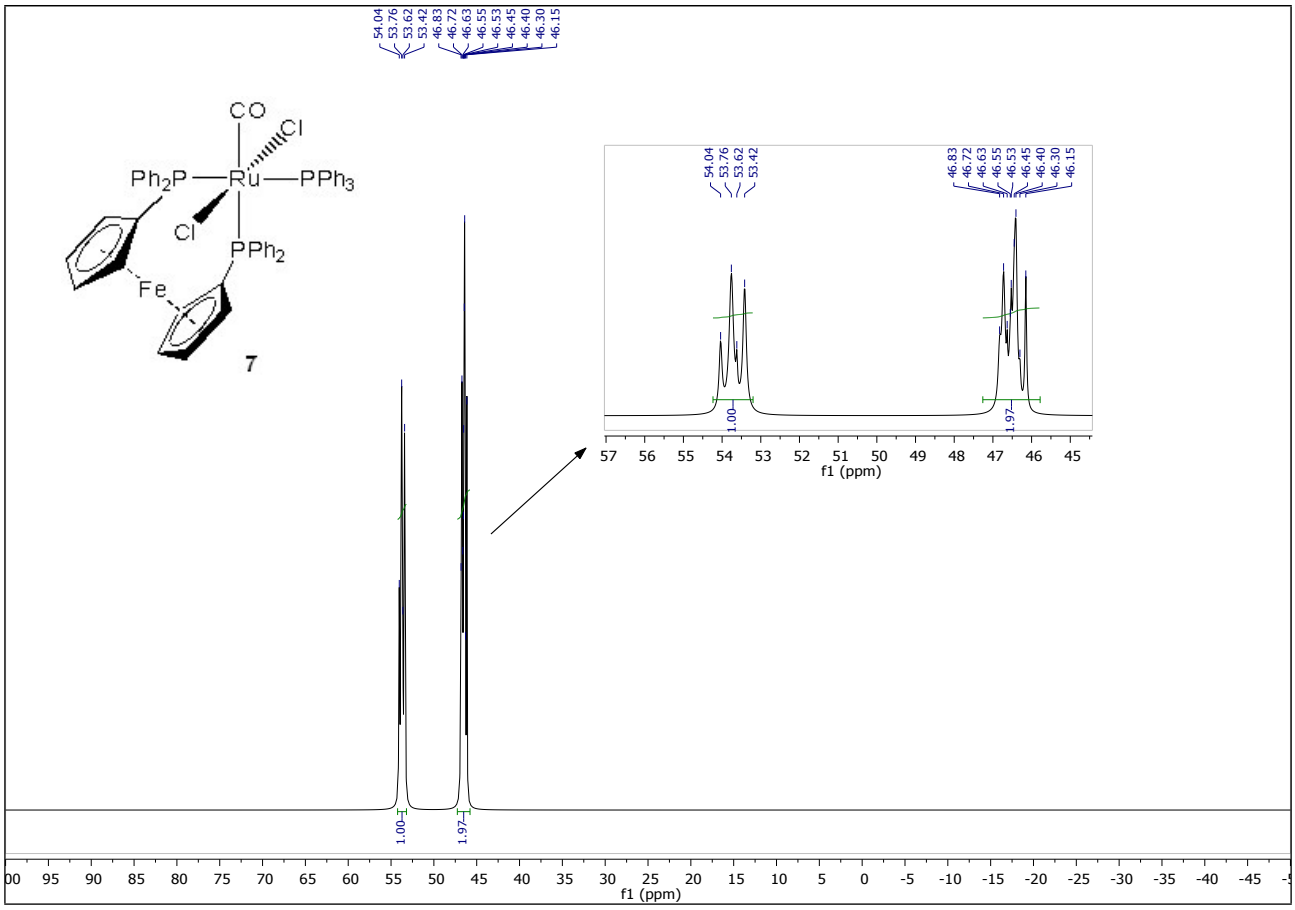

Figure S24. $^{31}P\{^{1}H\}$ NMR spectrum (81.0 MHz) of *trans*-[$RuCl_2(CO)(dppf)(PPh_3)$] (**7**) in CD_2Cl_2 at 20 °C.

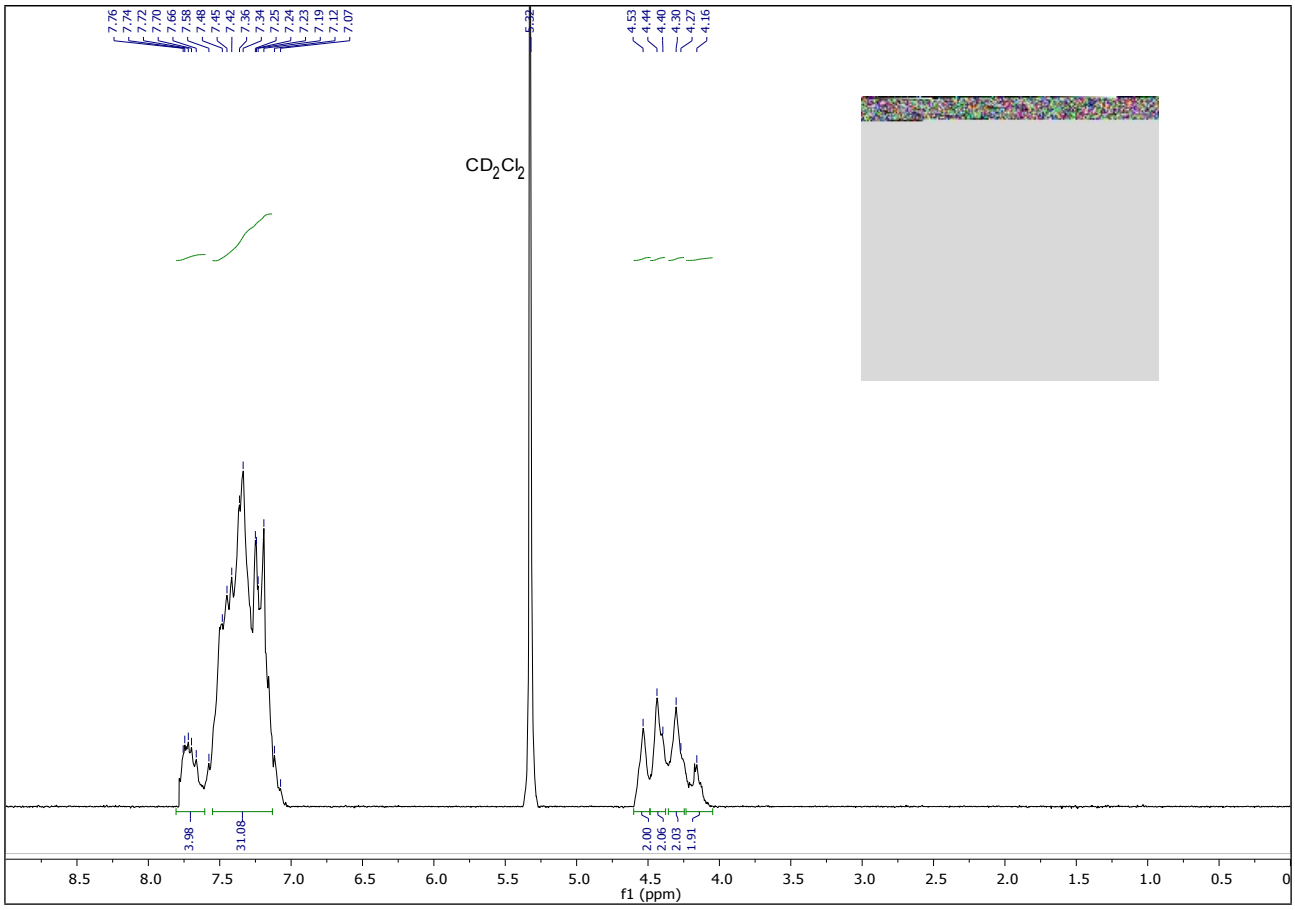

Figure S25. ^{1}H NMR spectrum (200.1 MHz) of *trans*-[$RuCl_2(CO)(dppf)(PPh_3)$] (**7**) in CD_2Cl_2 at 20 °C.

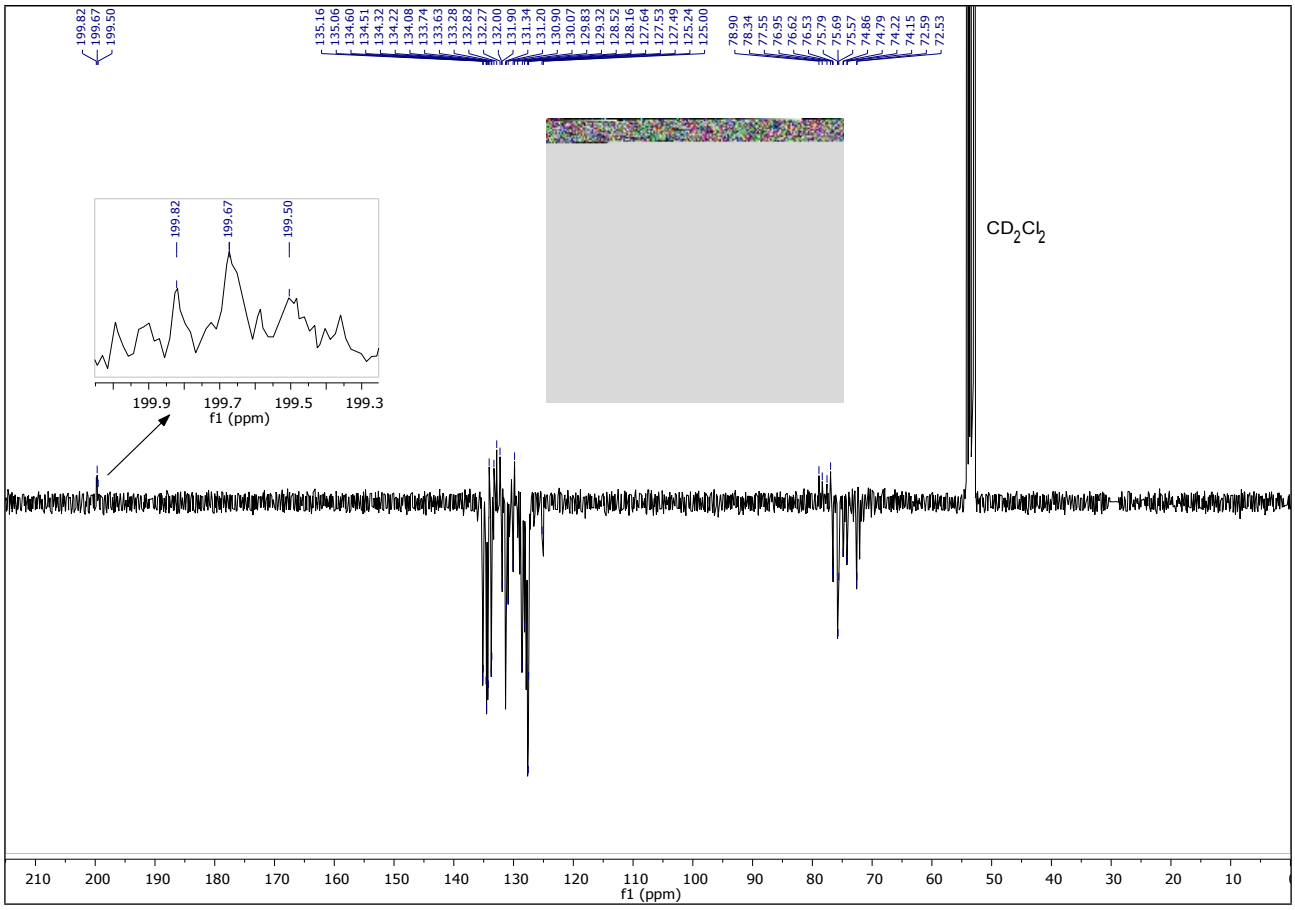

Figure S26. $^{13}C\{^{1}H\}$ DEPTQ NMR spectrum (100.6 MHz) of *trans*-[$RuCl_2(CO)(dppf)(PPh_3)$] (**7**) in CD_2Cl_2 at 20 °C.

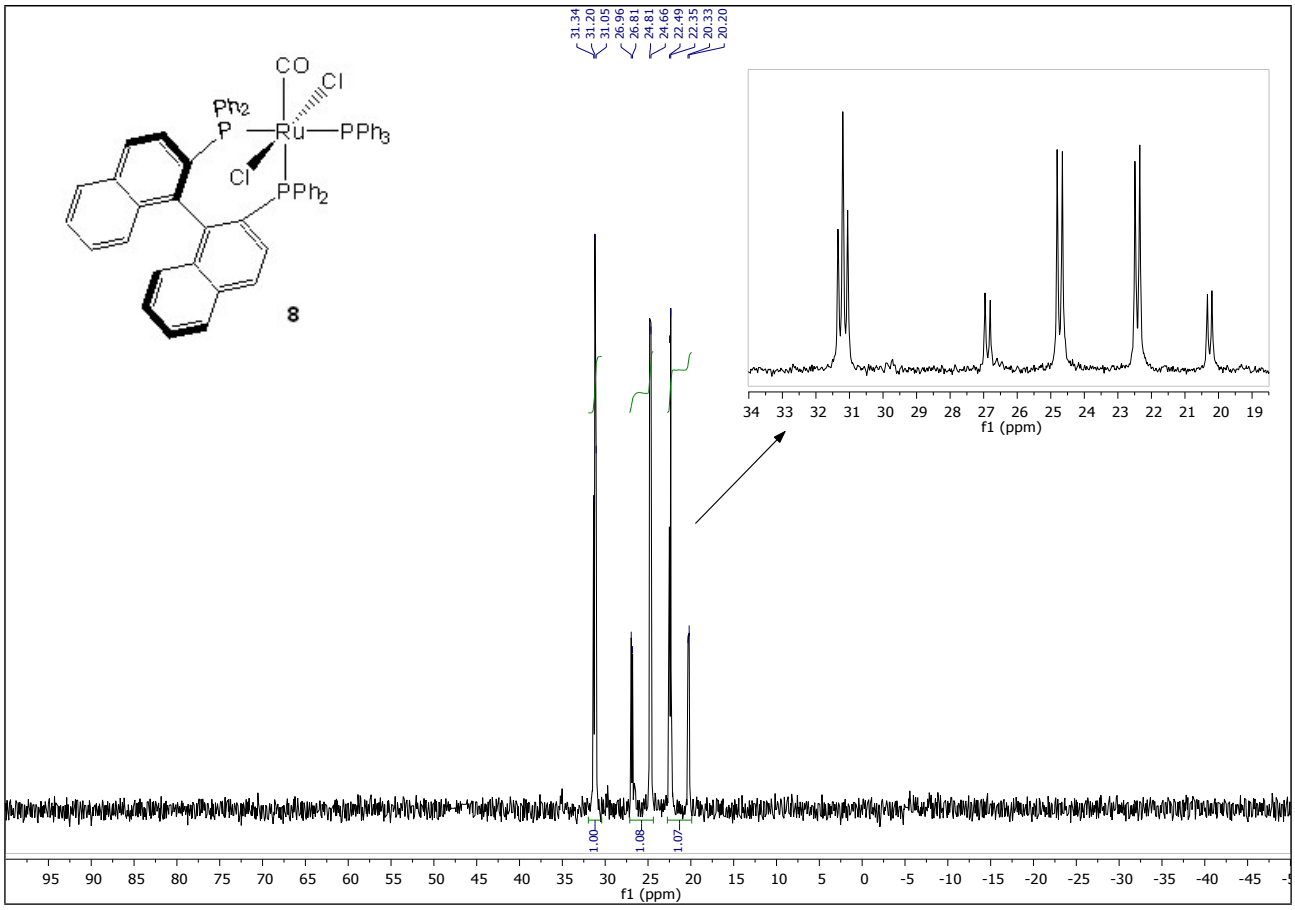

Figure S27. $^{31}P\{^{1}H\}$ NMR spectrum (162.0 MHz) of *trans*-[$RuCl_2$(CO)((*R*)-BINAP)(PPh_3)] (**8**) in [D8]toluene at 20 °C.

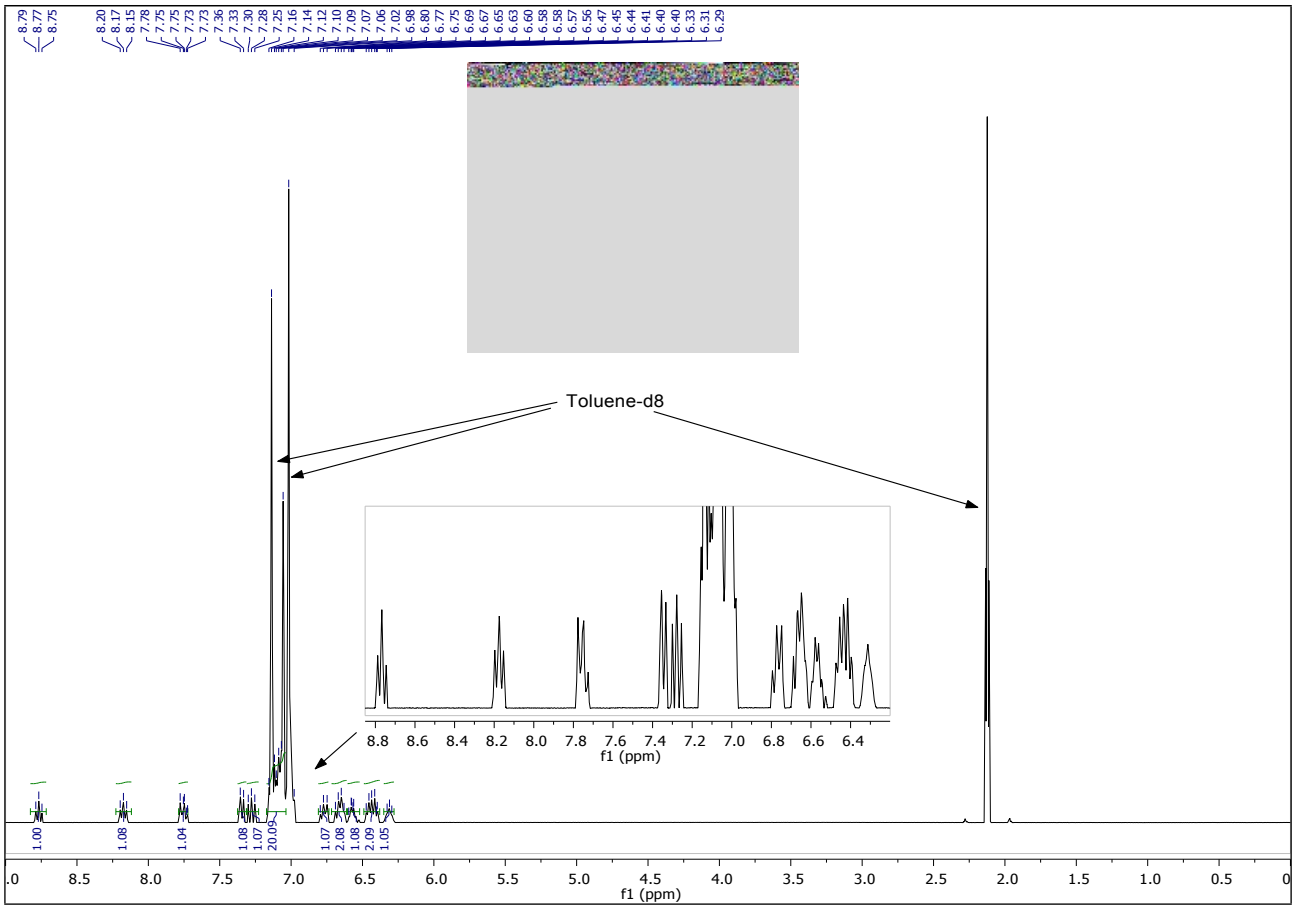

Figure S28. ^{1}H NMR spectrum (400.1 MHz) of *trans*-[$RuCl_2$(CO)((*R*)-BINAP)(PPh_3)] (**8**) in [D8]toluene at 20 °C.

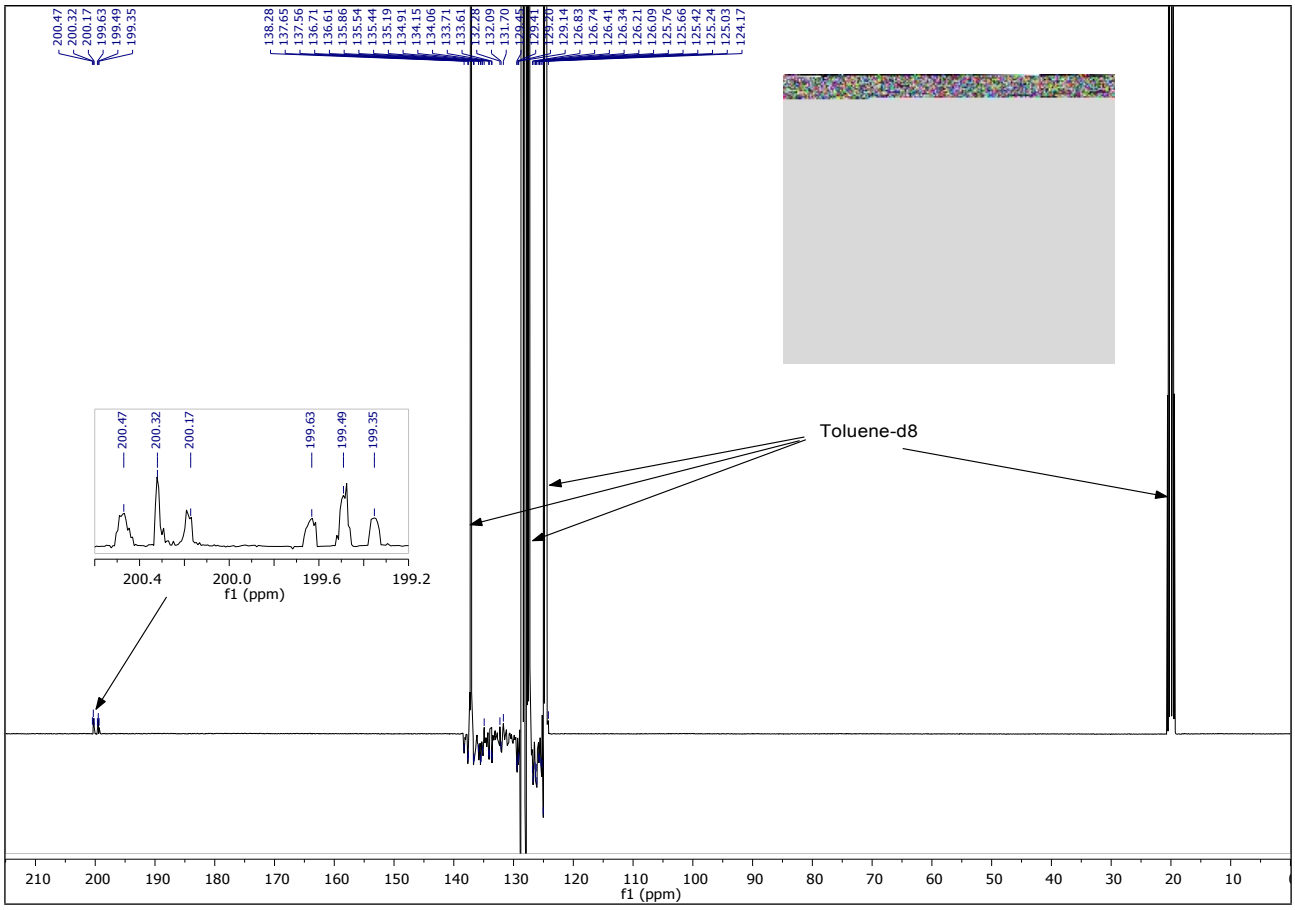

Figure S29. $^{13}C\{^{1}H\}$ DEPTQ NMR spectrum (100.6 MHz) of *trans*-[$RuCl_2$(CO)((*R*)-BINAP)(PPh_3)] (**8**) in [D8]toluene at 20 °C.

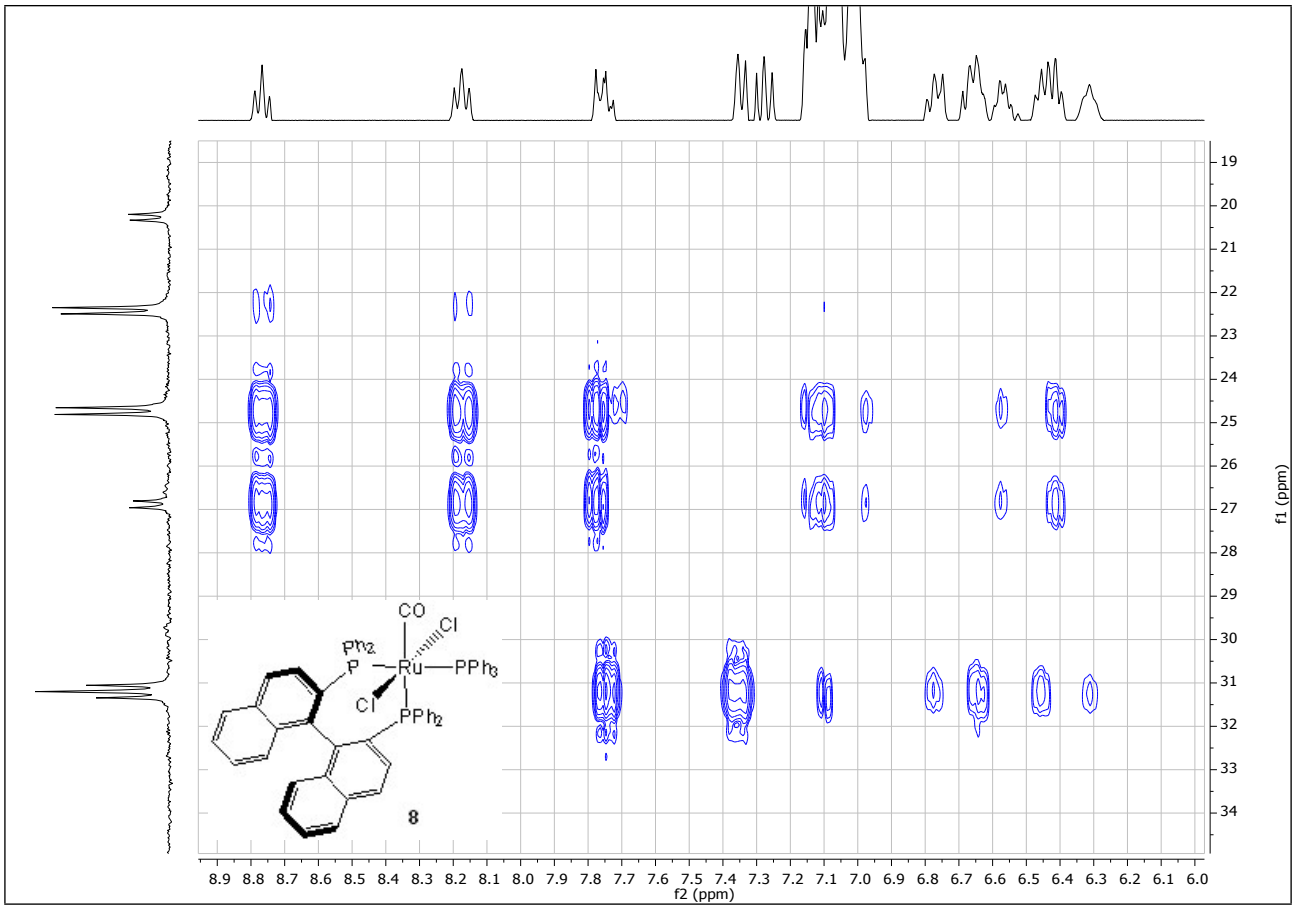

Figure S30. ^{31}P-^{1}H HMBC 2D NMR spectrum of *trans*-[$RuCl_2$(CO)((*R*)-BINAP)(PPh_3)] (**8**) in [D8]toluene at 20 °C.

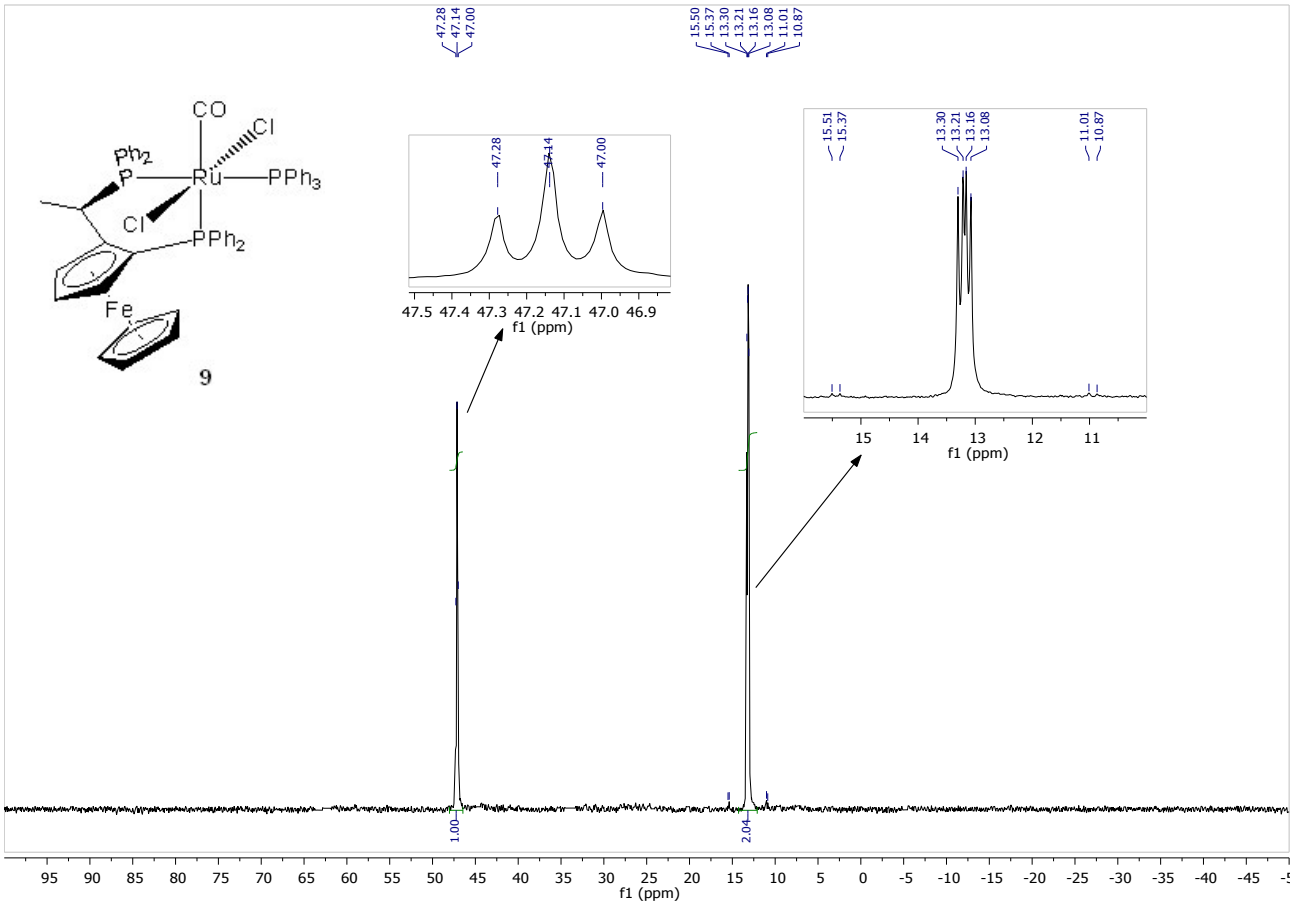

Figure S31. $^{31}P\{^{1}H\}$ NMR spectrum (162.0 MHz) of *trans*-[$RuCl_2$(CO)((*S*,*R*)-Josiphos)(PPh_3)] (**9**) in [D8]toluene at 20 °C.

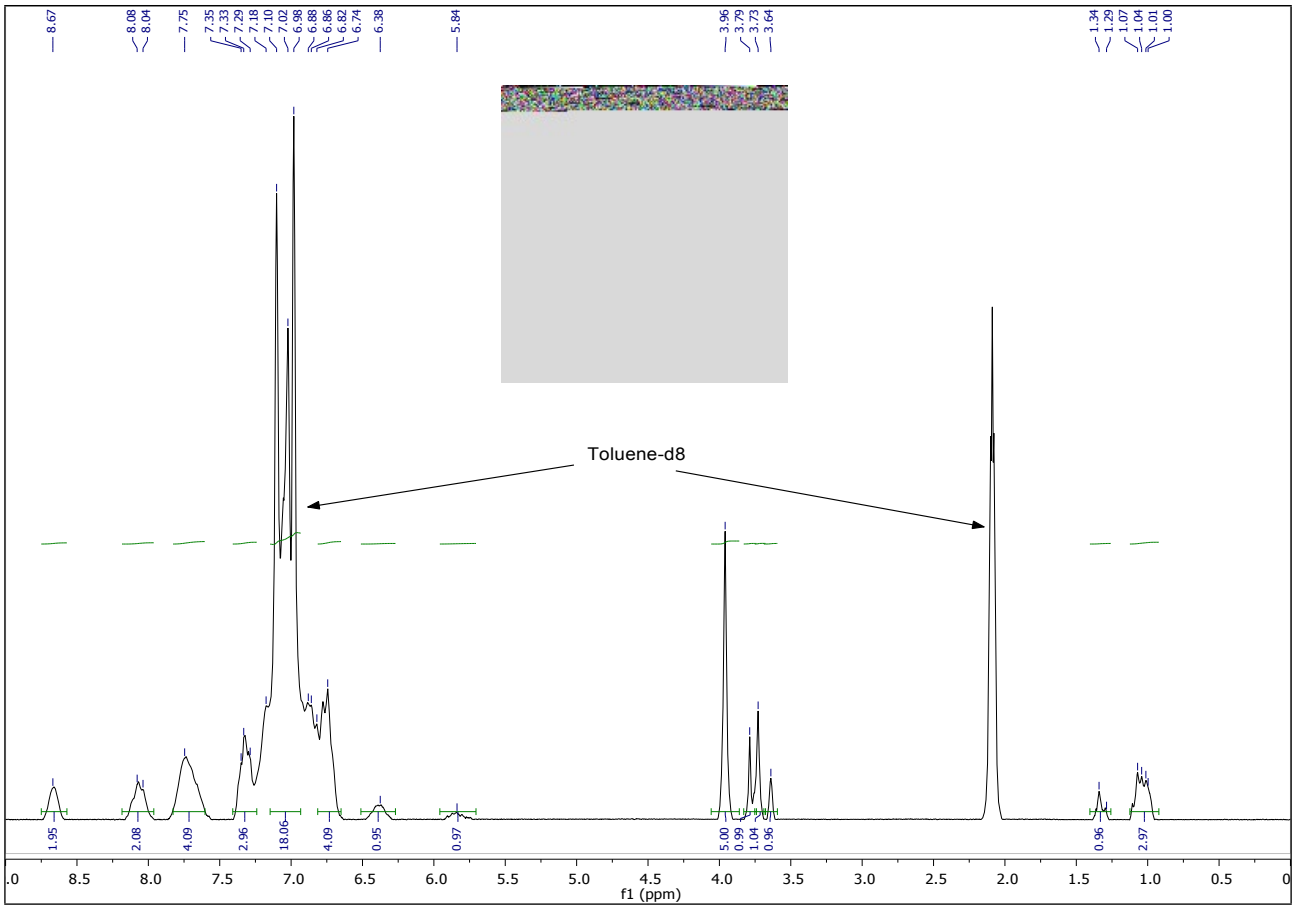

Figure S32. ^{1}H NMR spectrum (400.1 MHz) of *trans*-[$RuCl_2$(CO)((*S*,*R*)-Josiphos)(PPh_3)] (**9**) in [D8]toluene at 20 °C.

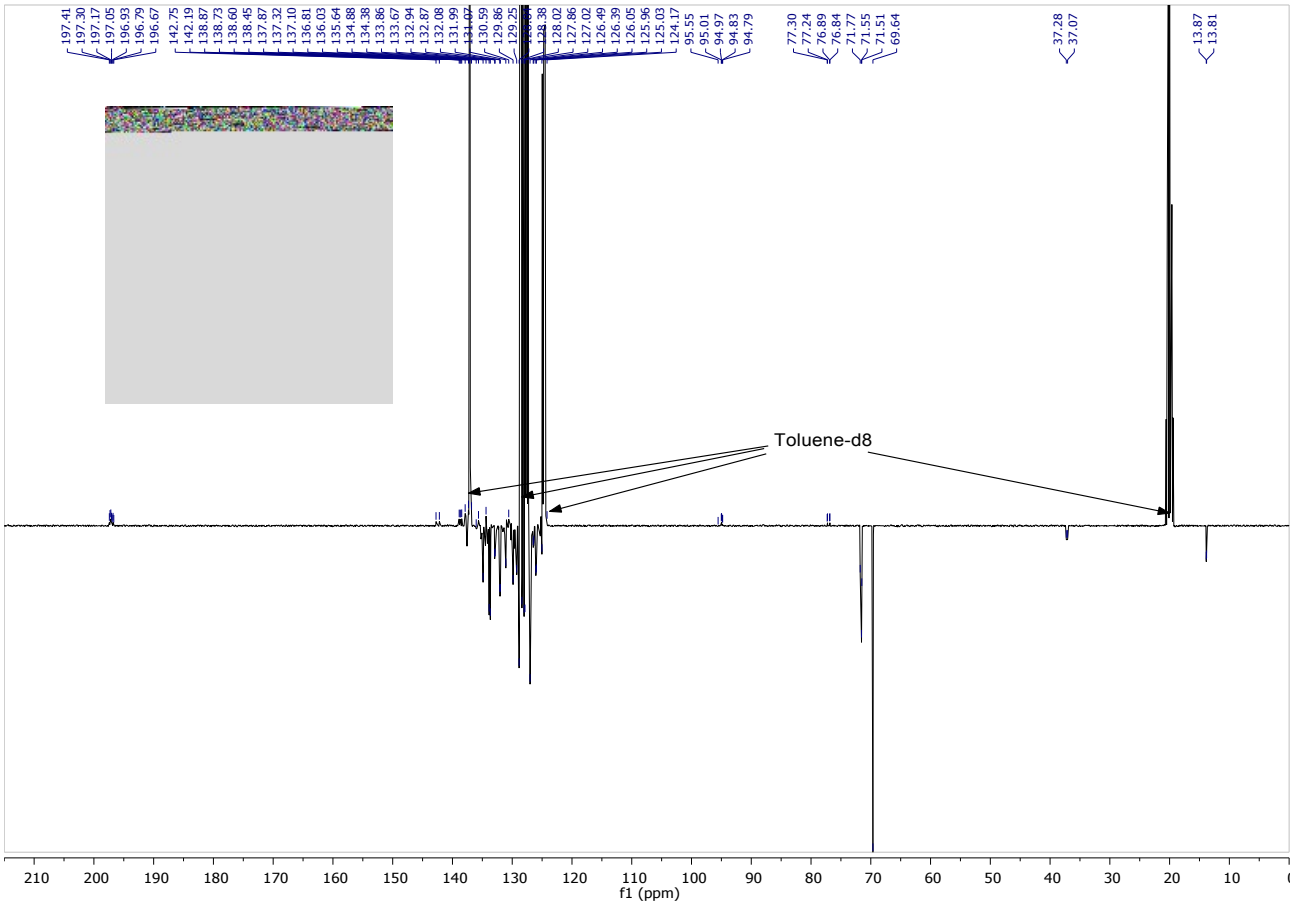

Figure S33. $^{13}C\{^{1}H\}$ DEPTQ NMR spectrum (100.6 MHz) of *trans*-[$RuCl_2$(CO)((*S*,*R*)-Josiphos)(PPh_3)] (**9**) in [D8]toluene at 20 °C.

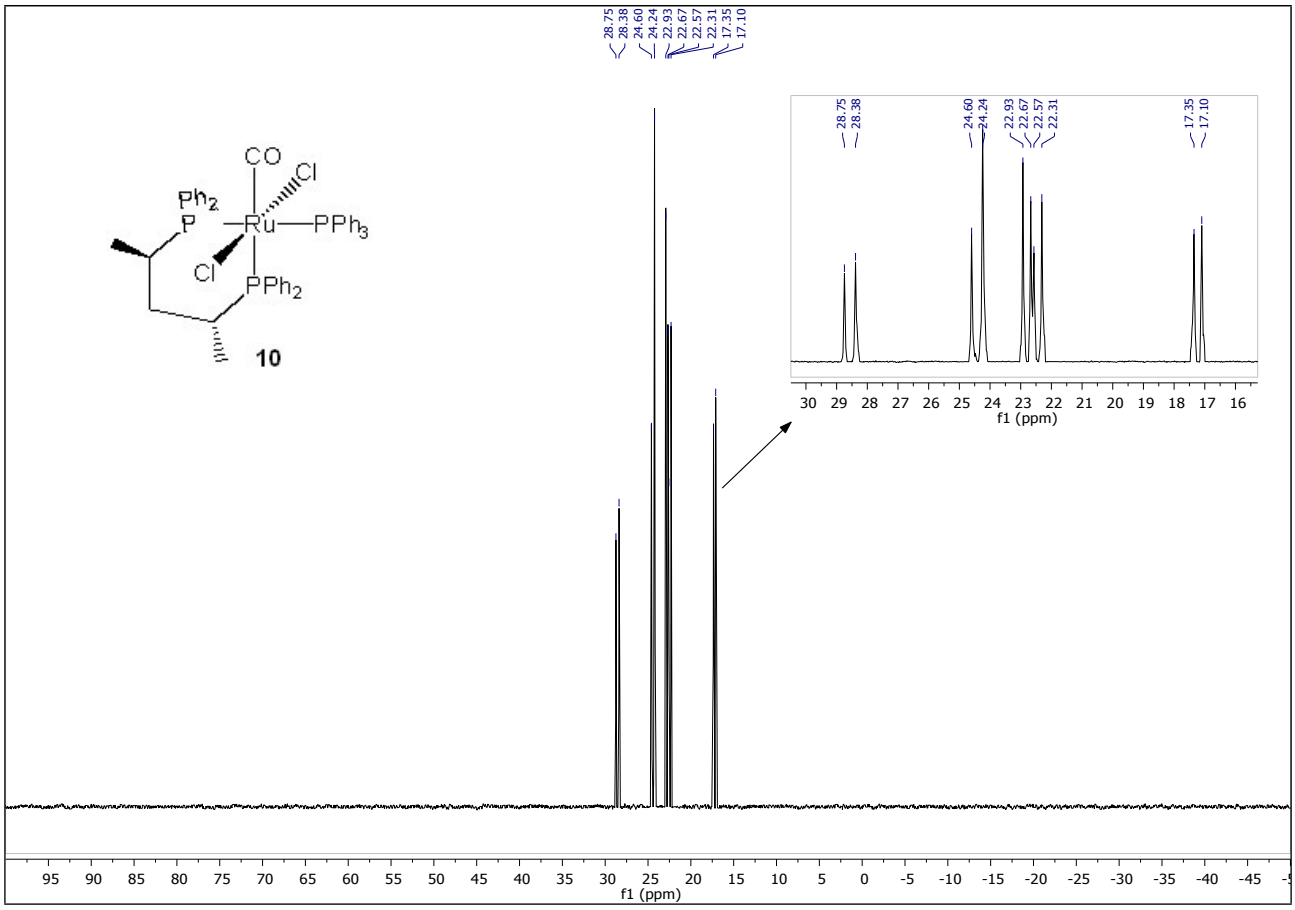

Figure S34. $^{31}P\{^{1}H\}$ NMR spectrum (81.0 MHz) of *trans*-[$RuCl_2$(CO)((*R*,*R*)-Skewphos)(PPh_3)] (**10**) in CD_2Cl_2 at 20 °C.

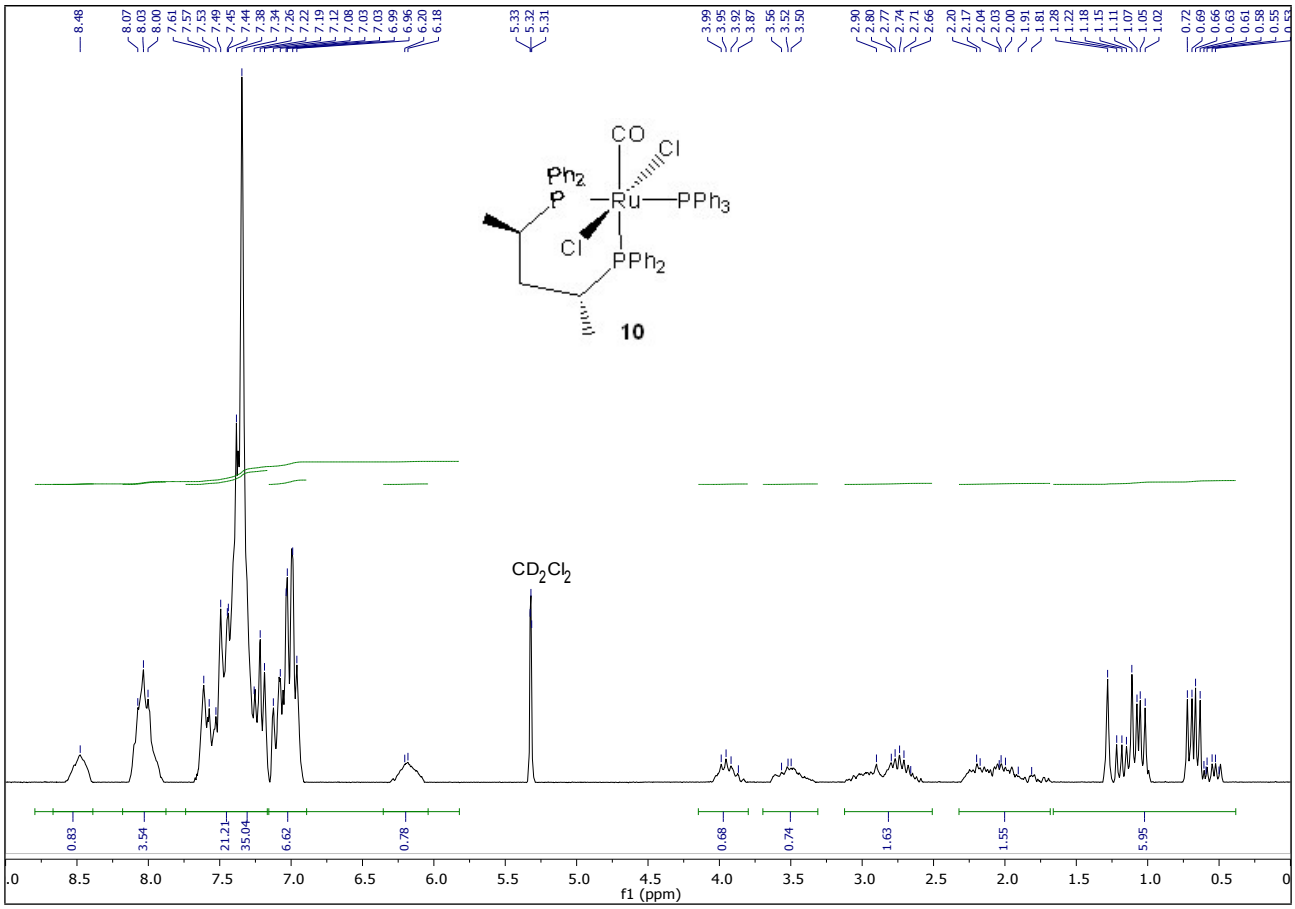

Figure S35. ^{1}H NMR spectrum (200.1 MHz) of *trans*-[$RuCl_2$(CO)((*R*,*R*)-Skewphos)(PPh_3)] (**10**) in CD_2Cl_2 at 20 °C.

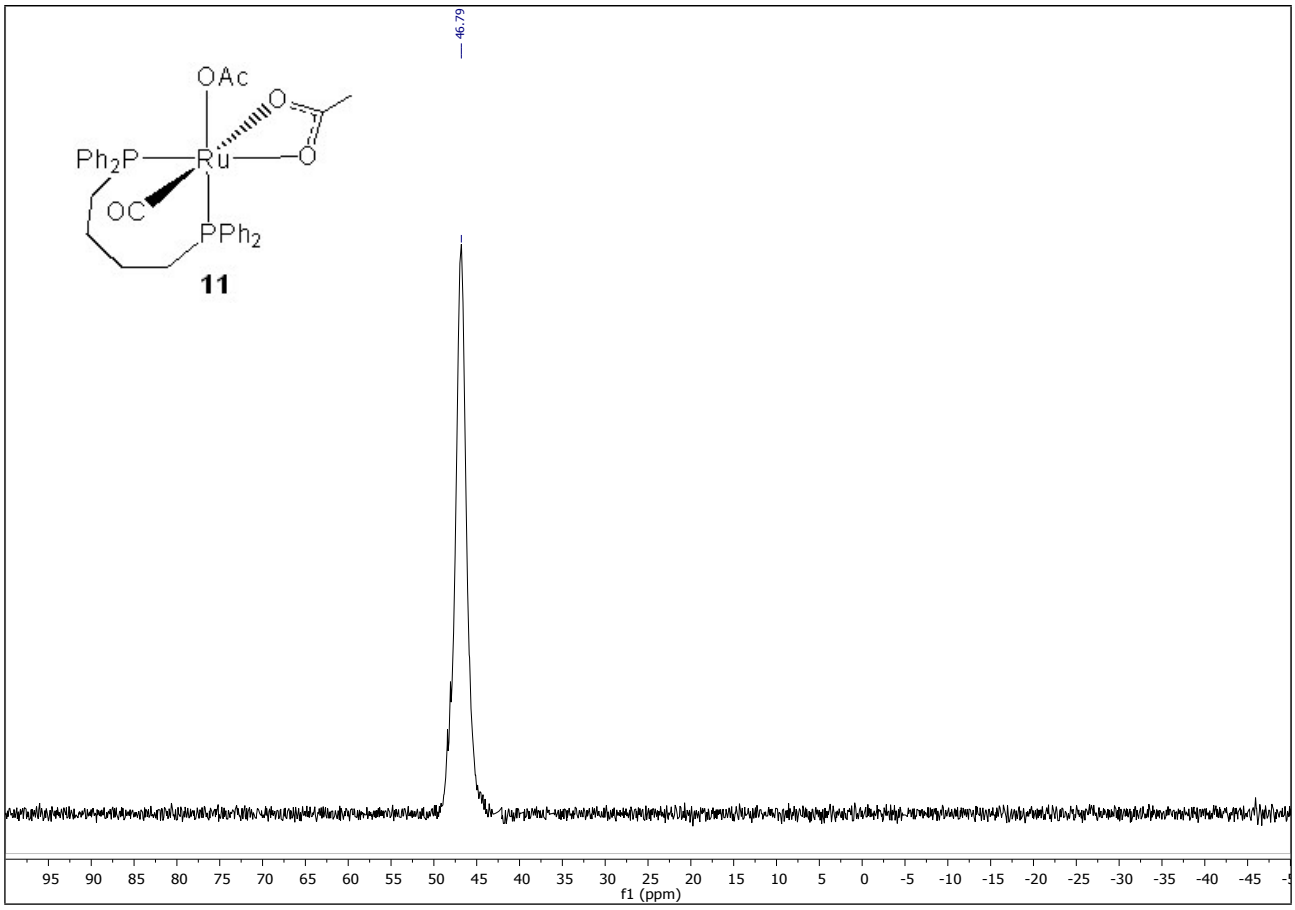

Figure S36. $^{31}P\{^{1}H\}$ NMR spectrum (81.0 MHz) of $[Ru(OAc)_2(CO)(dppb)]$ (**11**) in CD_2Cl_2 at 20 °C.

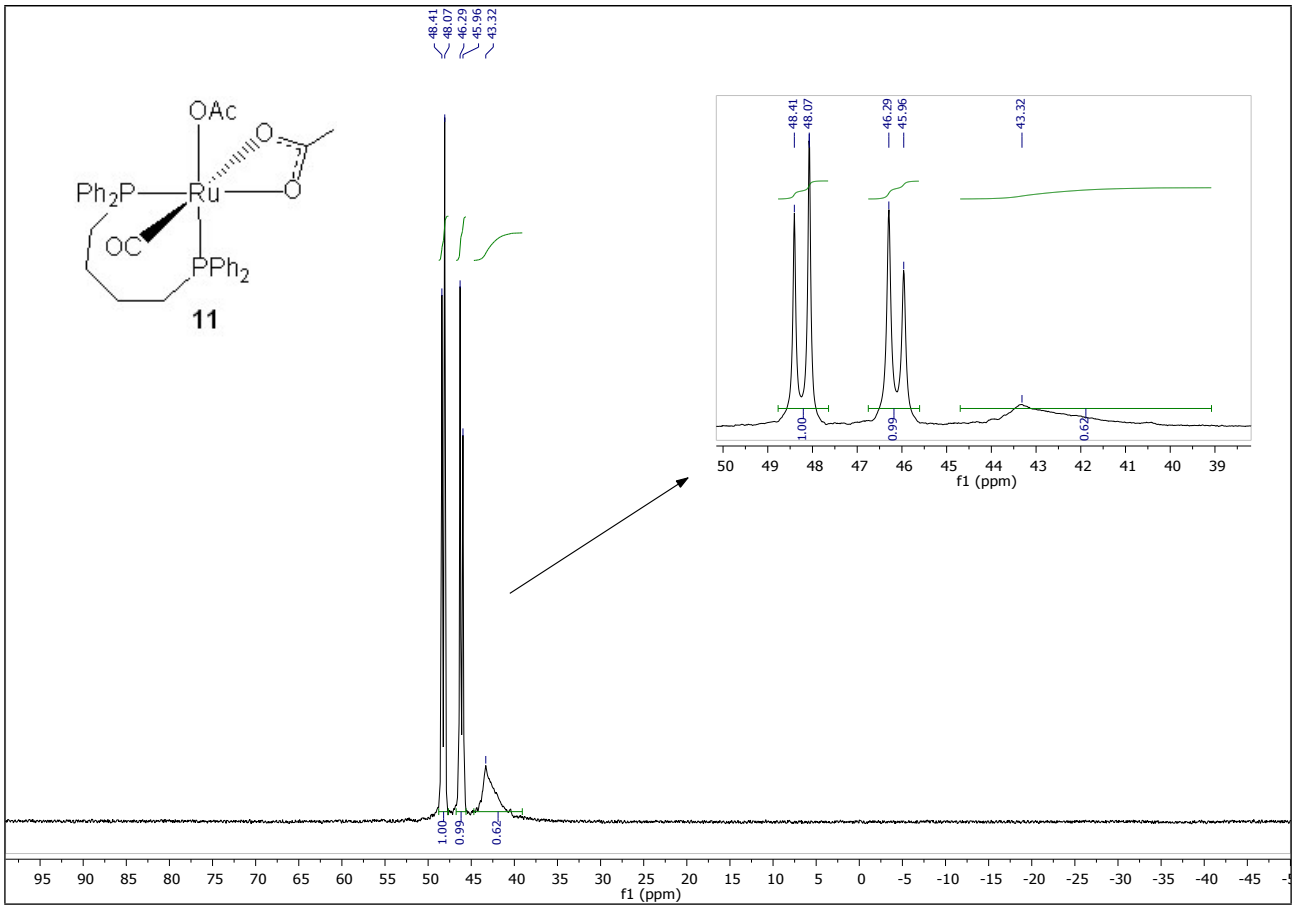

Figure S37. $^{31}P\{^{1}H\}$ NMR spectrum (81.0 MHz) of $[Ru(OAc)_2(CO)(dppb)]$ (**11**) in CD_2Cl_2 at - 60 °C.

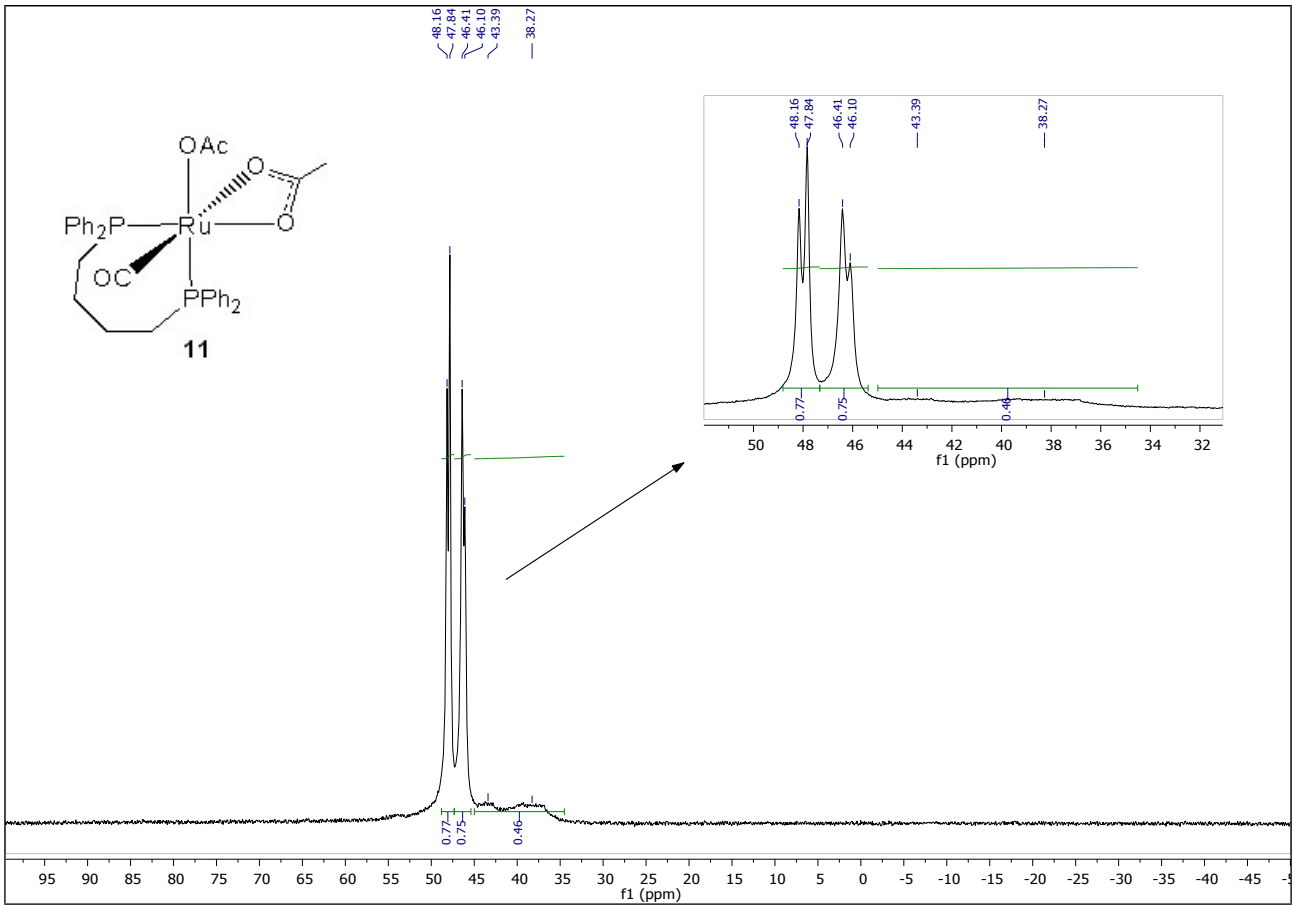

Figure S38. $^{31}P\{^{1}H\}$ NMR spectrum (81.0 MHz) of $[Ru(OAc)_2(CO)(dppb)]$ (**11**) in CD_2Cl_2 at - 80 °C.

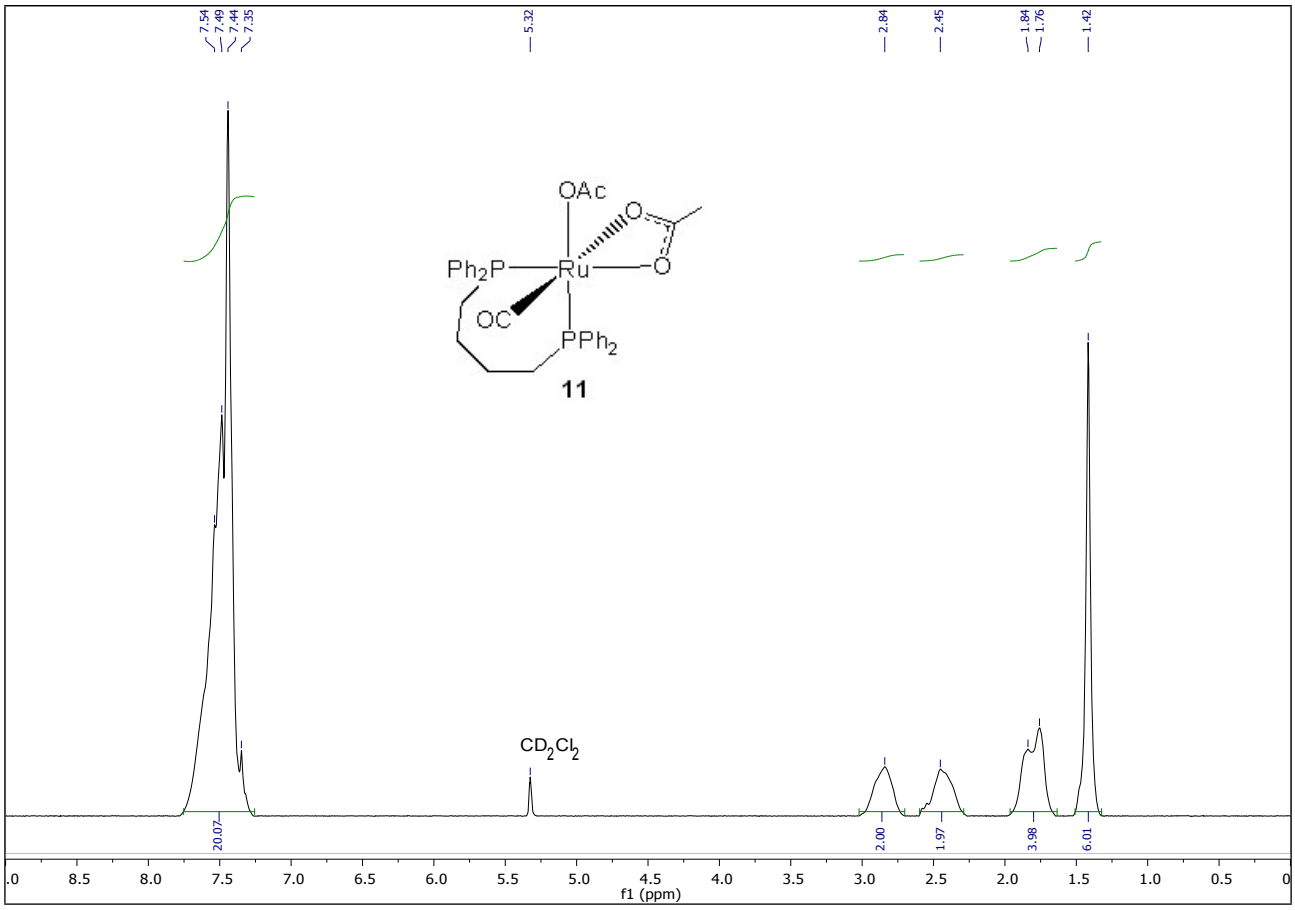

Figure S39. ^{1}H NMR spectrum (200.1 MHz) of [Ru(OAc)$_2$(CO)(dppb)] (**11**) in CD_2Cl_2 at 20 °C.

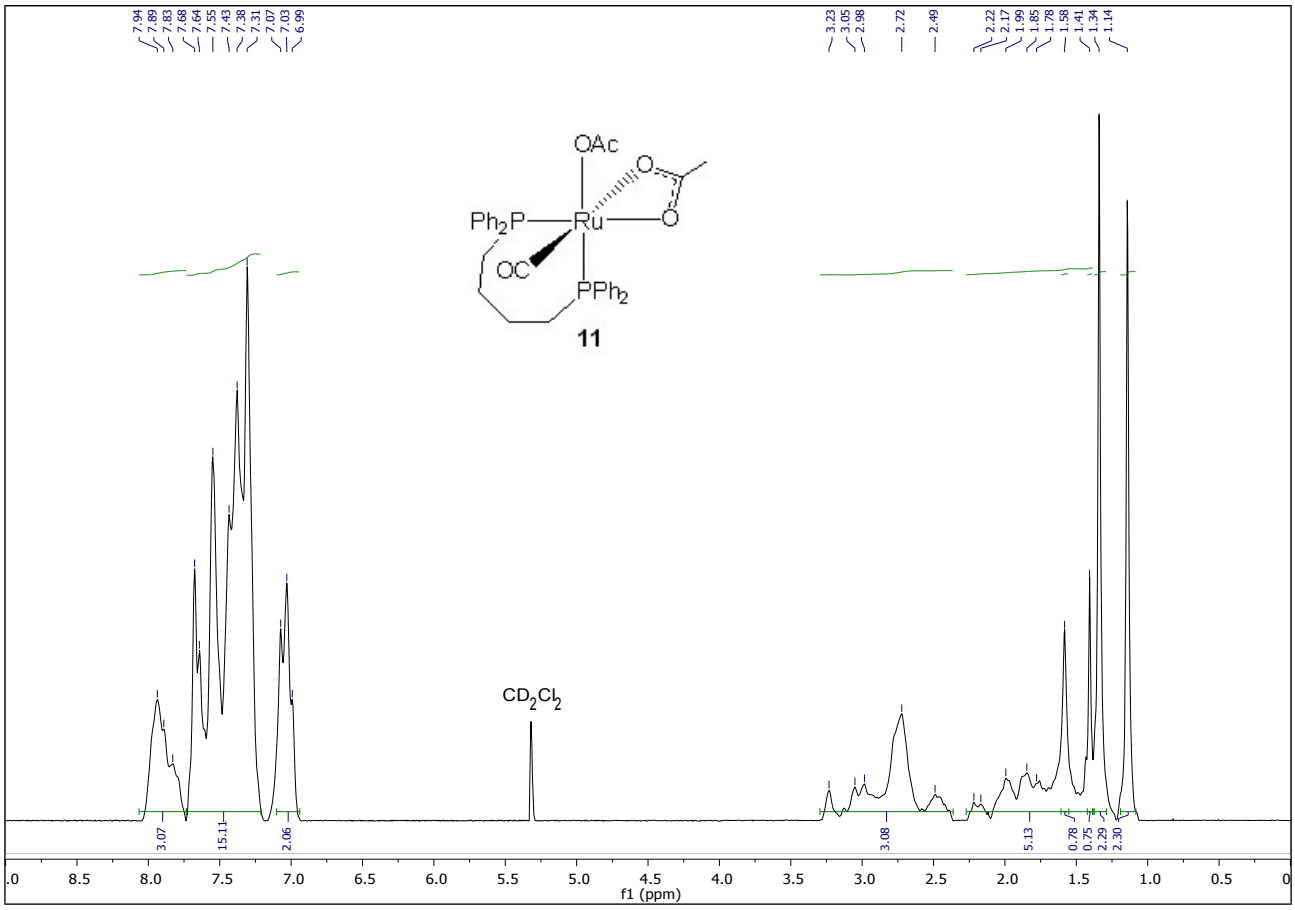

Figure S40. ^{1}H NMR spectrum (200.1 MHz) of [Ru(OAc)$_2$(CO)(dppb)] (**11**) in CD_2Cl_2 at - 80 °C.

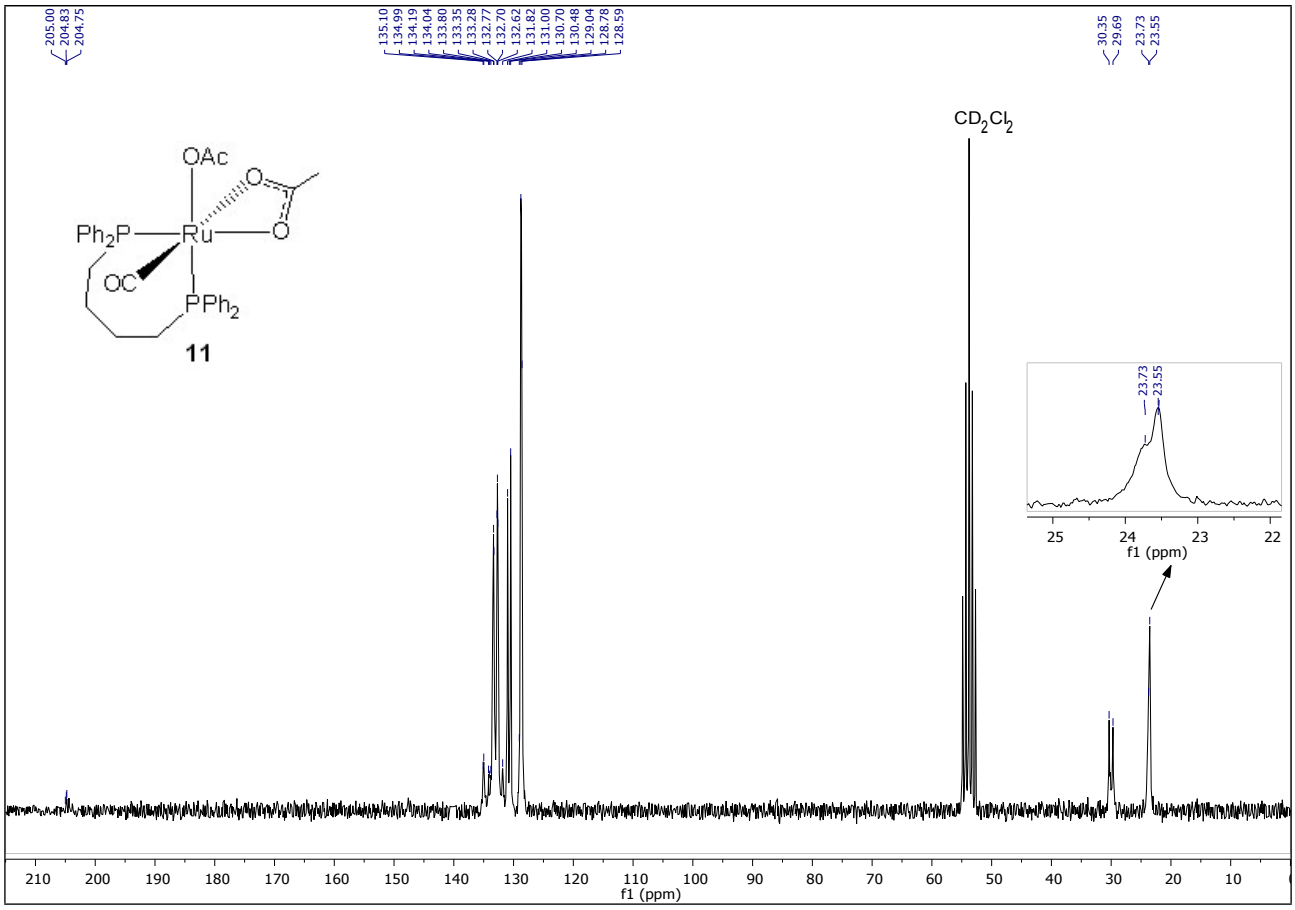

Figure S41. $^{13}C\{^{1}H\}$ NMR spectrum (50.3 MHz) of $[Ru(OAc)_2(CO)(dppb)]$ (**11**) in CD_2Cl_2 at 20 °C.

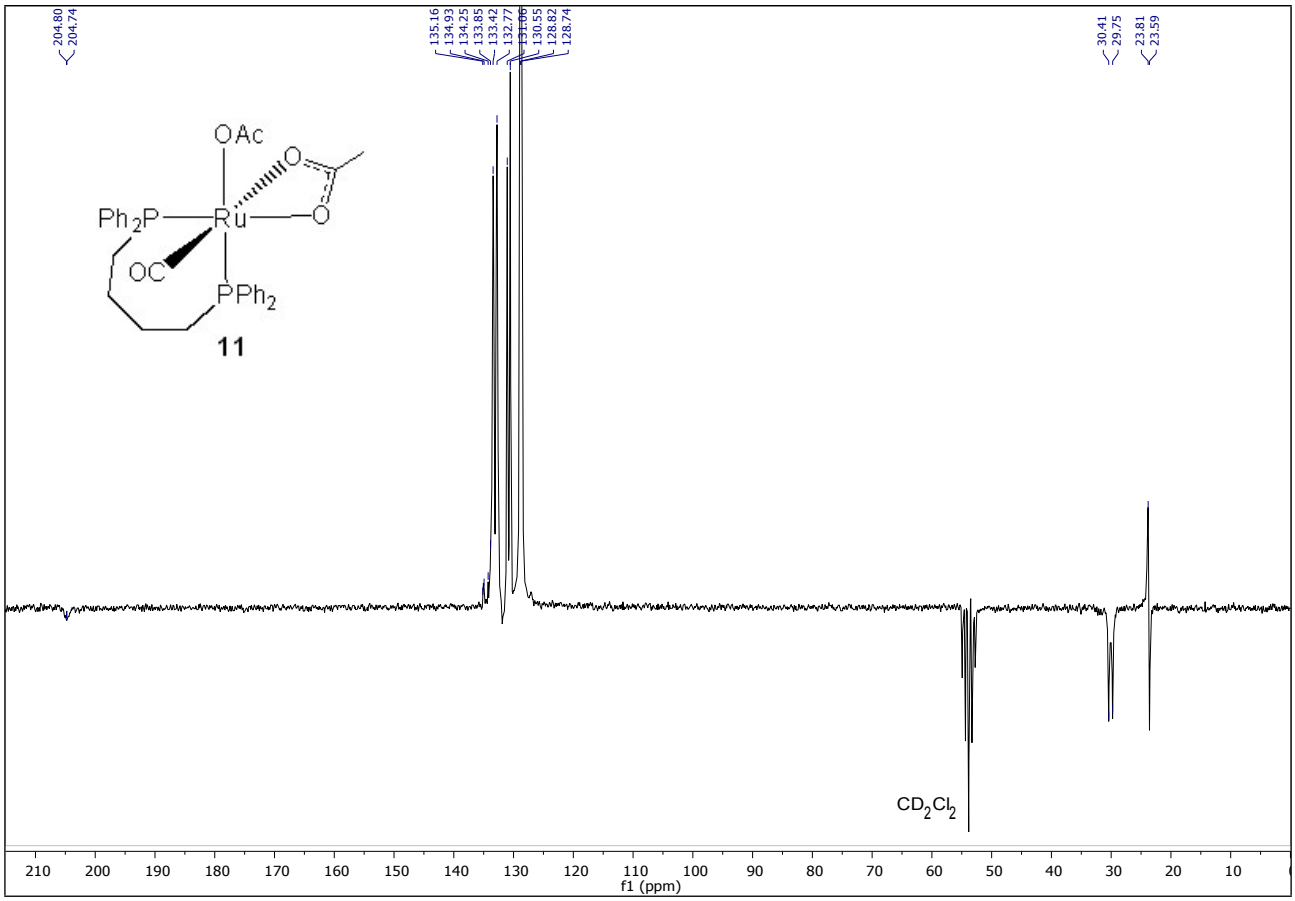

Figure S42. $^{13}C\{^{1}H\}$ PENDANT NMR spectrum (50.3 MHz) of $[Ru(OAc)_2(CO)(dppb)]$ (**11**) in CD_2Cl_2 at 20 °C.

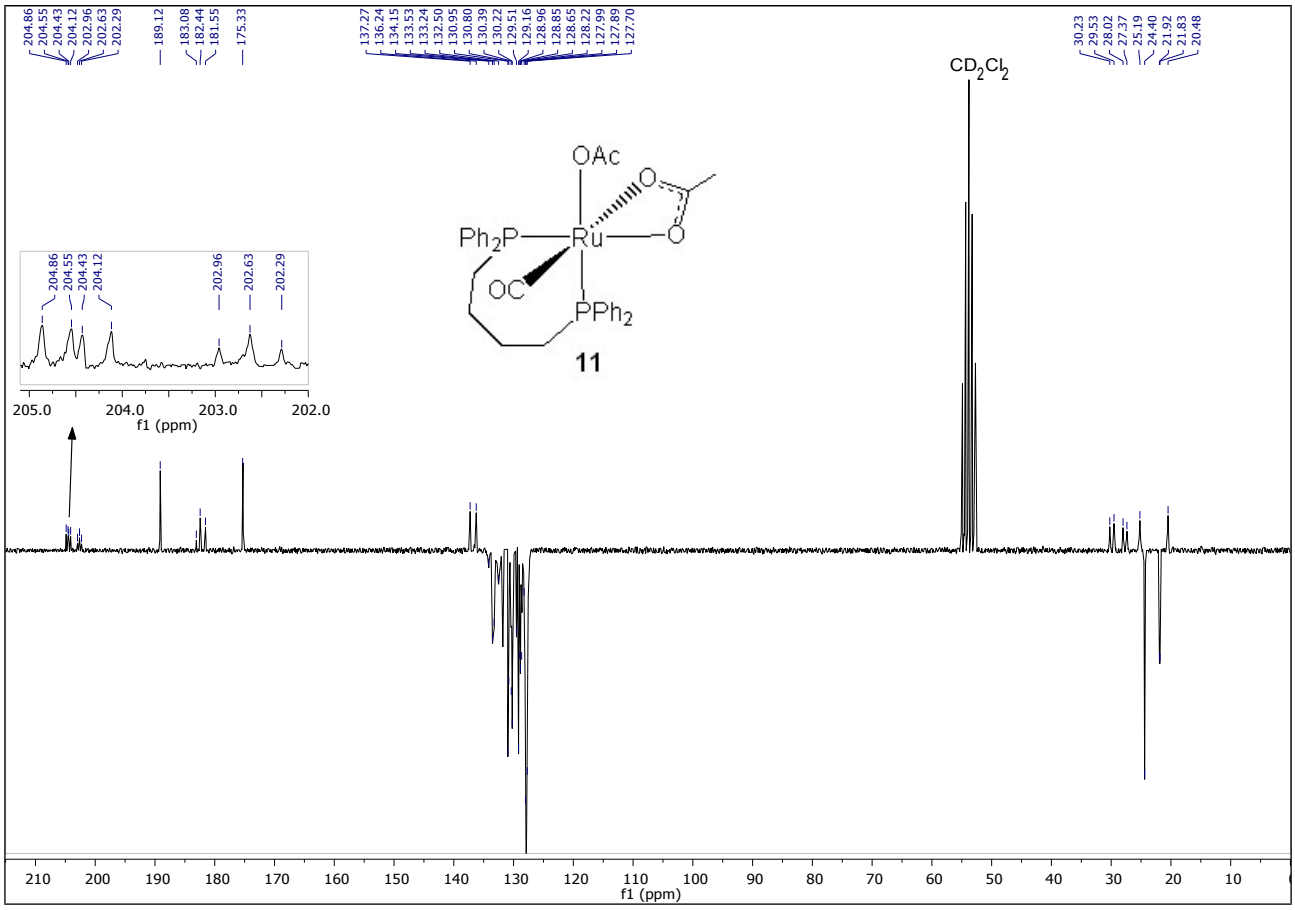

Figure S43. $^{13}C\{^{1}H\}$ PENDANT NMR spectrum (50.3 MHz) of $[Ru(OAc)_2(CO)(dppb)]$ (**11**) in CD_2Cl_2 at - 80 °C.

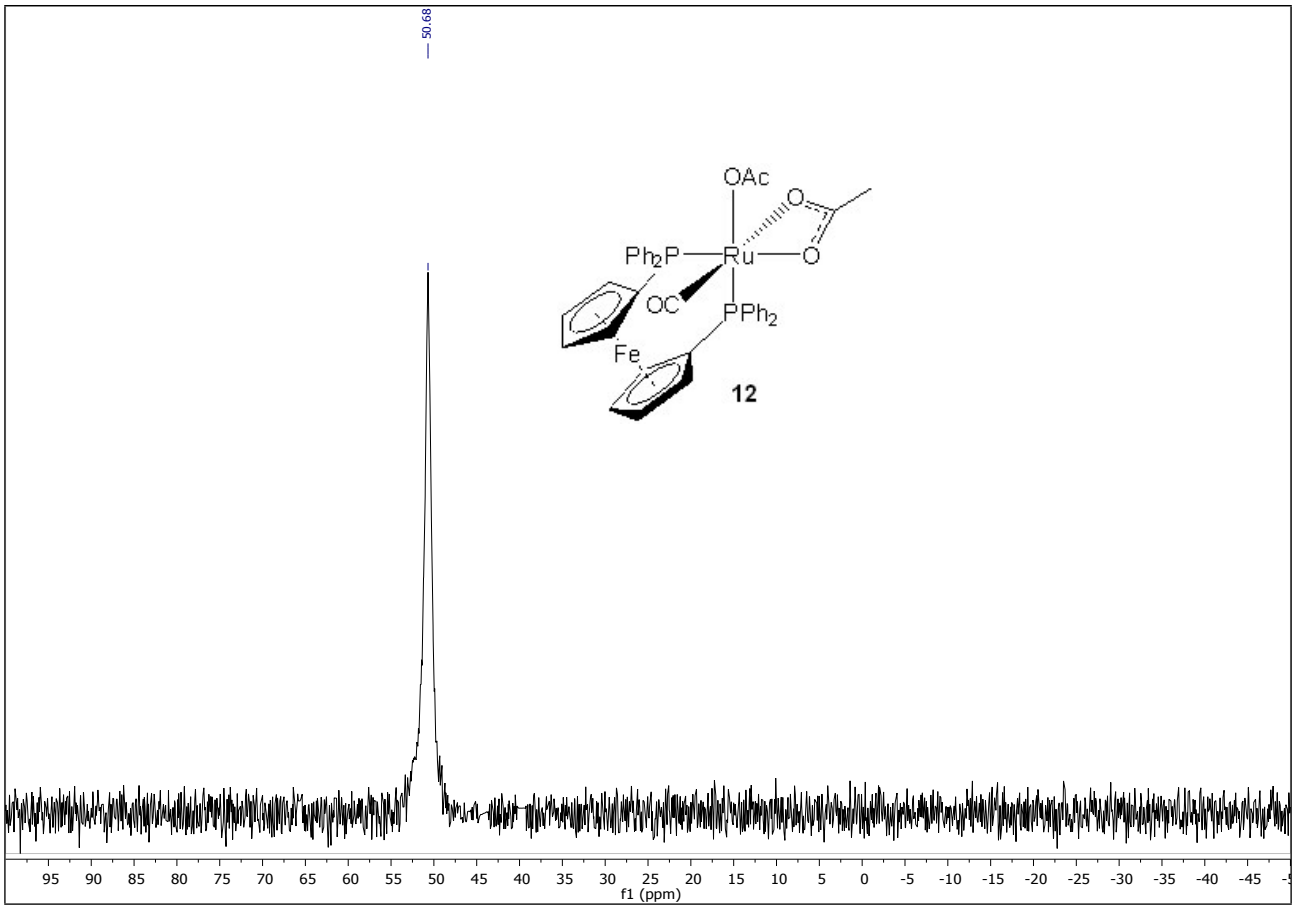

Figure S44. $^{31}P\{^{1}H\}$ NMR spectrum (81.0 MHz) of $[Ru(OAc)_2(CO)(dppf)]$ (**12**) in CD_2Cl_2 at 20 °C.

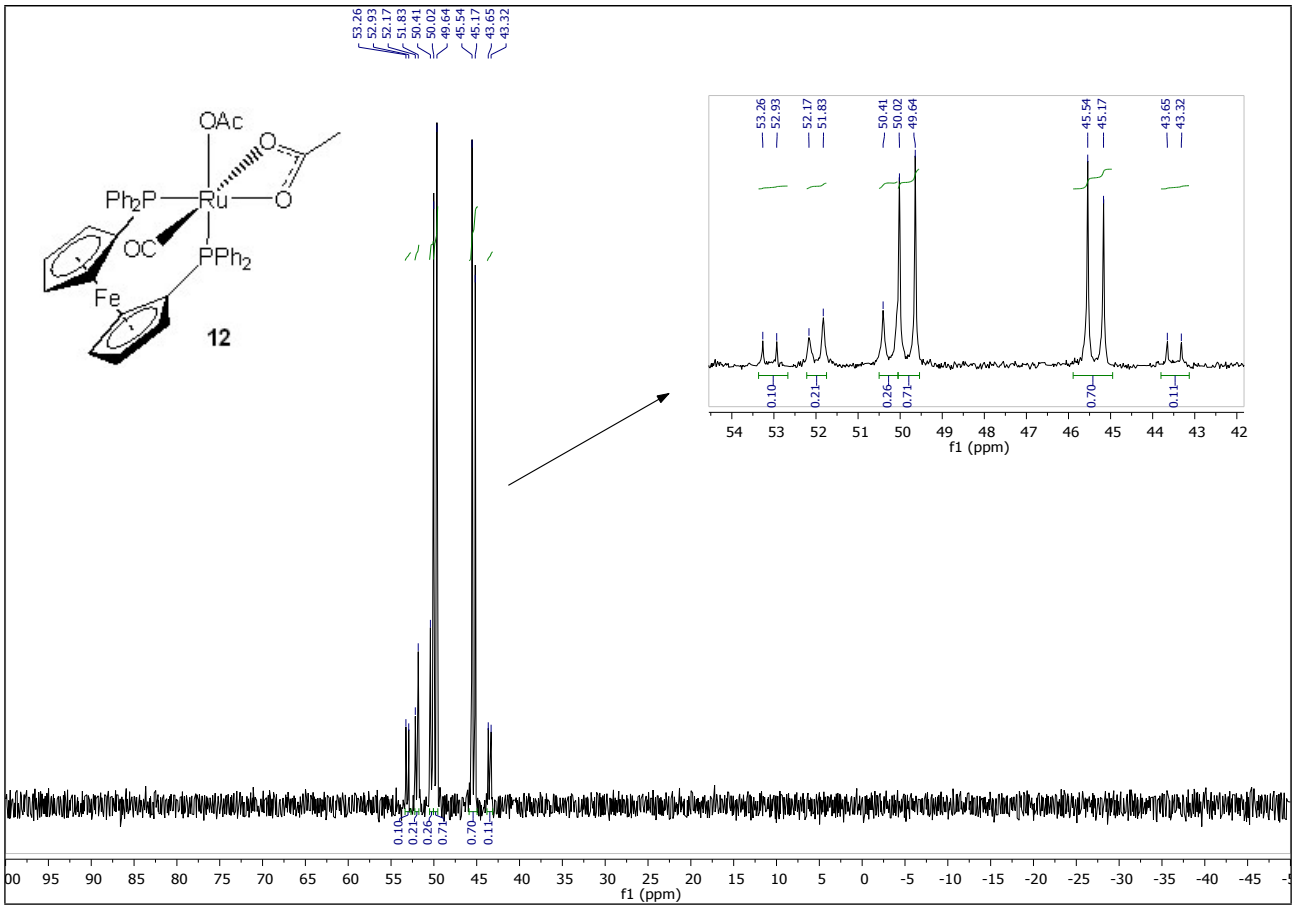

Figure S45. $^{31}P\{^{1}H\}$ NMR spectrum (81.0 MHz) of $[Ru(OAc)_2(CO)(dppf)]$ (**12**) in CD_2Cl_2 at - 70 °C.

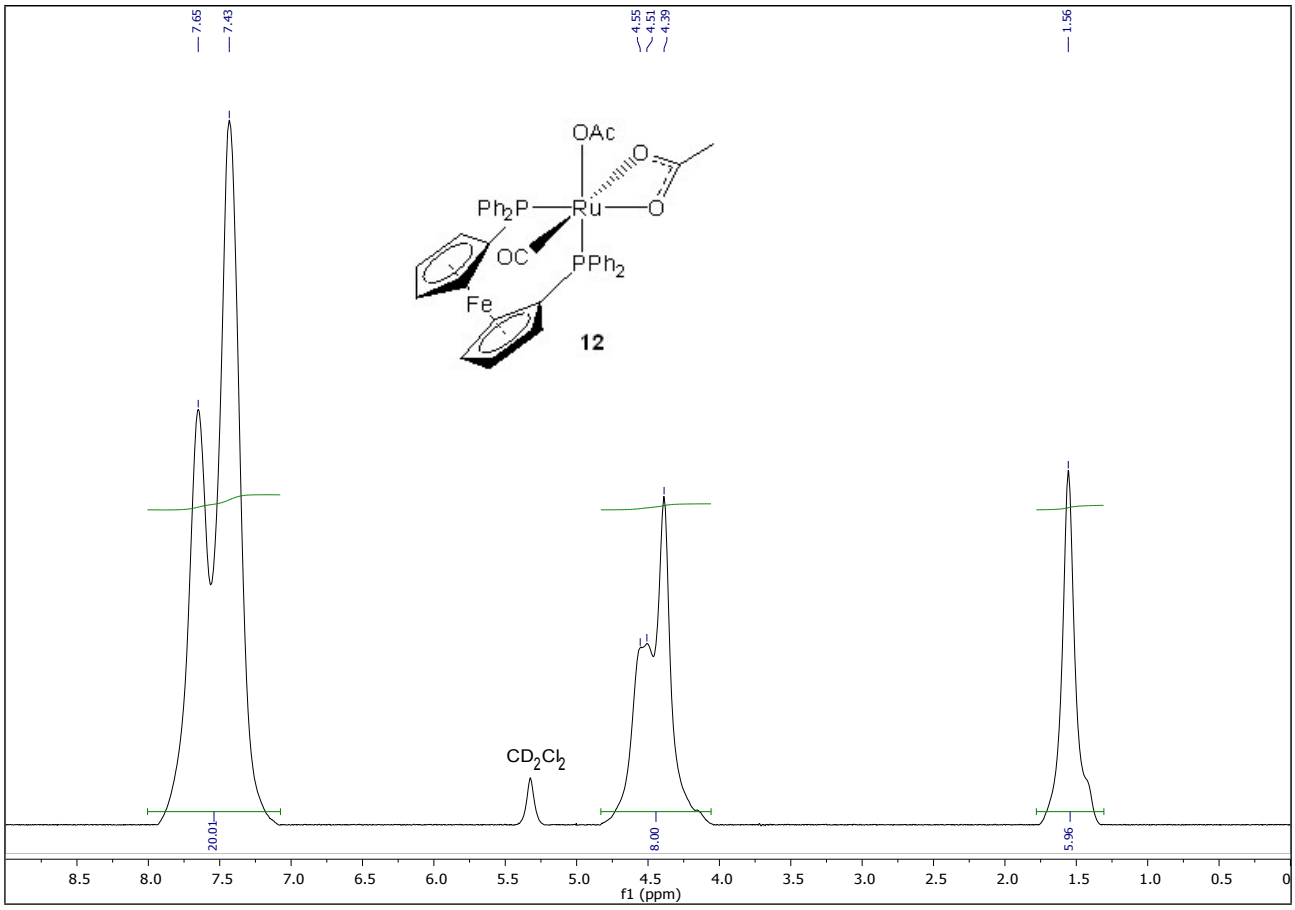

Figure S46. ^{1}H NMR spectrum (200.1 MHz) of [Ru(OAc)$_2$(CO)(dppf)] (**12**) in CD_2Cl_2 at 20 °C.

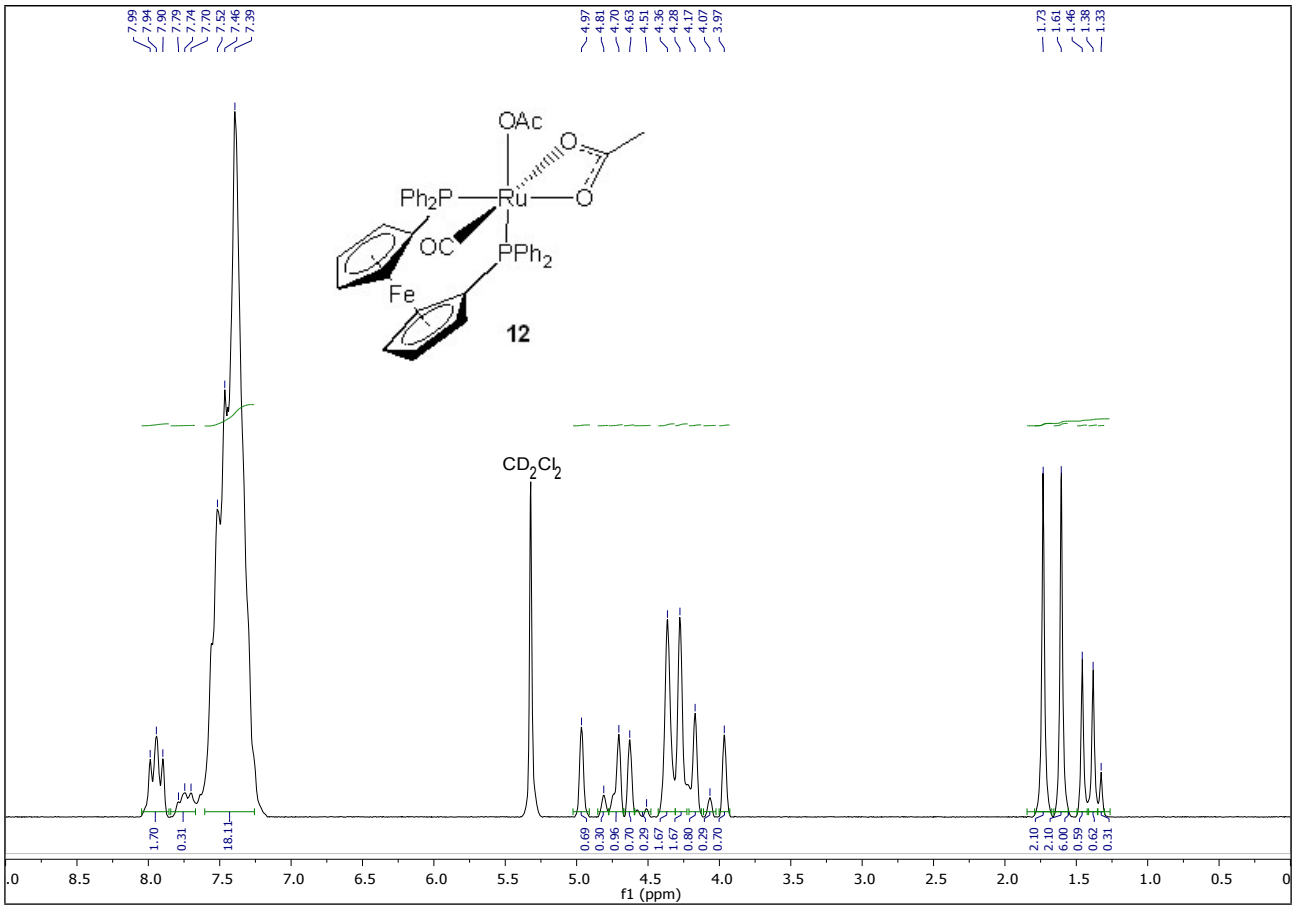

Figure S47. ^{1}H NMR spectrum (200.1 MHz) of [Ru(OAc)$_2$(CO)(dppf)] (**12**) in CD_2Cl_2 at - 70 °C.

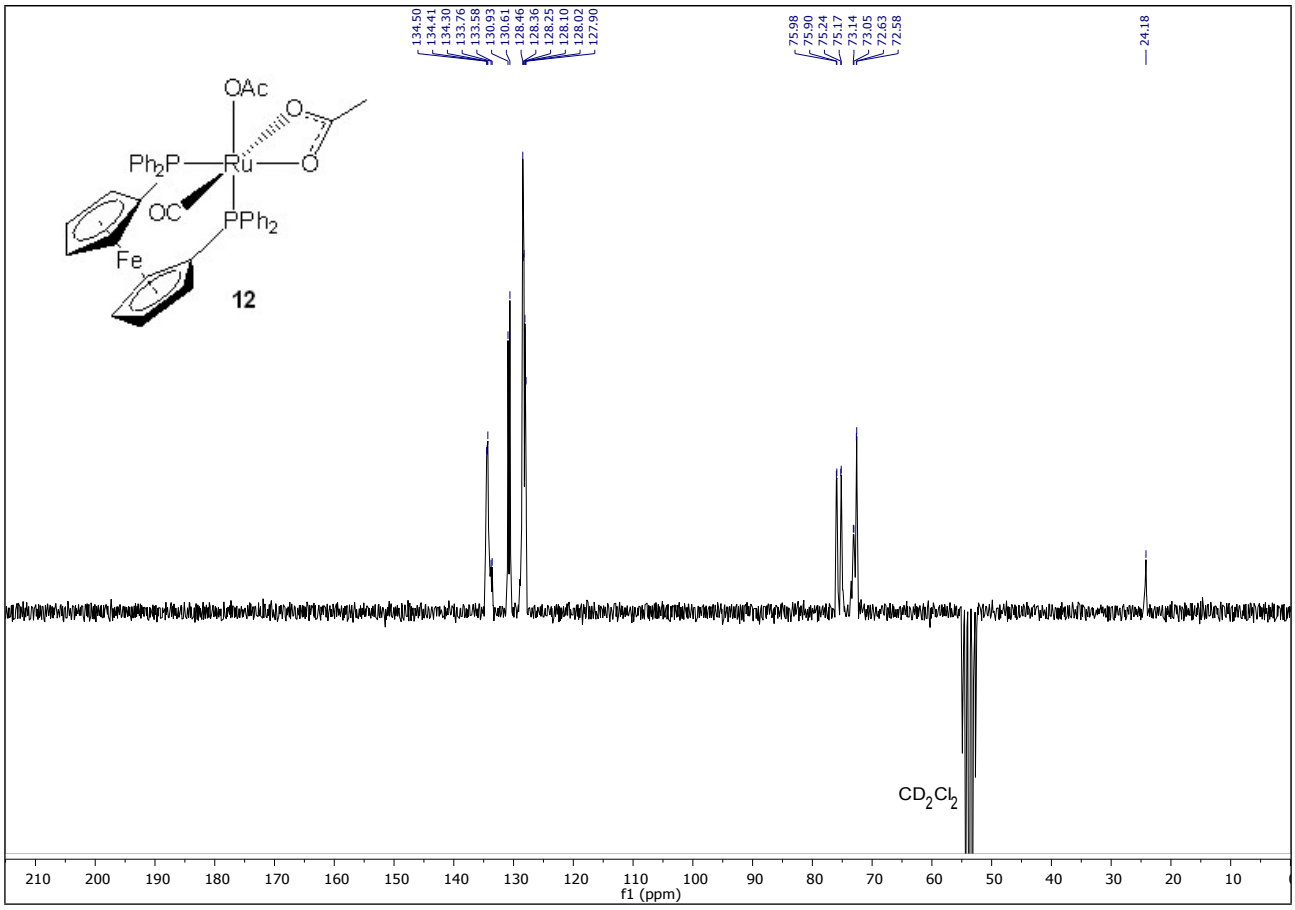

Figure S48. $^{13}C\{^{1}H\}$ PENDANT NMR spectrum (50.3 MHz) of $[Ru(OAc)_2(CO)(dppf)]$ (**12**) in CD_2Cl_2 at 20 °C.

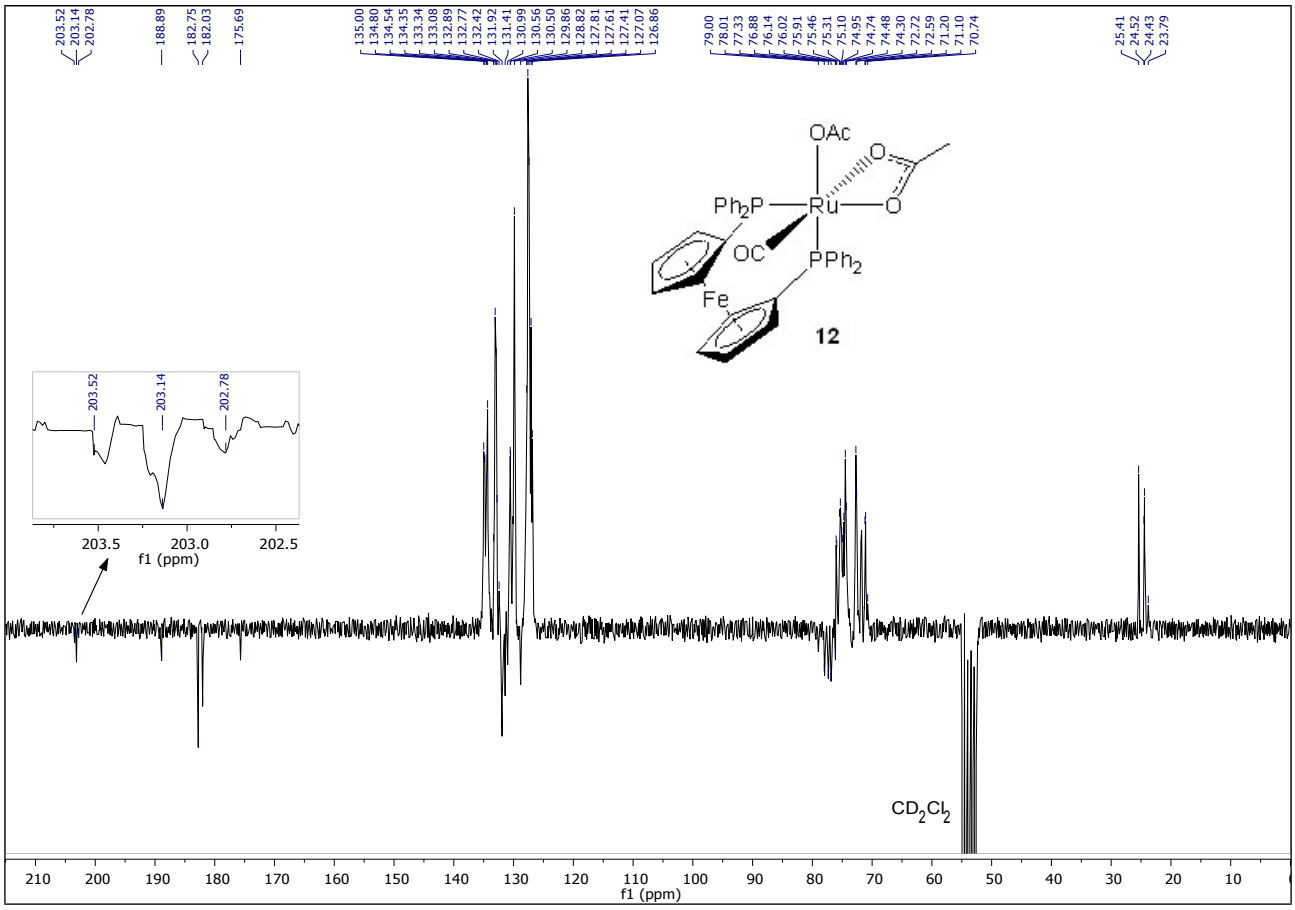

Figure S49. $^{13}C\{^{1}H\}$ PENDANT NMR spectrum (50.3 MHz) of $[Ru(OAc)_2(CO)(dppf)]$ (**12**) in CD_2Cl_2 at - 70 °C.

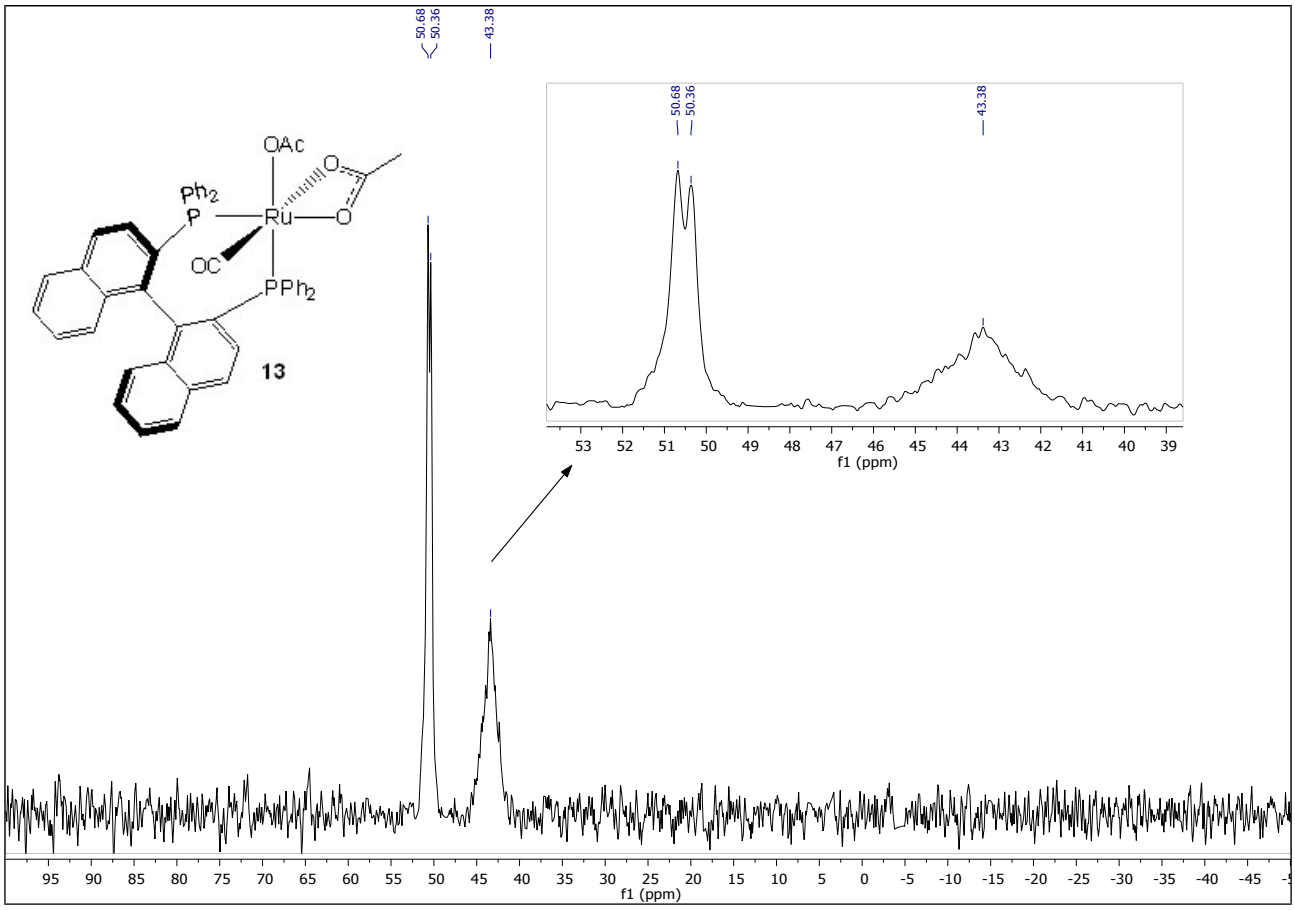

Figure S50. $^{31}P\{^{1}H\}$ NMR spectrum (81.0 MHz) of $[Ru(OAc)_2(CO)((R)\text{-BINAP})]$ (**13**) in CD_2Cl_2 at 20 °C.

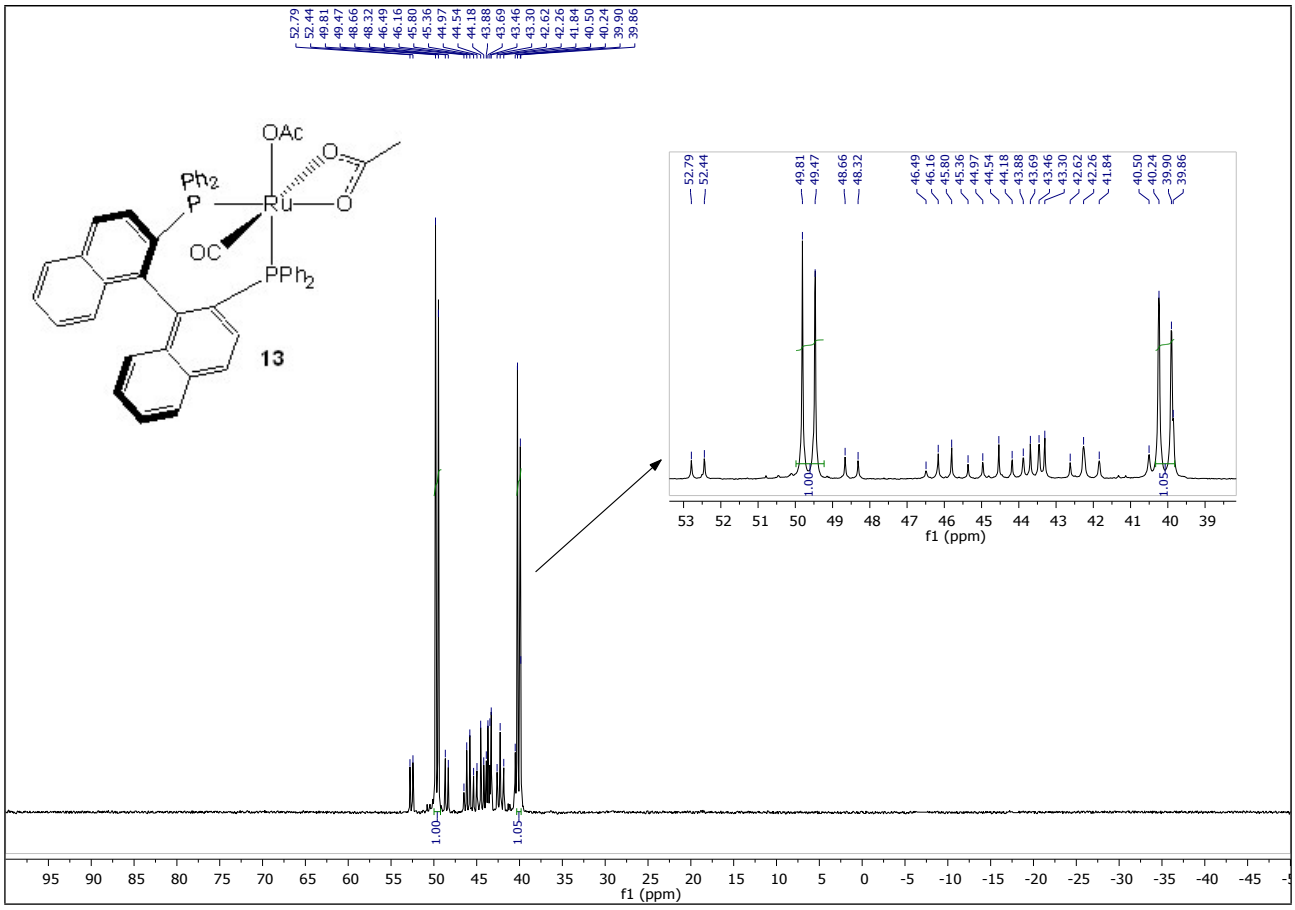

Figure S51. $^{31}P\{^{1}H\}$ NMR spectrum (81.0 MHz) of $[Ru(OAc)_2(CO)((R)\text{-BINAP})]$ (**13**) in CD_2Cl_2 at - 60 °C.

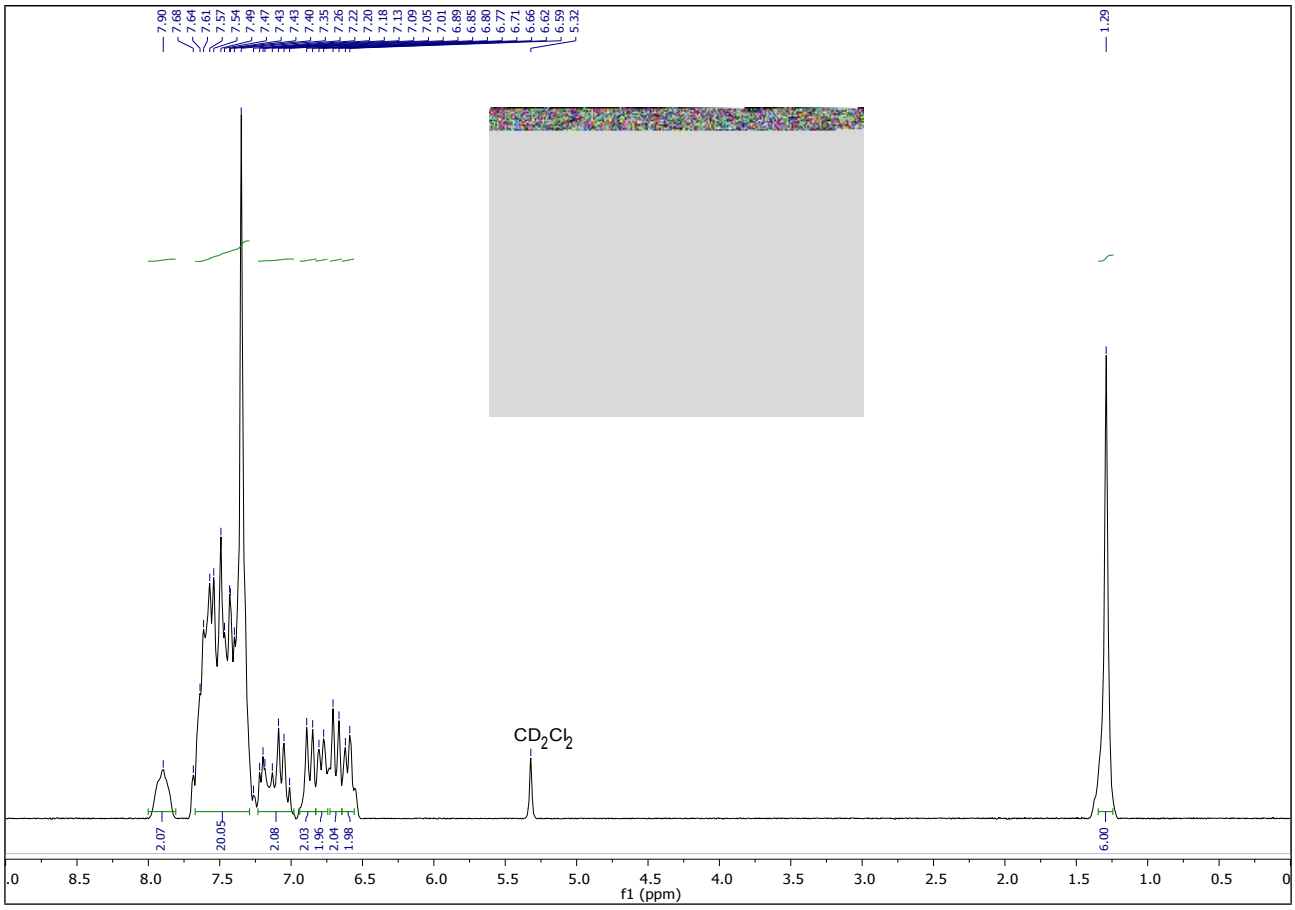

Figure S52. ^{1}H NMR spectrum (200.1 MHz) of [Ru(OAc)$_2$(CO)((*R*)-BINAP)] (**13**) in CD_2Cl_2 at 20 °C.

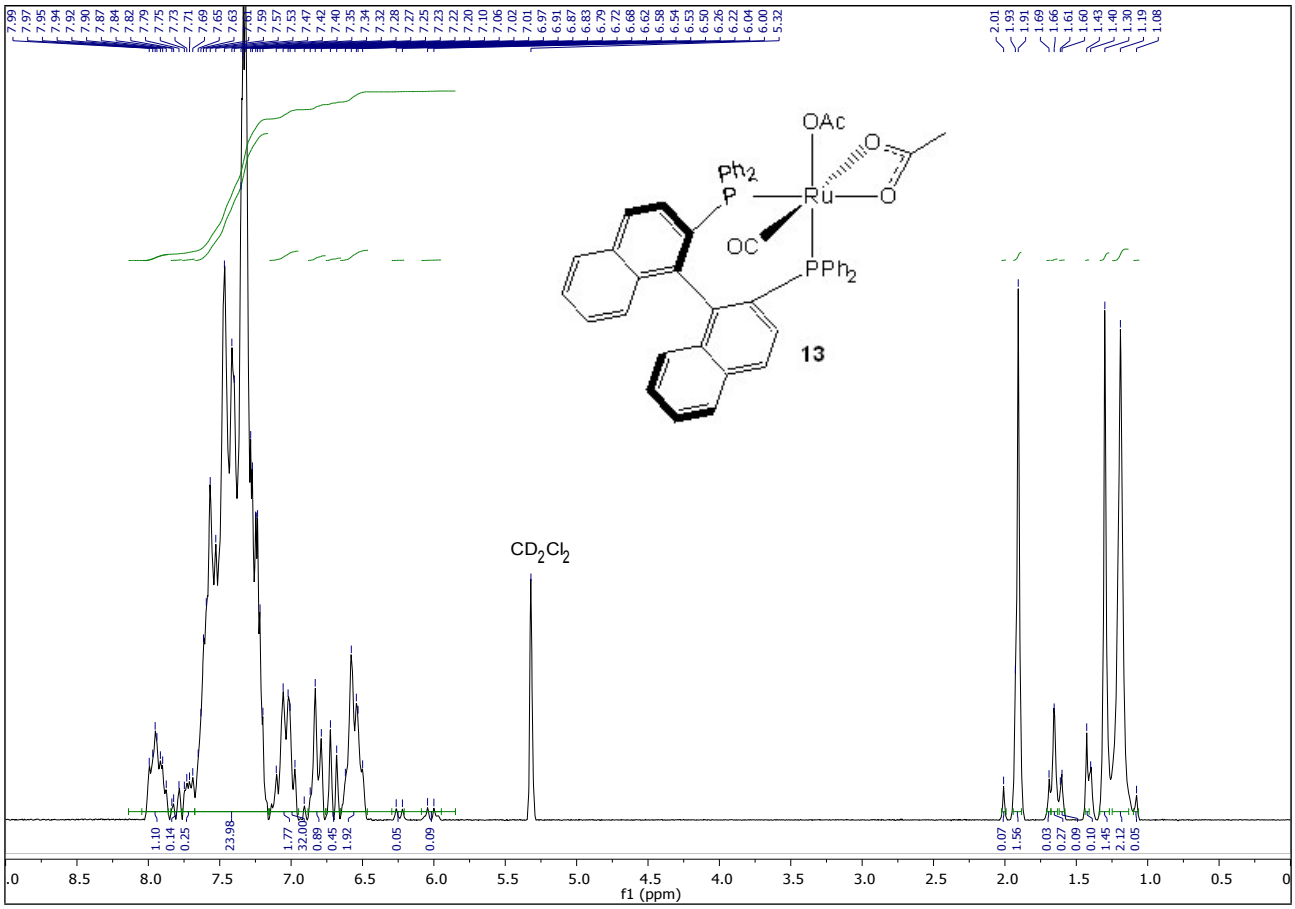

Figure S53. ^{1}H NMR spectrum (200.1 MHz) of [Ru(OAc)$_2$(CO)((*R*)-BINAP)] (**13**) in CD_2Cl_2 at -60 °C.

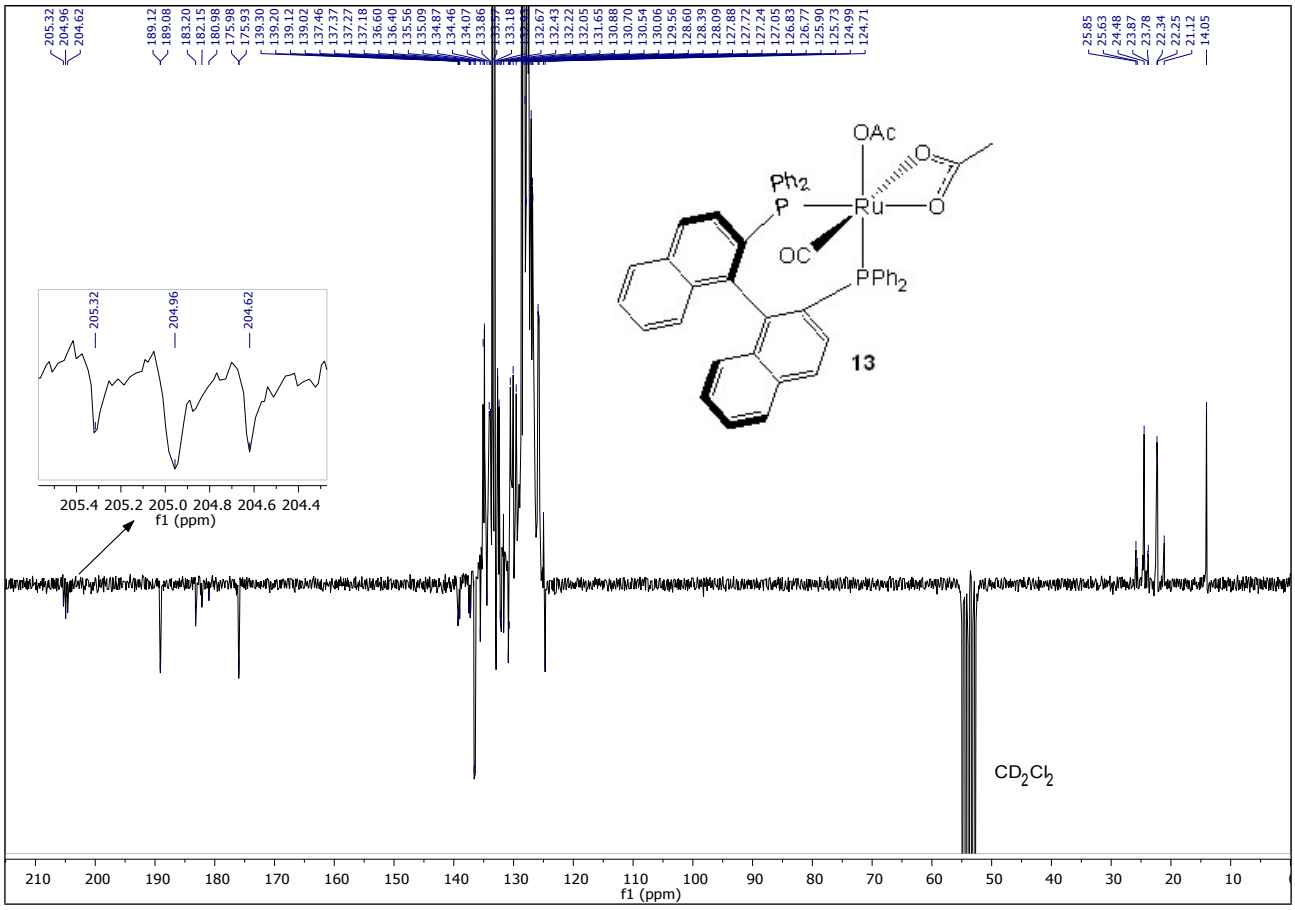

Figure S54. $^{13}C\{^{1}H\}$ PENDANT NMR spectrum (50.3 MHz) of $[Ru(OAc)_2(CO)((R)\text{-BINAP})]$ (**13**) in CD_2Cl_2 at - 60 °C.

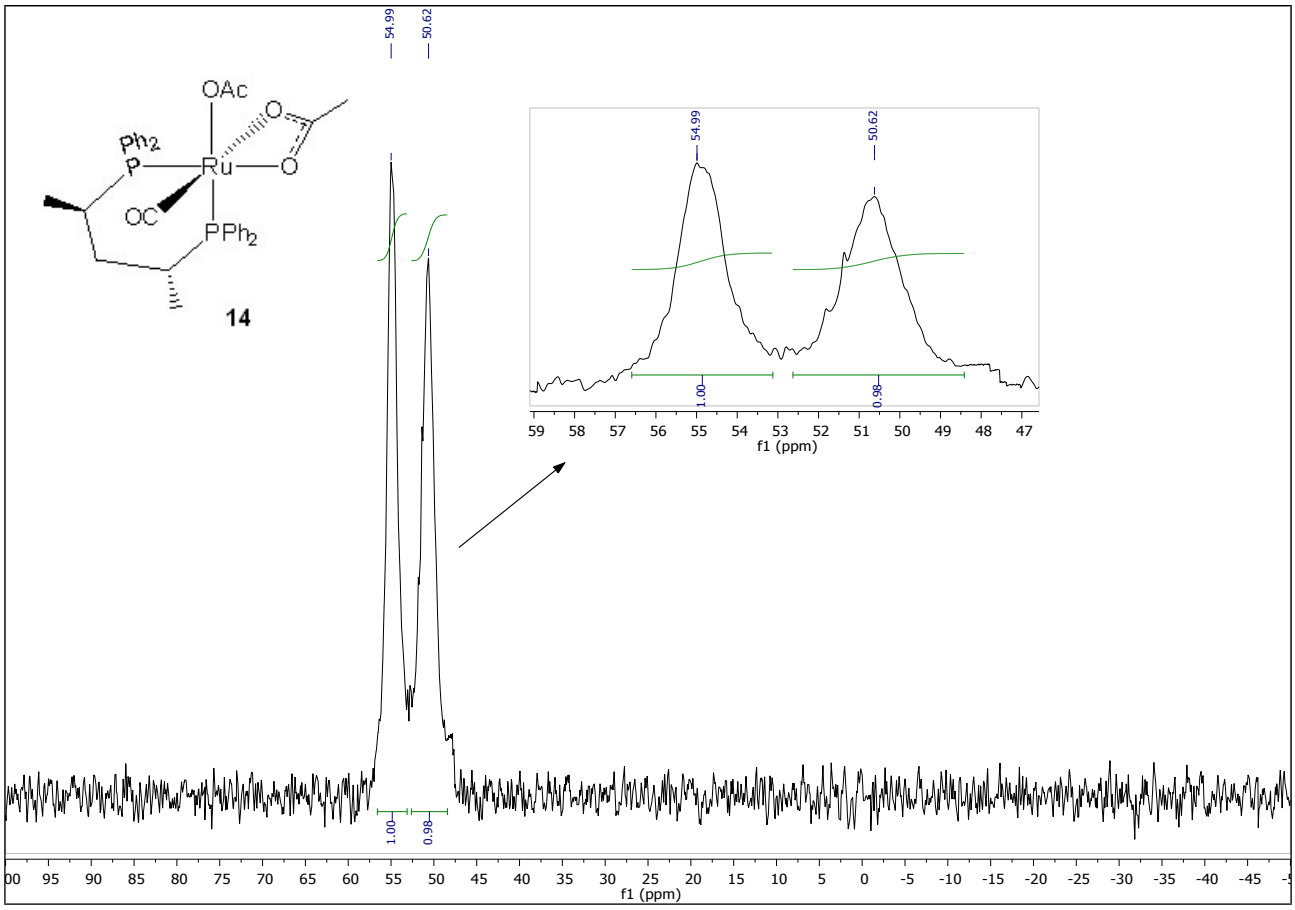

Figure S55. $^{31}P\{^{1}H\}$ NMR spectrum (81.0 MHz) of $[Ru(OAc)_2(CO)((R,R)\text{-Skewphos})]$ (**14**) in CD_2Cl_2 at 20 °C.

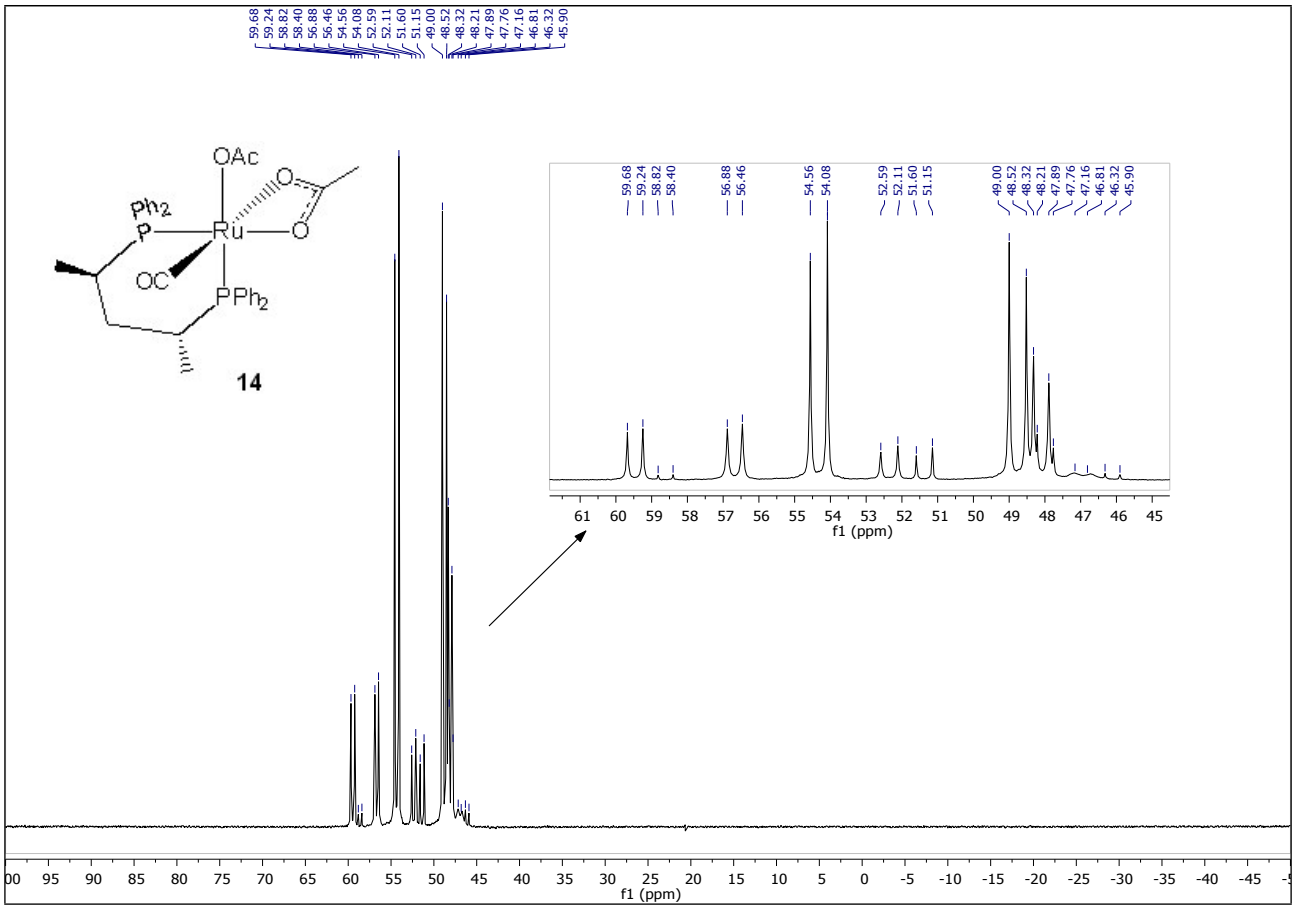

Figure S56. $^{31}P\{^{1}H\}$ NMR spectrum (81.0 MHz) of $[Ru(OAc)_2(CO)((R,R)\text{-Skewphos})]$ (**14**) in CD_2Cl_2 at - 60 °C.

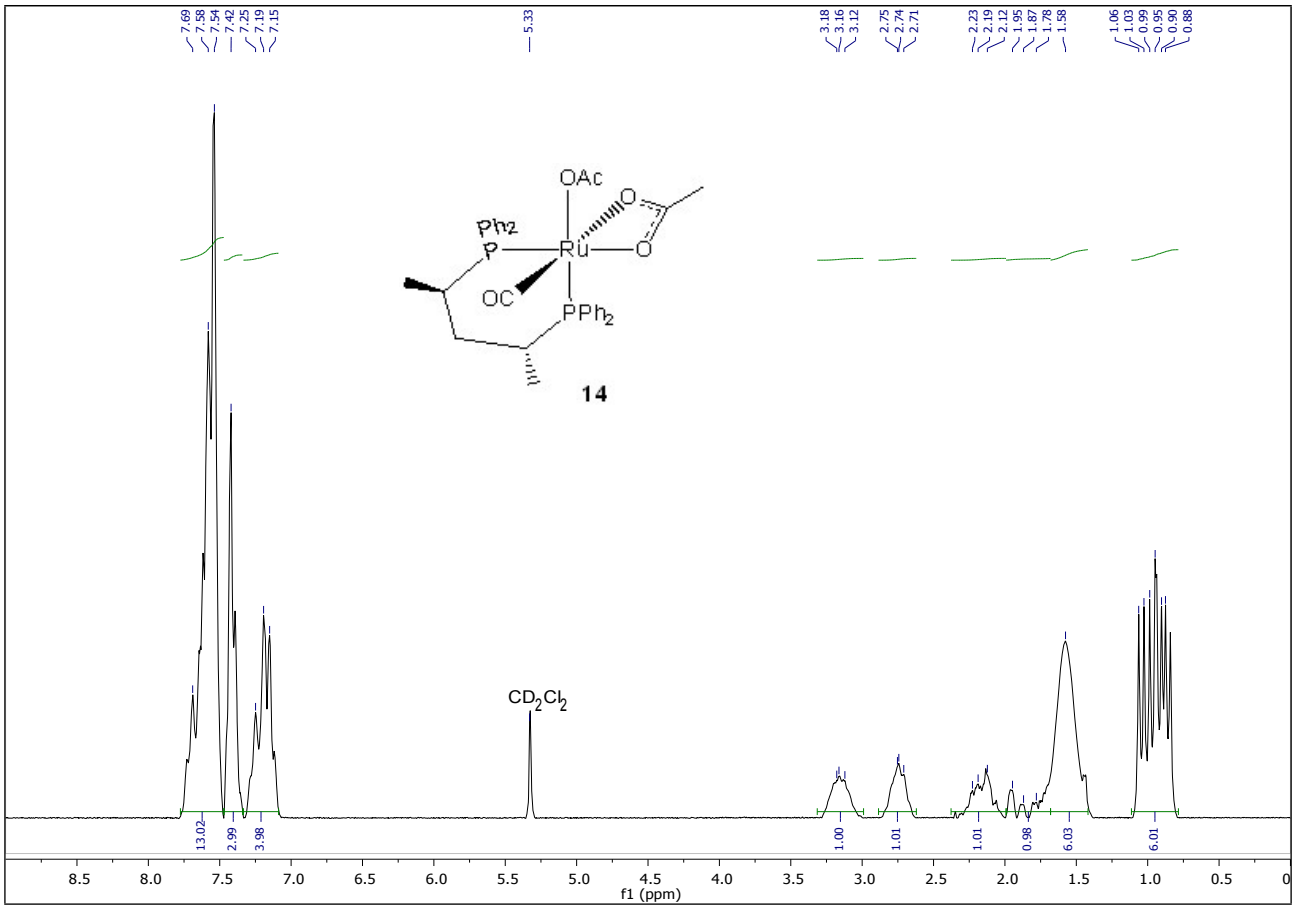

Figure S57. ^{1}H NMR spectrum (200.1 MHz) of [Ru(OAc)$_2$(CO)((*R*,*R*)-Skewphos)] (**14**) in CD_2Cl_2 at 20 °C.

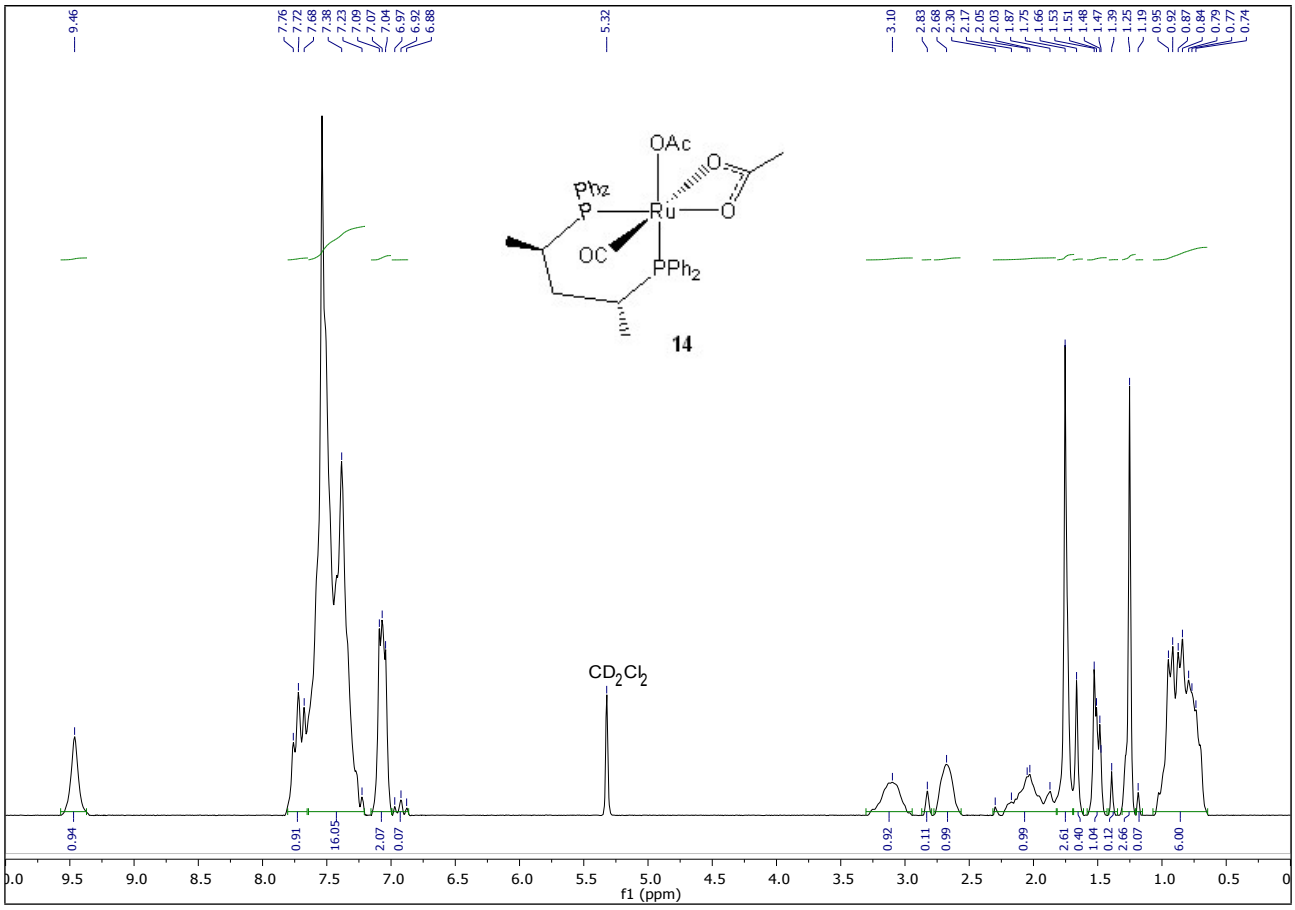

Figure S58. ^{1}H NMR spectrum (200.1 MHz) of [Ru(OAc)$_2$(CO)((*R*,*R*)-Skewphos)] (**14**) in CD_2Cl_2 at - 60 °C.

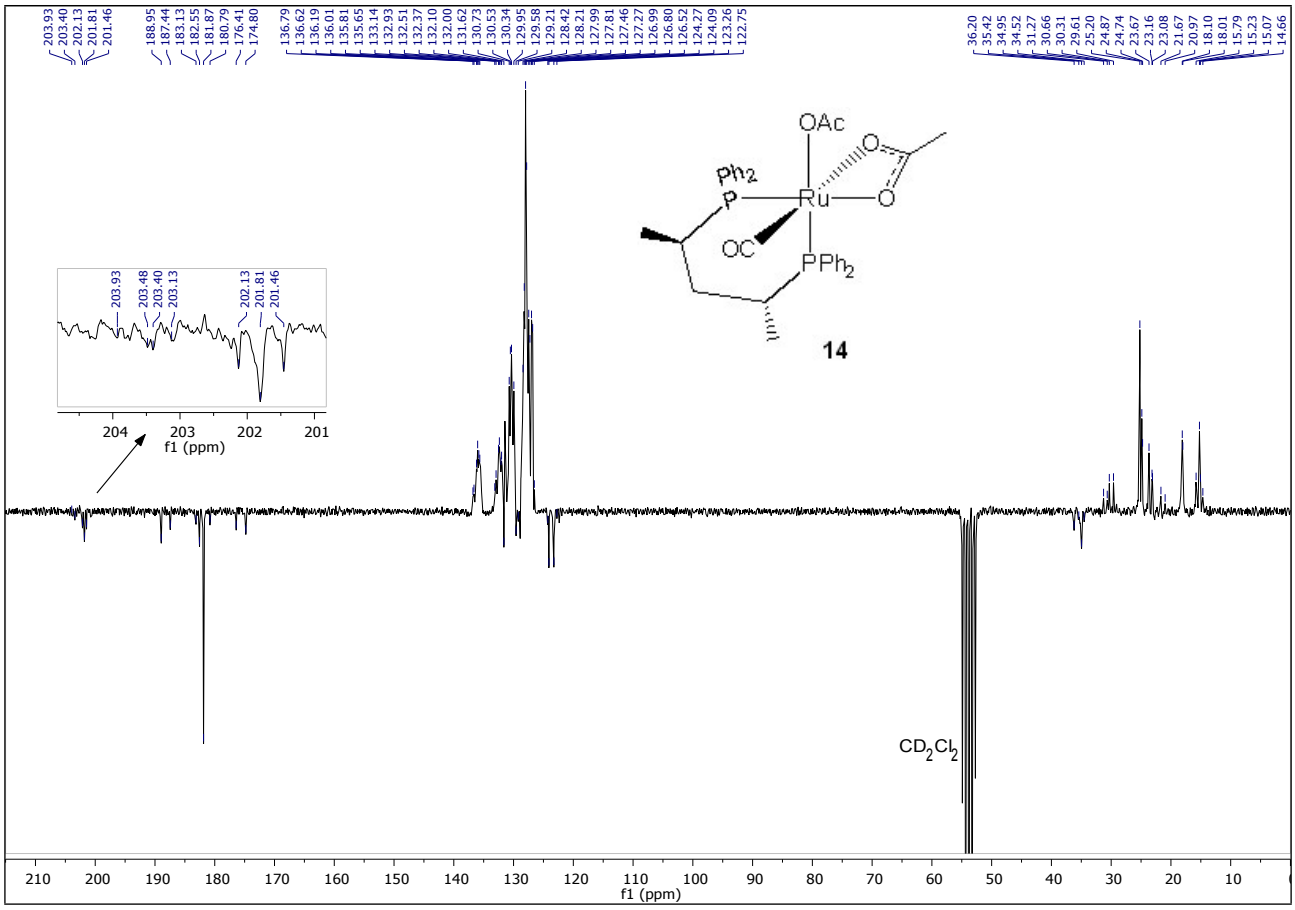

Figure S59. $^{13}C\{^{1}H\}$ PENDANT NMR spectrum (50.3 MHz) of $[Ru(OAc)_2(CO)((R,R)$-Skewphos)] (**14**) in CD_2Cl_2 at - 60 °C.

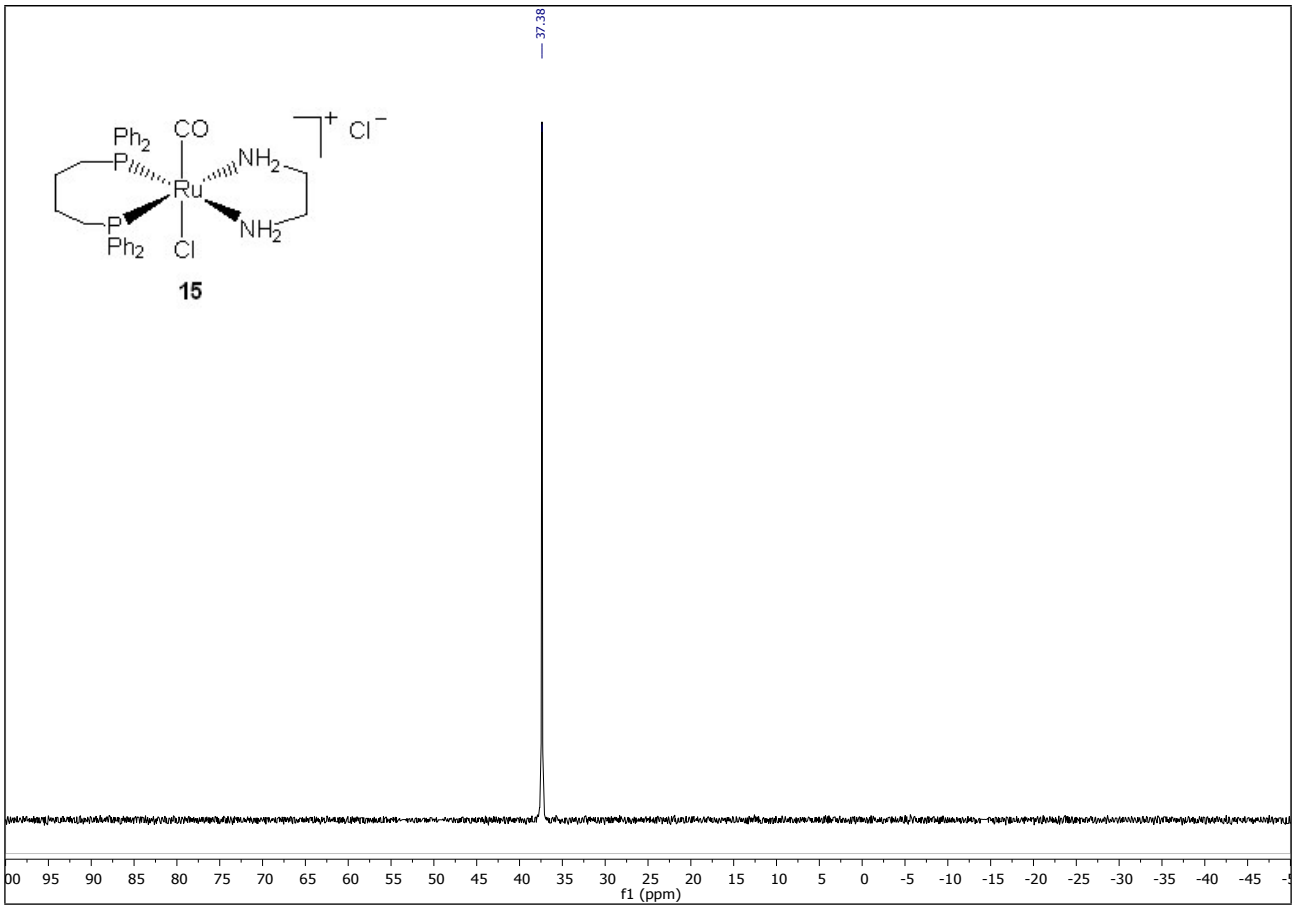

Figure S60. $^{31}P\{^{1}H\}$ NMR spectrum (81.0 MHz) of [RuCl(CO)(dppb)(en)]Cl (**15**) in CD_2Cl_2 at 20 °C.

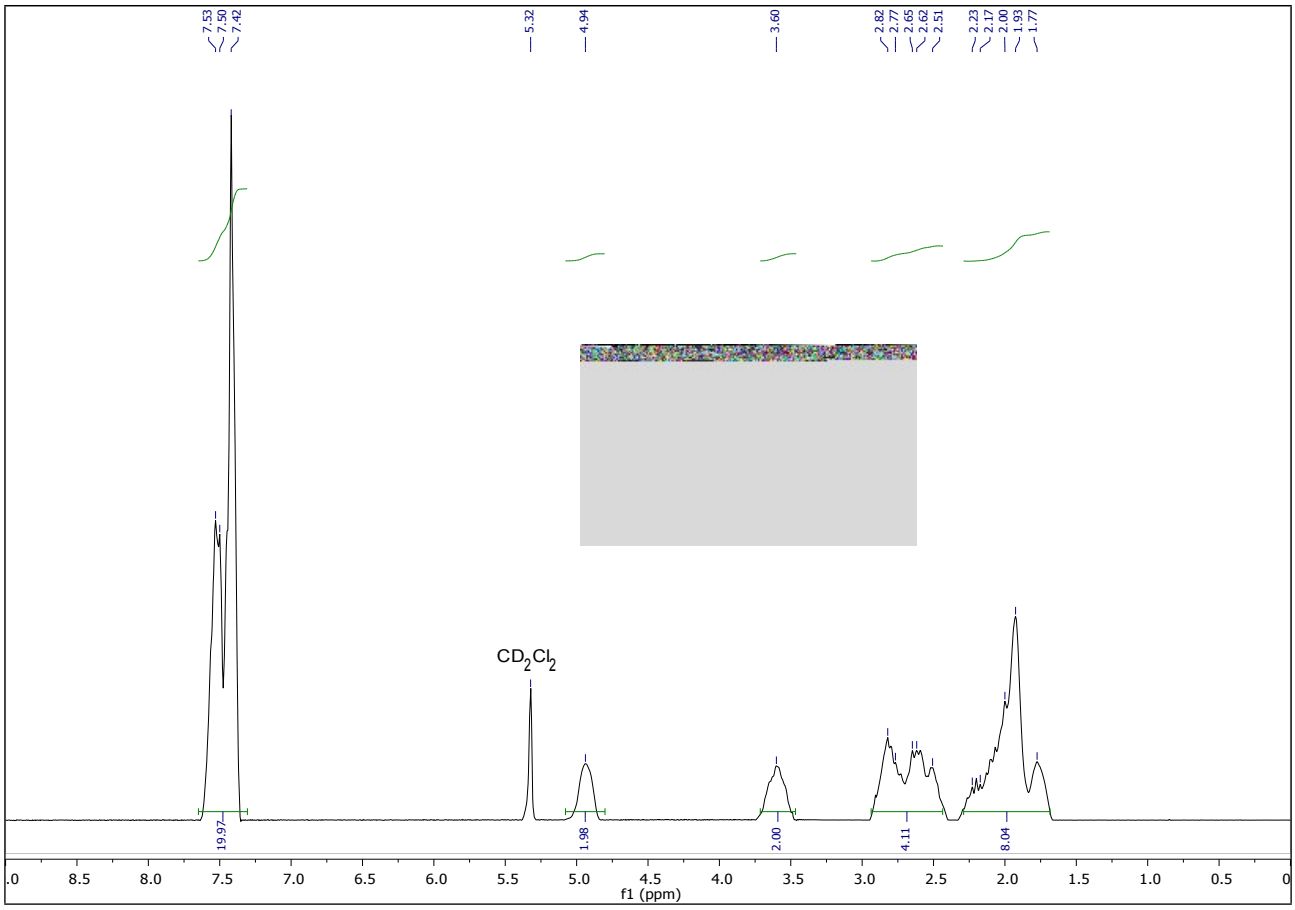

Figure S61. ^{1}H NMR spectrum (200.1 MHz) of [RuCl(CO)(dppb)(en)]Cl (**15**) in CD_2Cl_2 at 20 °C.

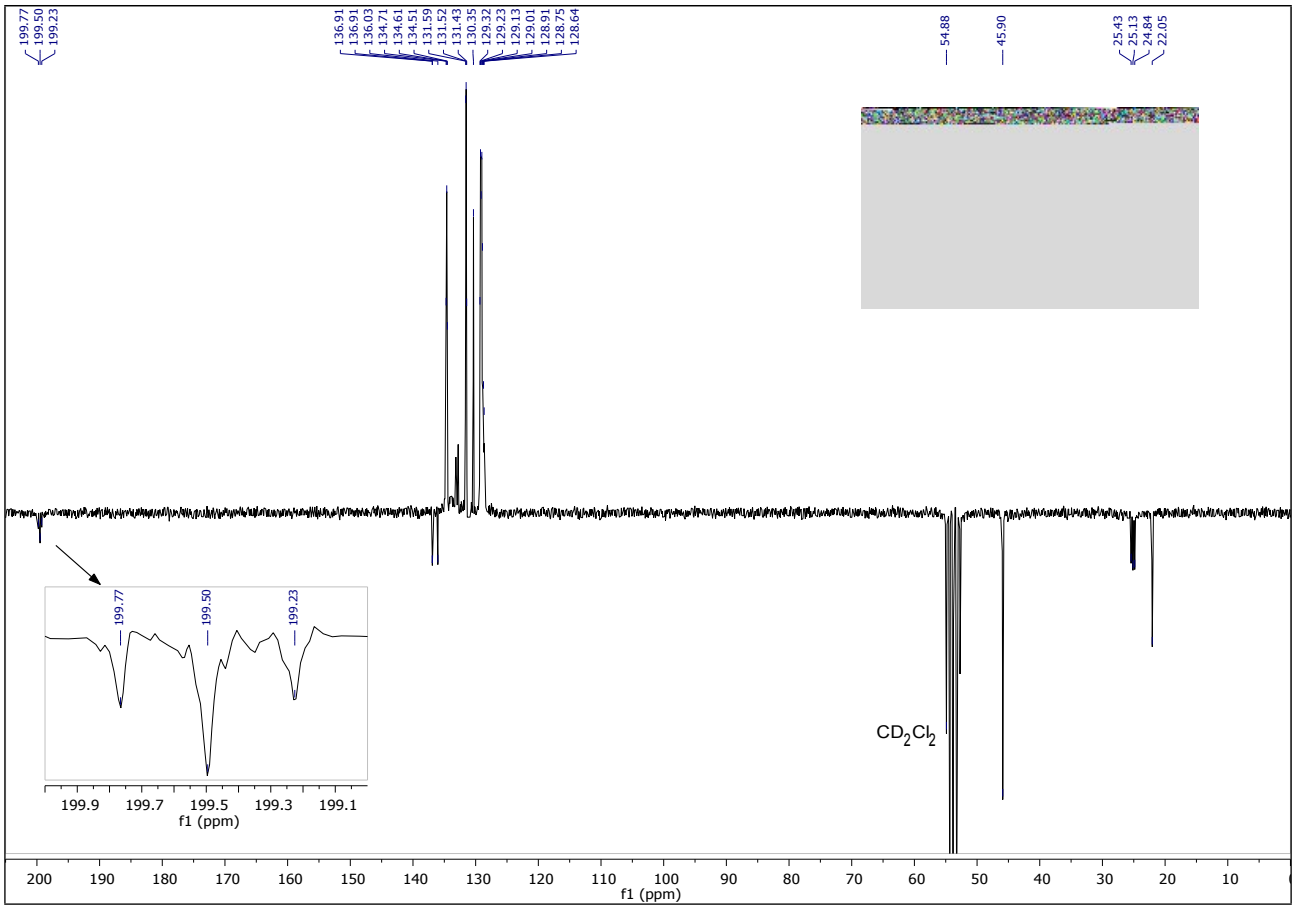

Figure S62. $^{13}C\{^{1}H\}$ PENDANT NMR spectrum (50.3 MHz) of [RuCl(CO)(dppb)(en)]Cl (**15**) in CD_2Cl_2 at 20 °C

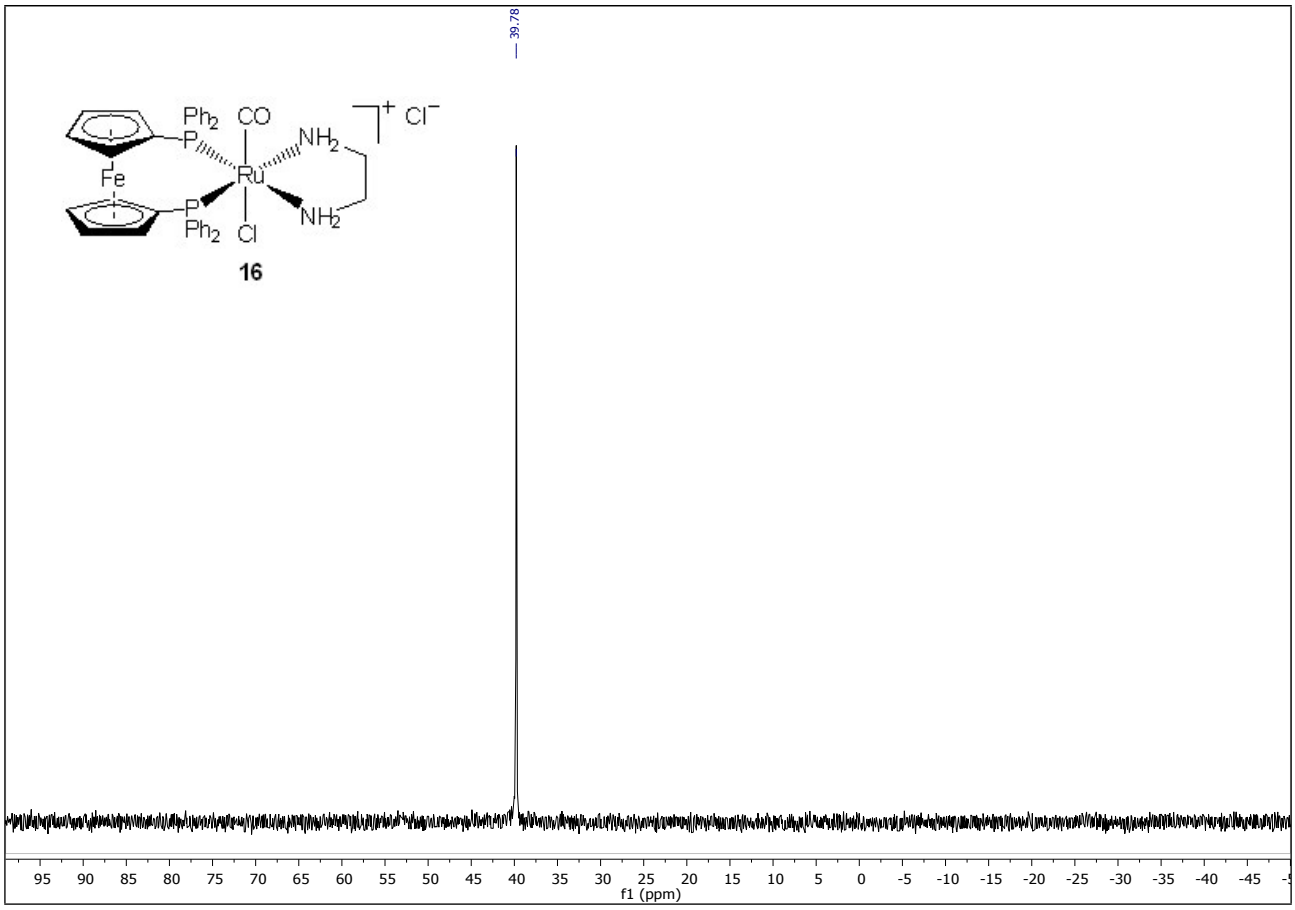

Figure S63. $^{31}P\{^{1}H\}$ NMR spectrum (81.0 MHz) of [RuCl(CO)(dppf)(en)]Cl (**16**) in CD_2Cl_2 at 20 °C.

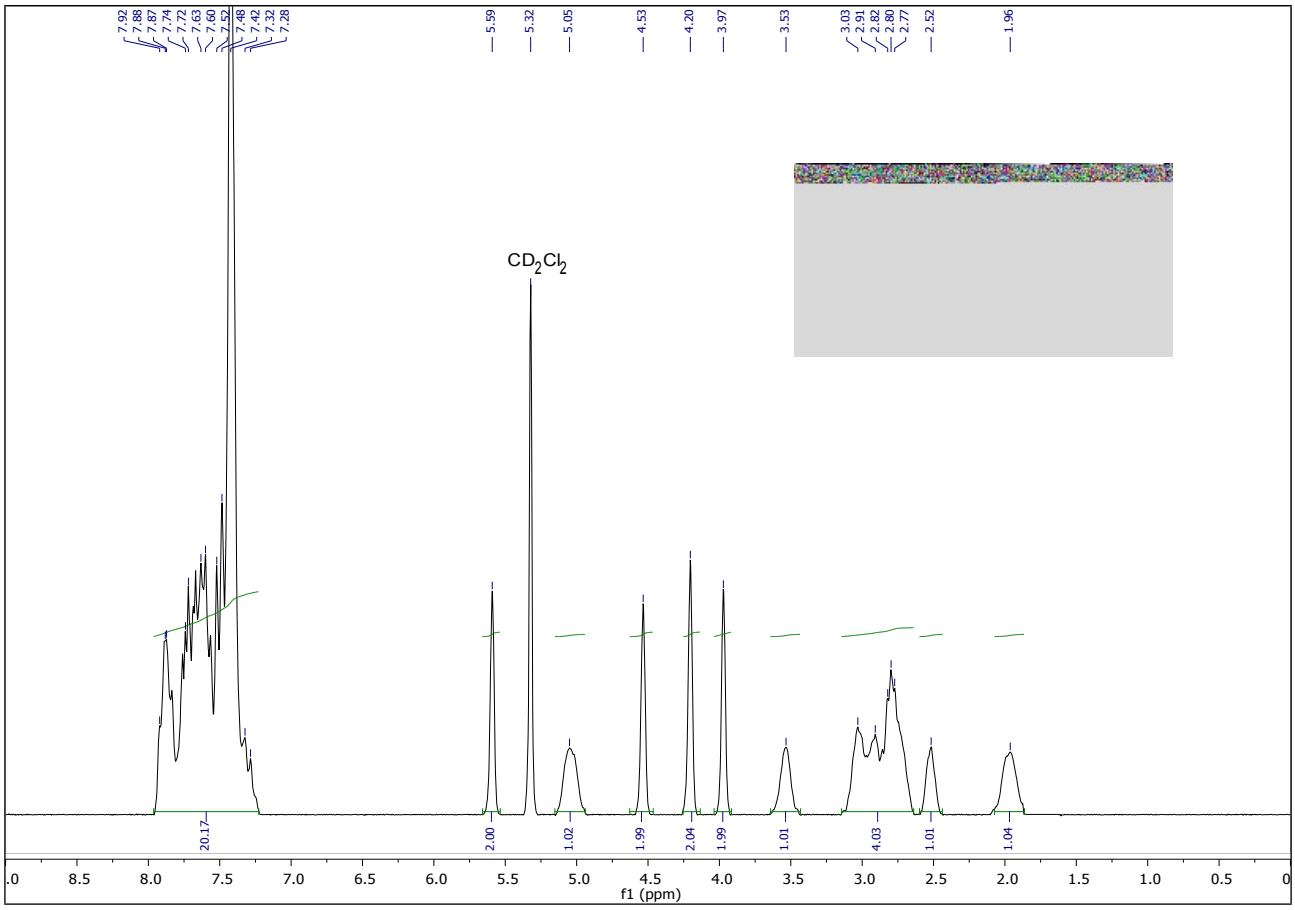

Figure S64. ^{1}H NMR spectrum (200.1 MHz) of [RuCl(CO)(dppf)(en)]Cl (**16**) in CD_2Cl_2 at 20 °C.

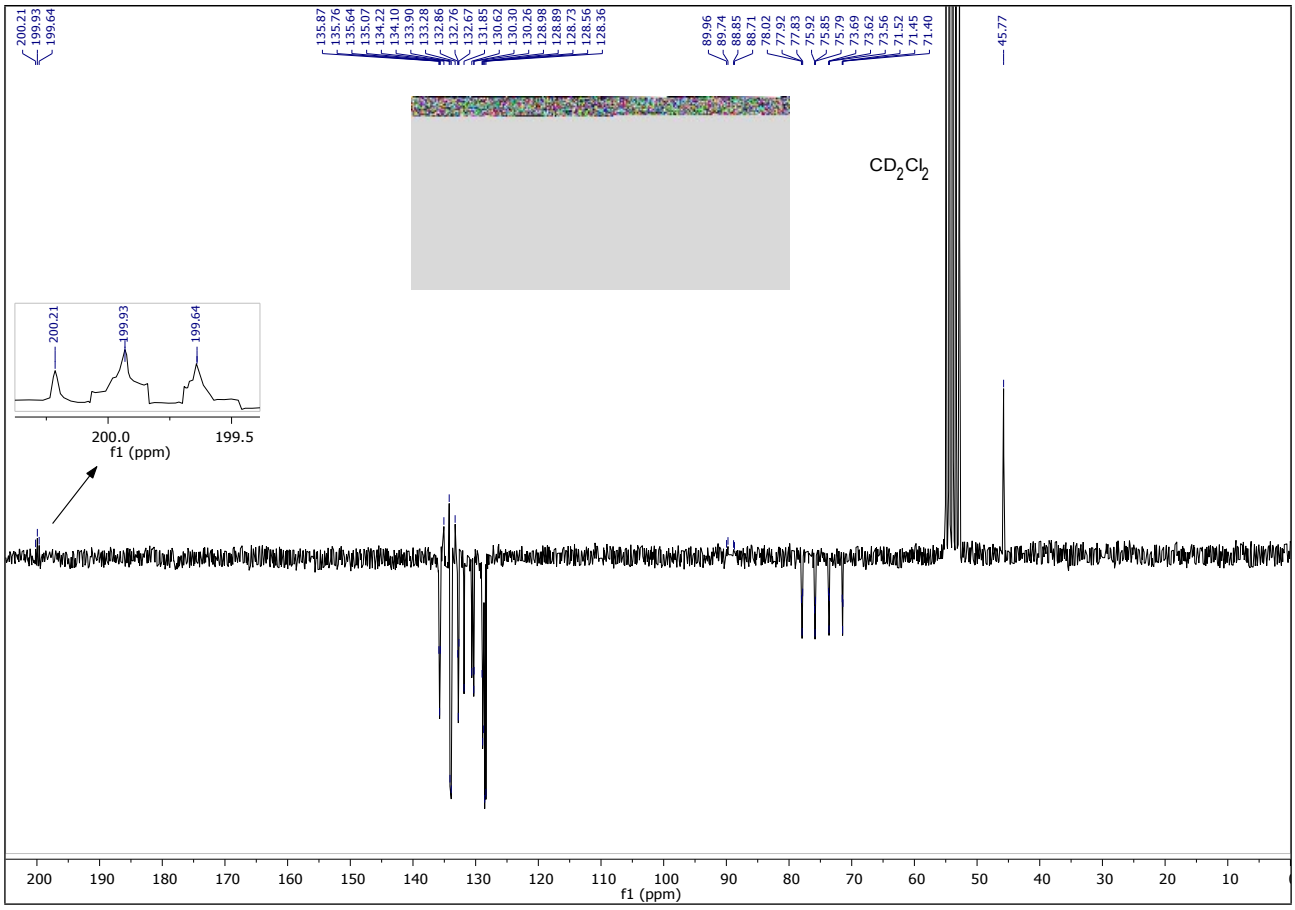

Figure S65. $^{13}C\{^{1}H\}$ PENDANT NMR spectrum (50.3 MHz) of [RuCl(CO)(dppf)(en)]Cl (**16**) in CD_2Cl_2 at 20 °C.

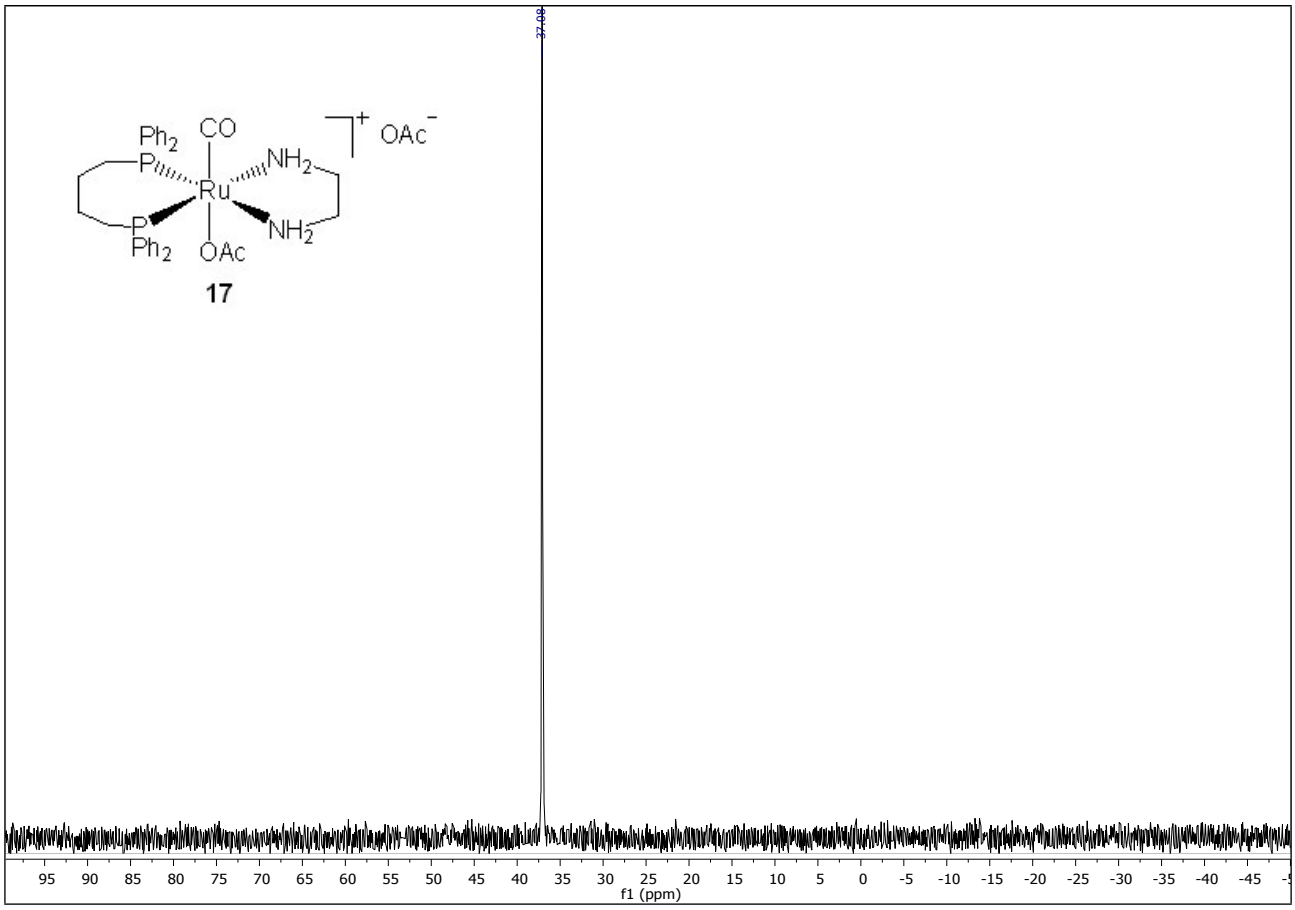

Figure S66. $^{31}P\{^{1}H\}$ NMR spectrum (81.0 MHz) of [Ru(OAc)(CO)(dppb)(en)]OAc (**17**) in CD_3OD at 20 °C.

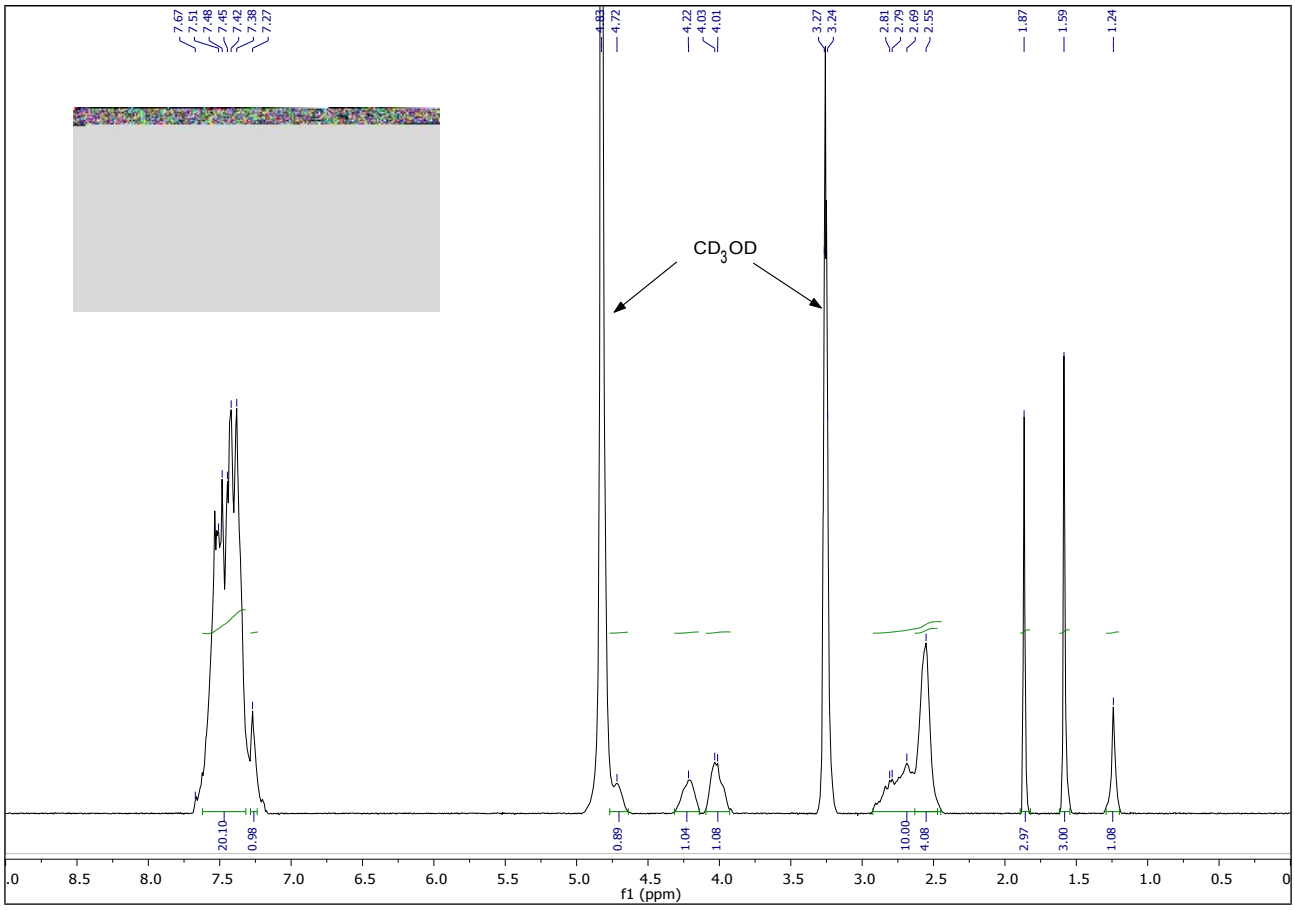

Figure S67. ^{1}H NMR spectrum (200.1 MHz) of [Ru(OAc)(CO)(dppb)(en)]OAc (**17**) in CD_3OD at 20 °C.

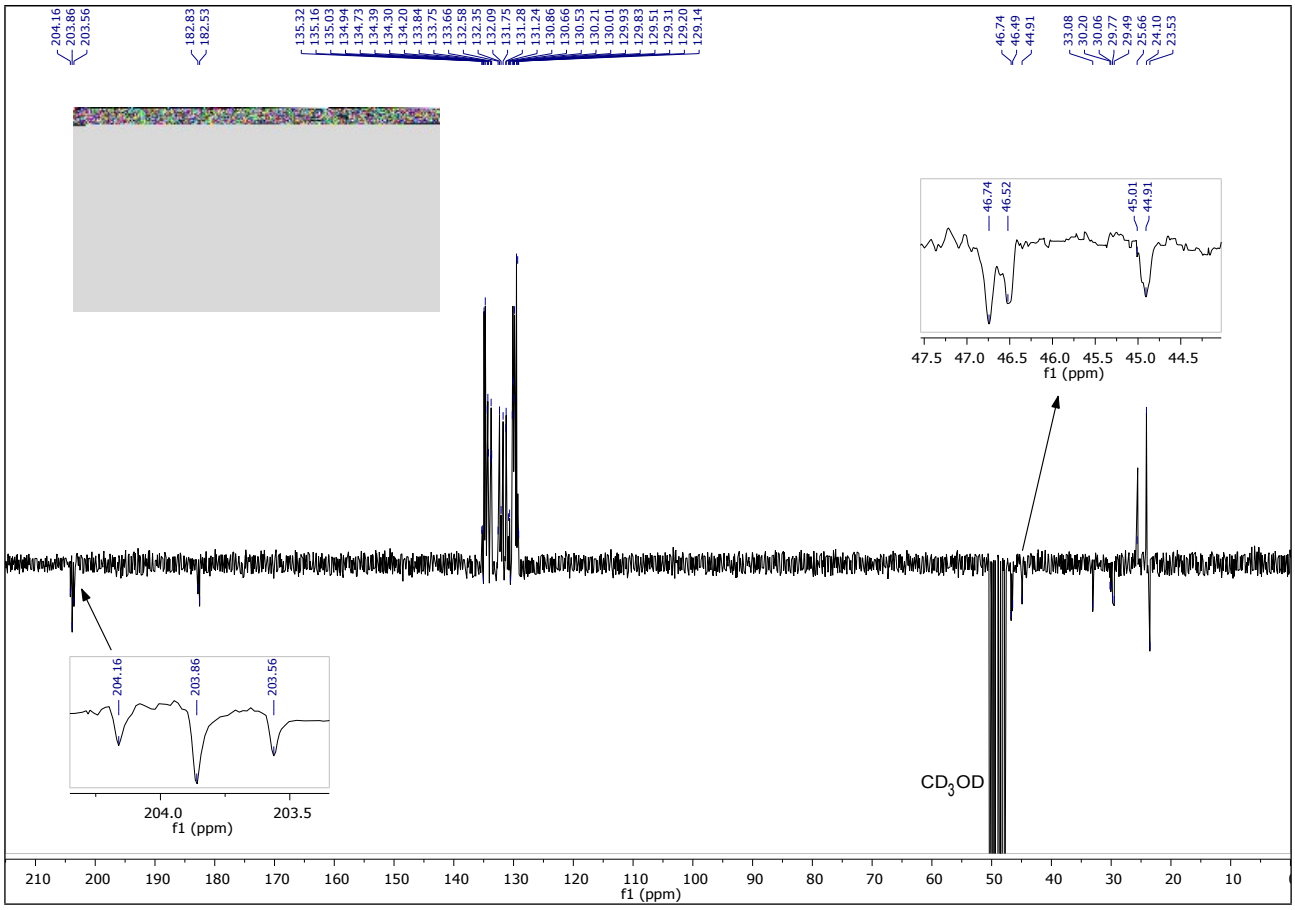

Figure S68. $^{13}C\{^{1}H\}$ PENDANT NMR spectrum (50.3 MHz) of [Ru(OAc)(CO)(dppb)(en)]OAc (**17**) in CD_3OD at 20 °C.

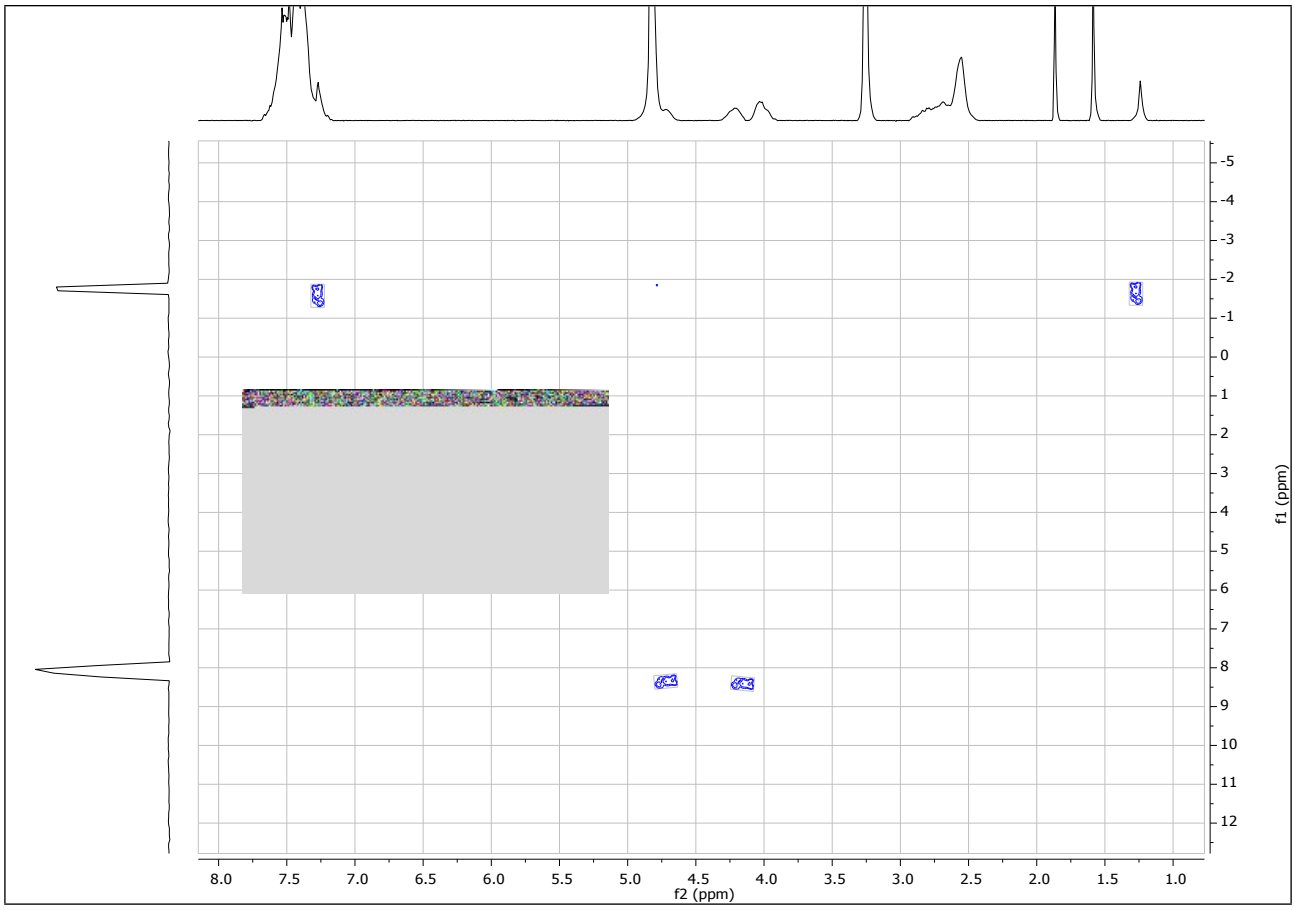

Figure S69. ^{15}N-^{1}H HSQC 2D NMR spectrum of [Ru(OAc)(CO)(dppb)(en)]OAc (**17**) in CD_3OD at 20 °C.

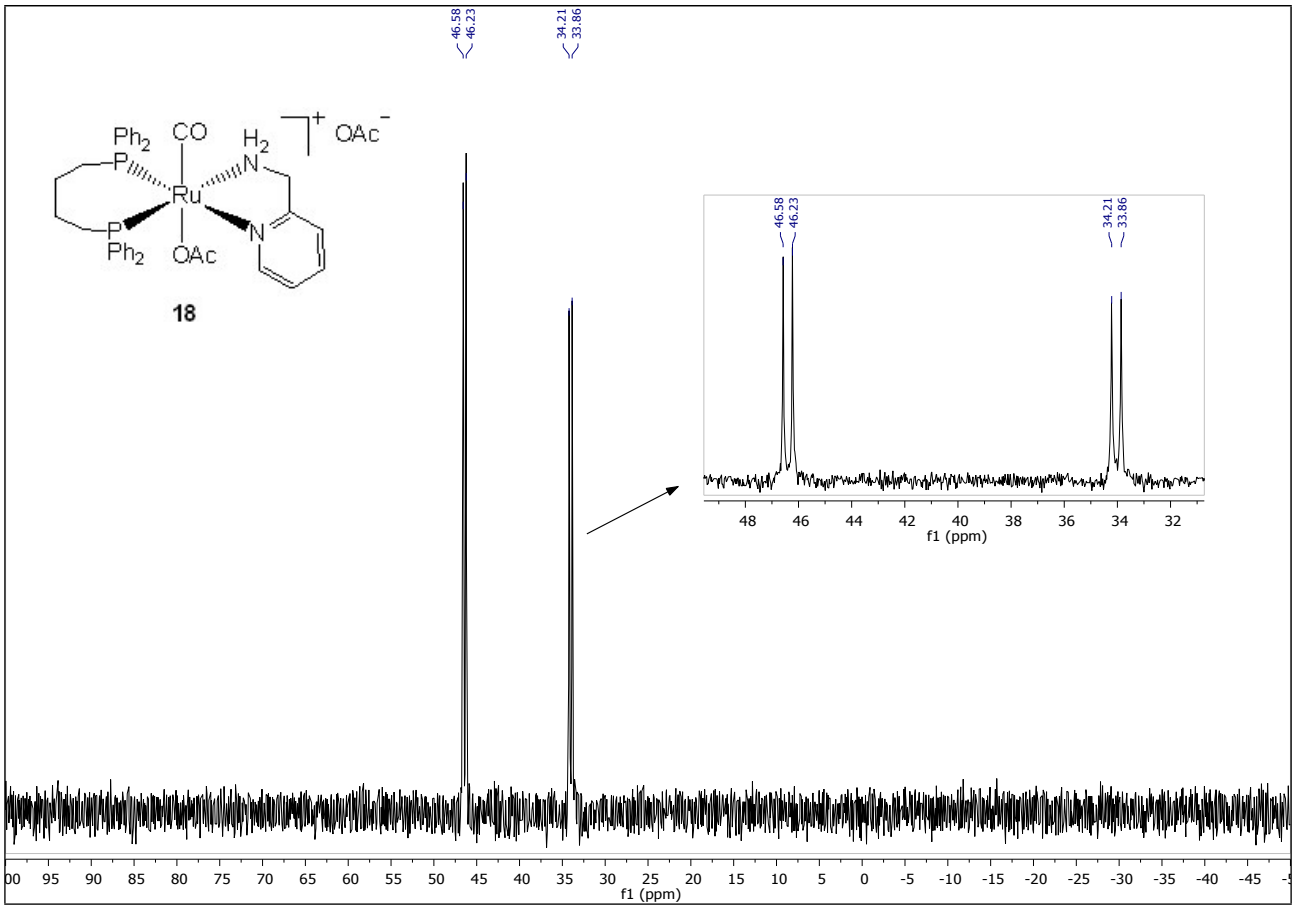

Figure S70. $^{31}P\{^{1}H\}$ NMR spectrum (81.0 MHz) of [Ru(OAc)(CO)(dppb)(ampy)]OAc (**18**)) in [D8]toluene at 20 °C.

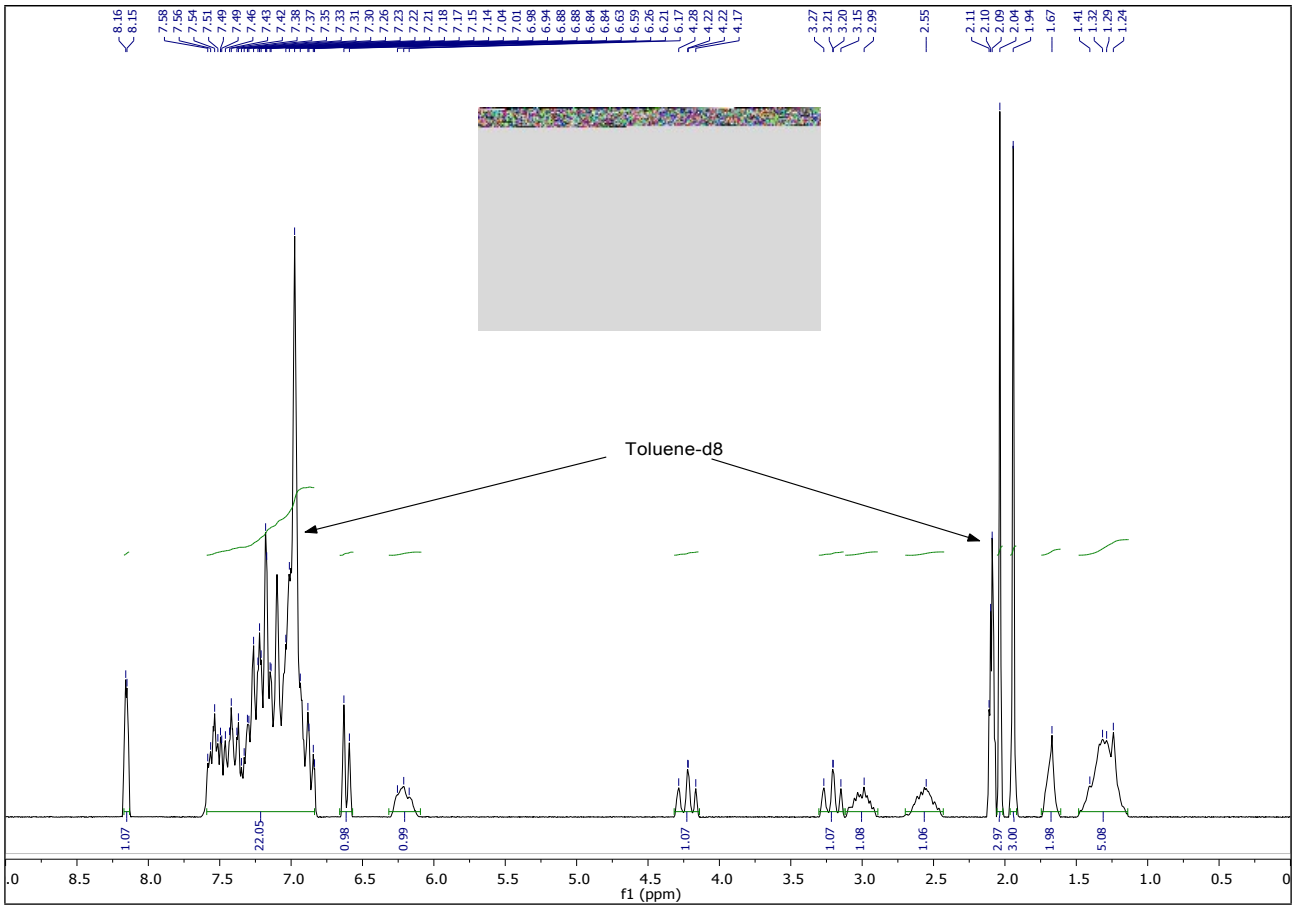

Figure S71. ^{1}H NMR spectrum (200.1 MHz) of [Ru(OAc)(CO)(dppb)(ampy)]OAc (**18**) in [D8]toluene at 20 °C.

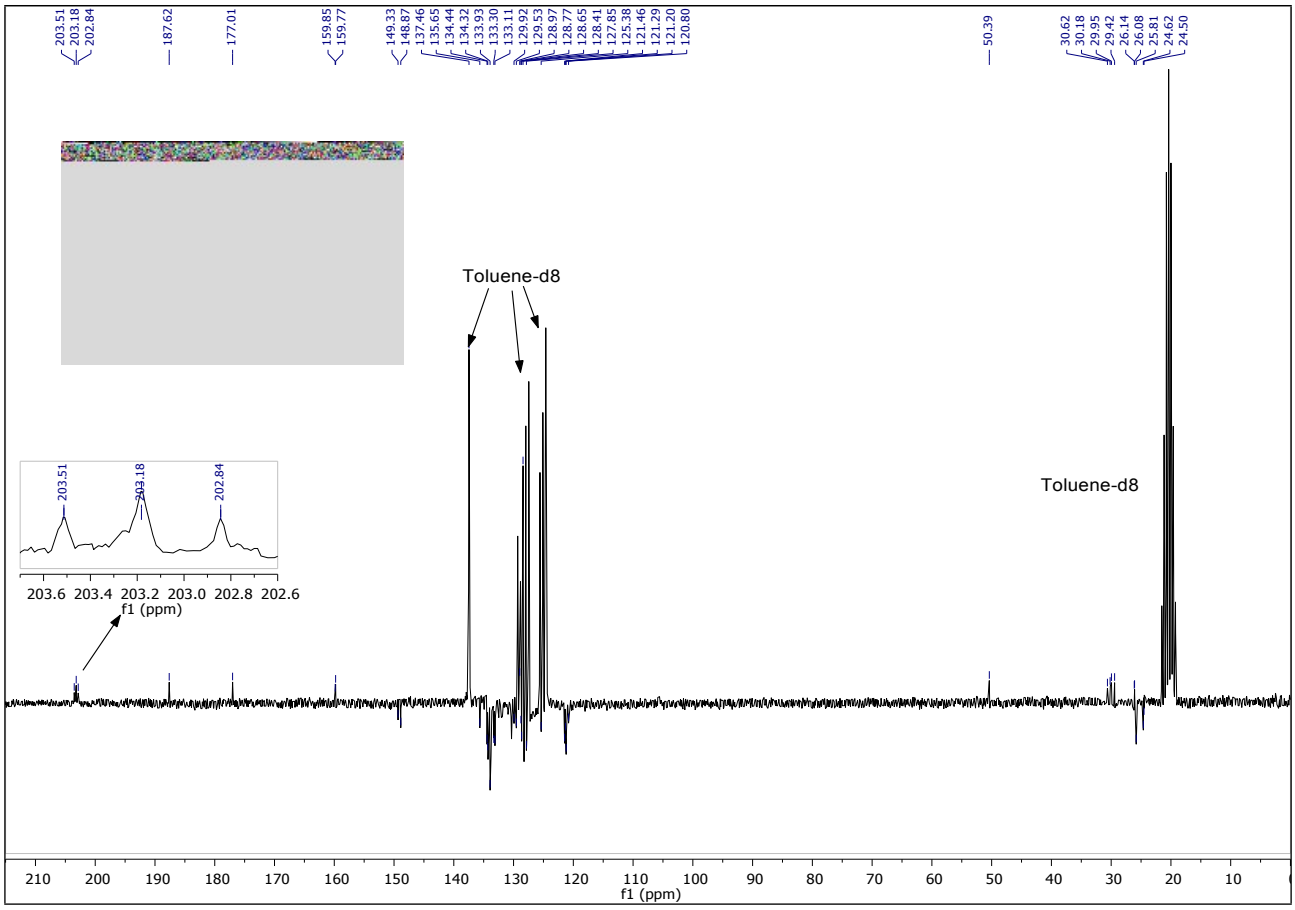

Figure S72. $^{13}C\{^{1}H\}$ PENDANT NMR spectrum (50.3 MHz) of [Ru(OAc)(CO)(dppb)(ampy)]OAc (**18**) in [D8]toluene at 20 °C.

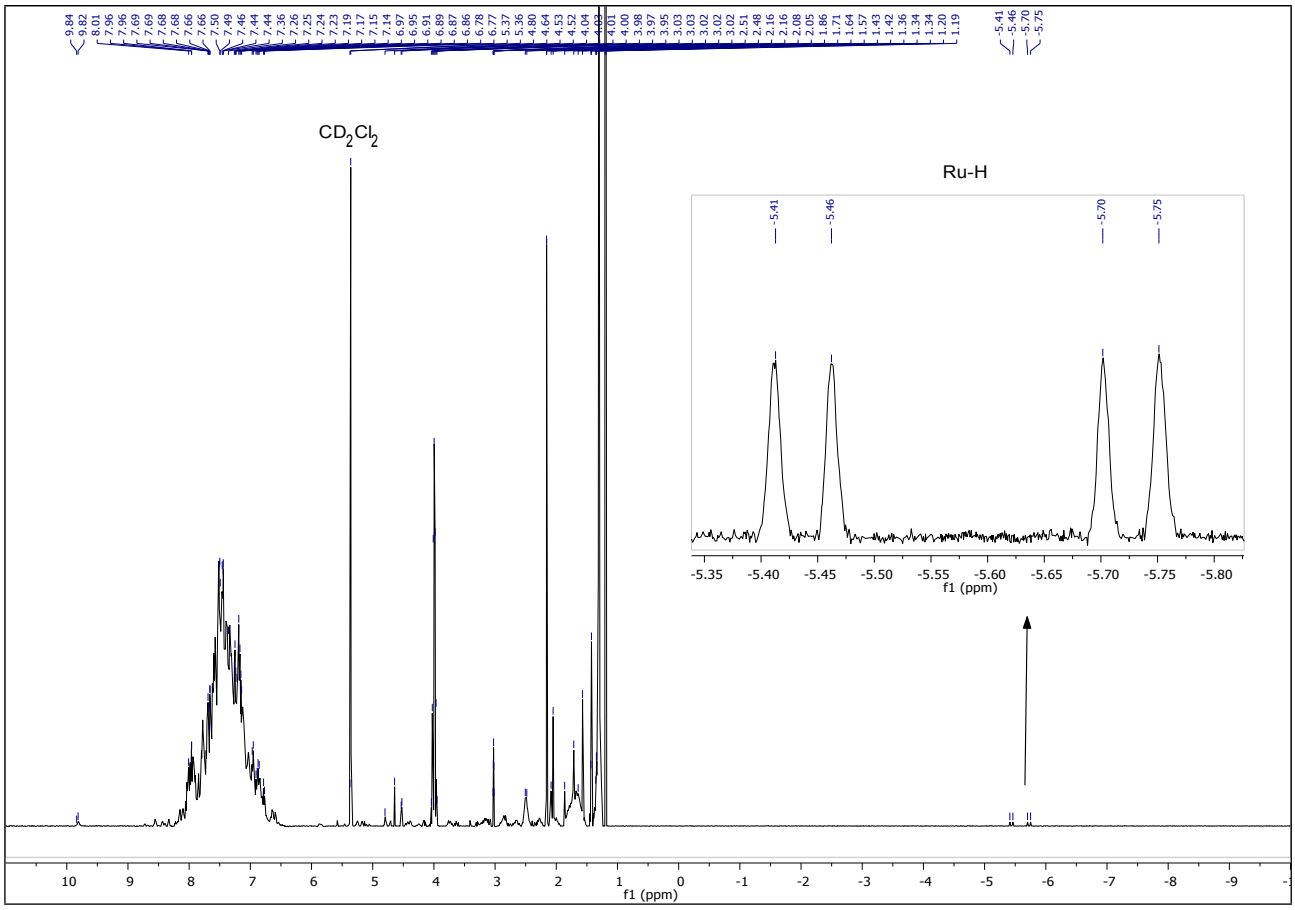

Figure S73. ^{1}H NMR spectrum (400.1 MHz, CD_2Cl_2, 20 °C) which evidences of the formation of a ruthenium monohydride species from [Ru(OAc)(CO)(dppb)(ampy)]OAc (**18**), by treatment with 2 eq. of NaO*i*Pr in 2-propanol.

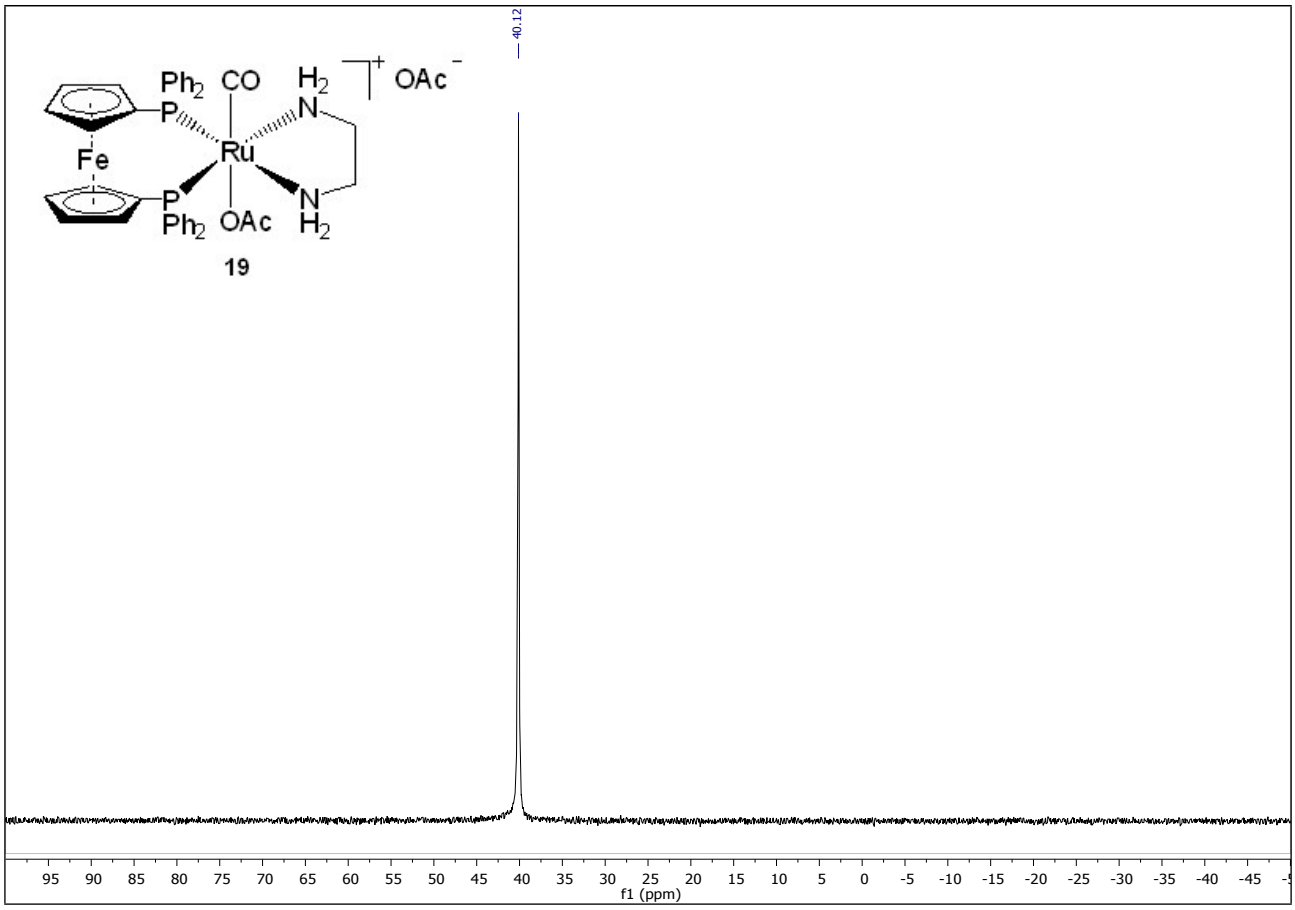

Figure S74. $^{31}P\{^{1}H\}$ NMR spectrum (81.0 MHz) of [Ru(OAc)(CO)(dppf)(en)]OAc (**19**) in CD_2Cl_2 at 20 °C.

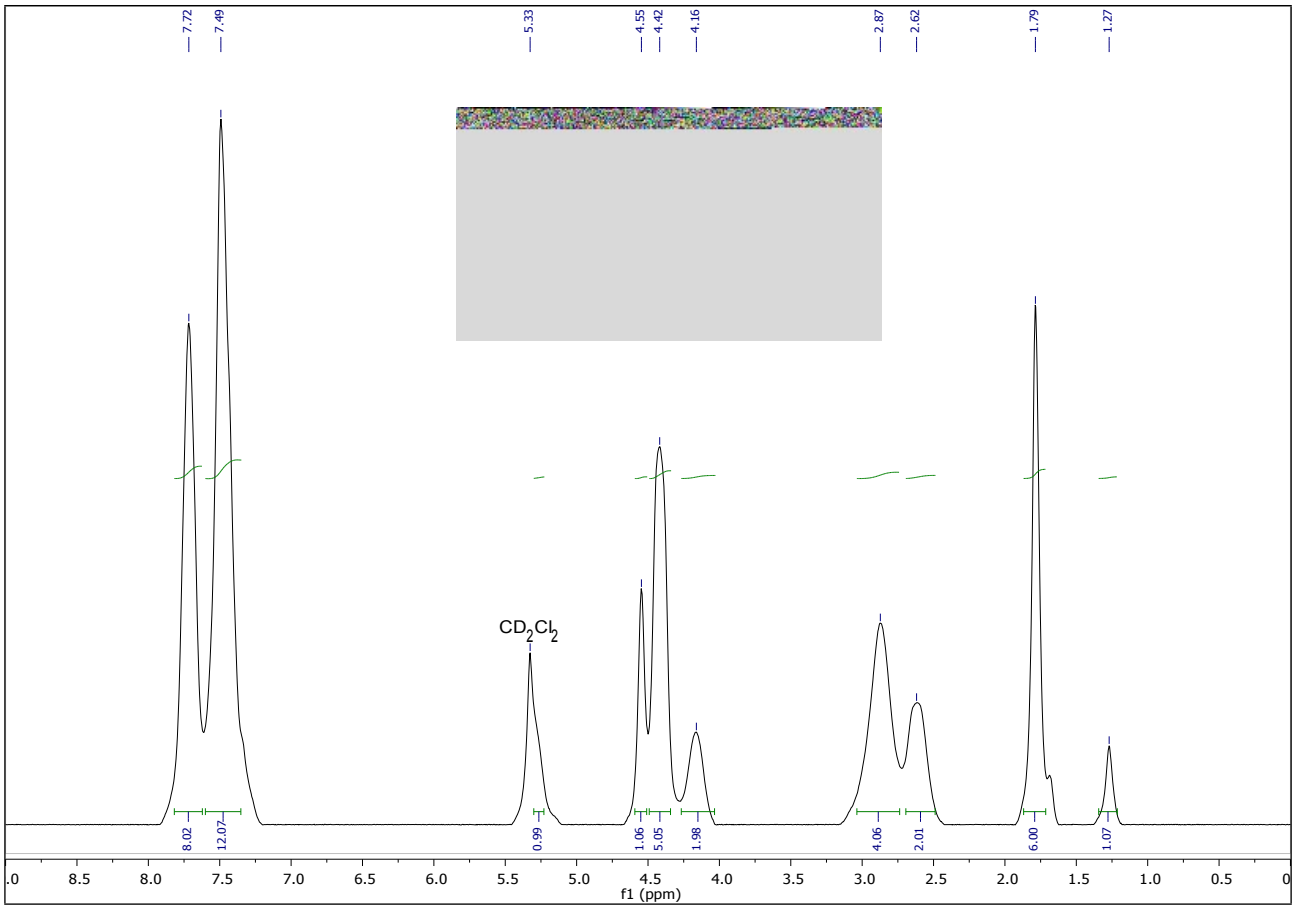

Figure S75. ^{1}H NMR spectrum (200.1 MHz) of [Ru(OAc)(CO)(dppf)(en)]OAc (**19**) in CD_2Cl_2 at 20 °C.

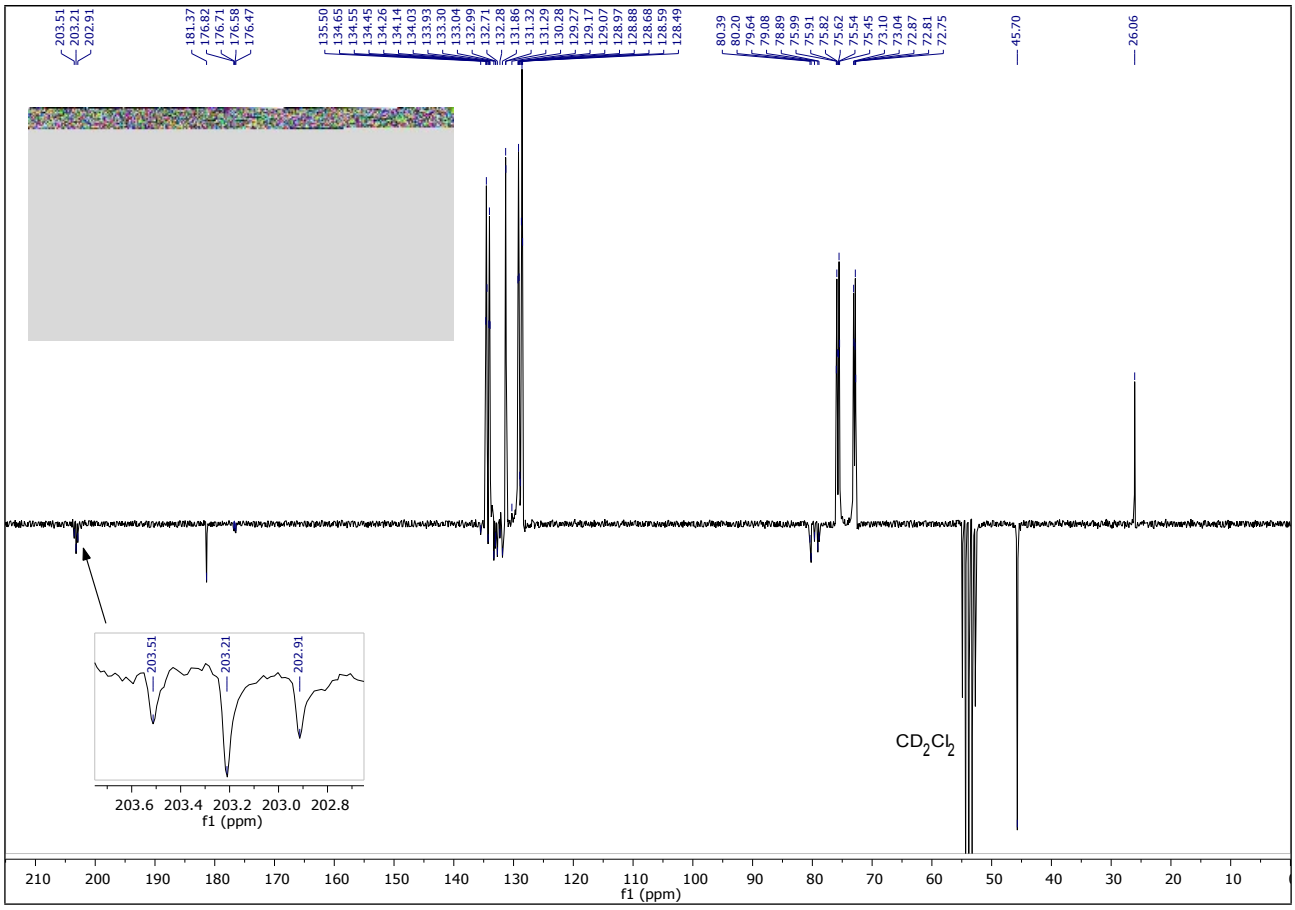

Figure S76. $^{13}C\{^{1}H\}$ PENDANT NMR spectrum (50.3 MHz) of [Ru(OAc)(CO)(dppf)(en)]OAc (**19**) in CD_2Cl_2 at 20 °C.

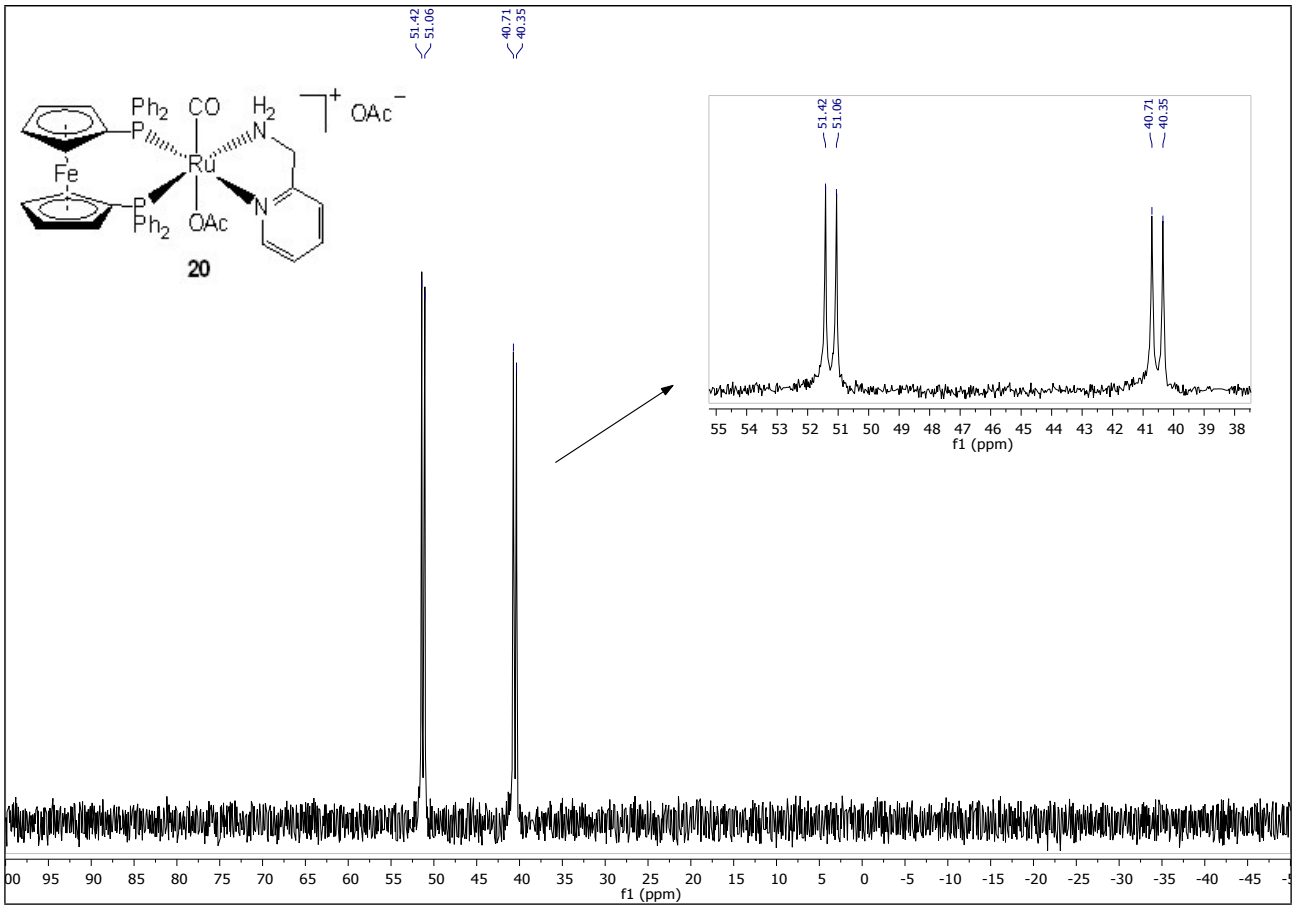

Figure S77. $^{31}P\{^{1}H\}$ NMR spectrum (81.0 MHz) of [Ru(OAc)(CO)(dppf)(ampy)]OAc (**20**) in [D8]toluene at 20 °C.

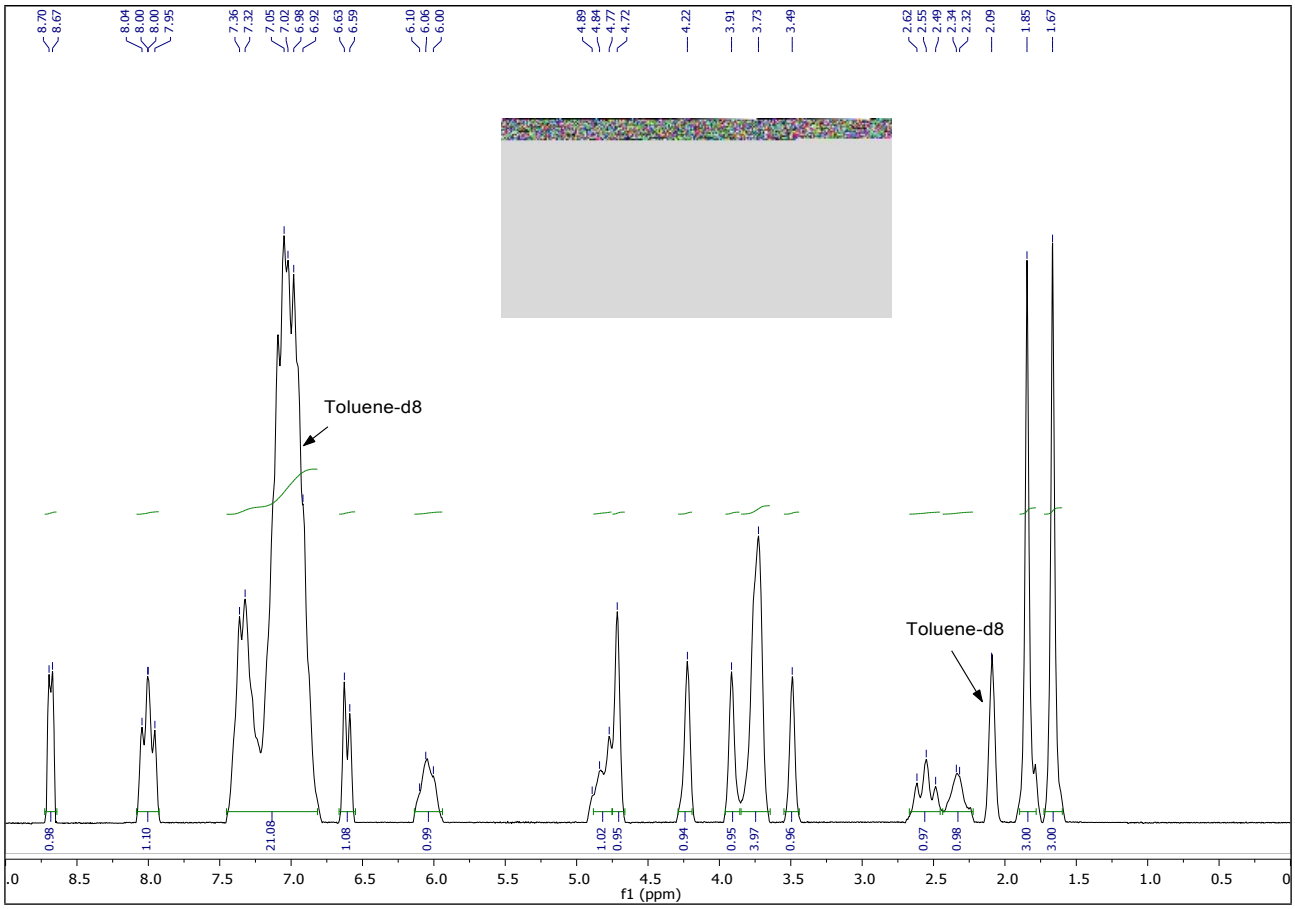

Figure S78. ^{1}H NMR spectrum (200.1 MHz) of [Ru(OAc)(CO)(dppf)(ampy)]OAc (**20**) in [D8]toluene at 20 °C.

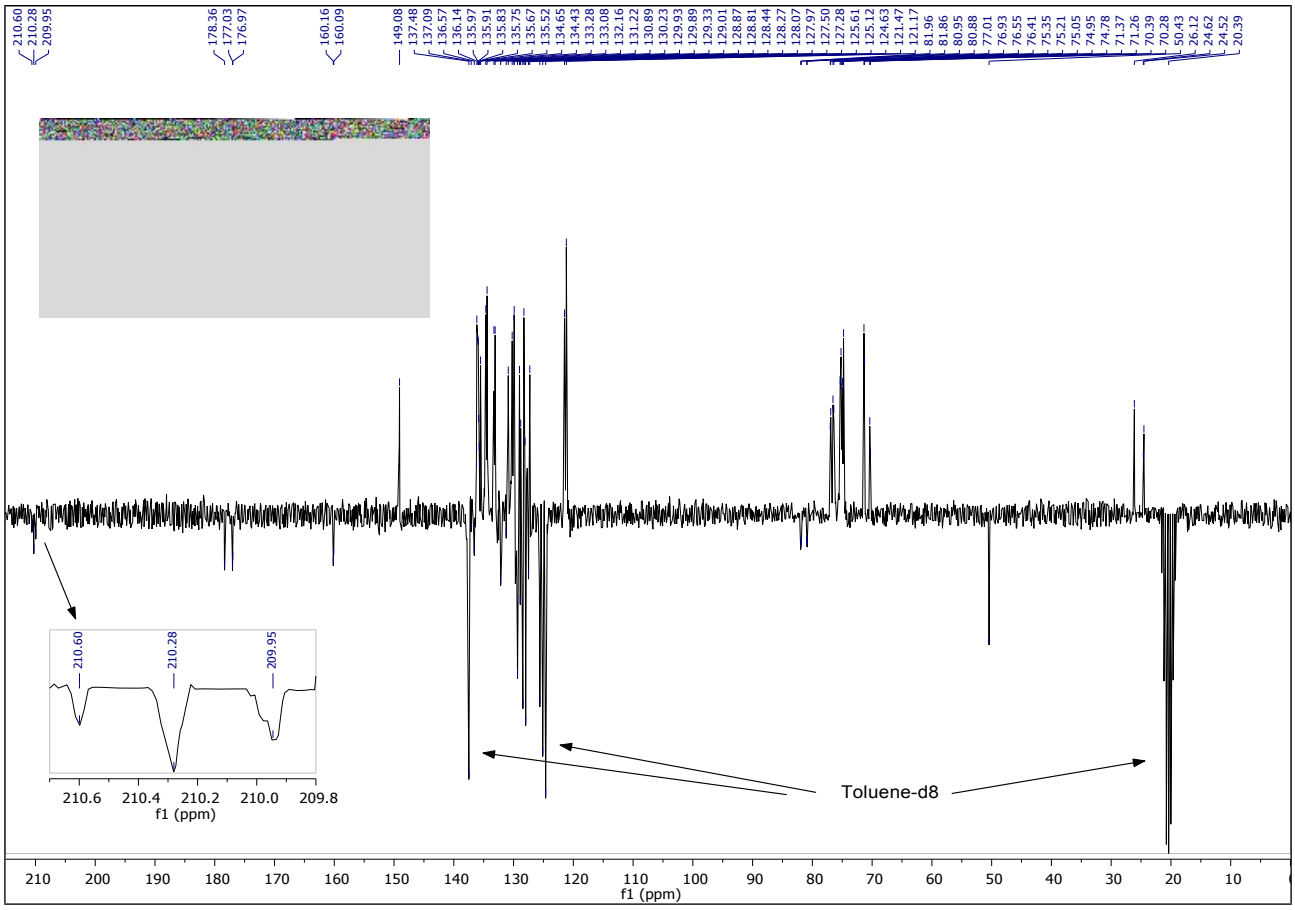

Figure S79. $^{13}C\{^{1}H\}$ NMR spectrum (81.0 MHz) of [Ru(OAc)(CO)(dppf)(ampy)]OAc (**20**) in [D8]toluene at 20 °C.

Table S1. Further data regarding the catalytic TH of acetophenone (0.1 M) with complexes **6-14** (S/C 1000) in 2-propanol at 82 °C, and in the presence of NaO*i*Pr 2 mol%.

Entry	Complex	Ligand (5 equiv.)	Time [min]	Conv.[a] [%]	TOF[b] [h^{-1}]	e.e. (%)
1	**6**	en	120	25	-	-
2	**7**	en	120	44	-	-
3	**8**	en	120	92	900	22 (*S*)
4	**8**	ampy	300	88	300	18 (*S*)
5	**8**	(±)-*i*Pr-ampy[c]	120	97	1200	25 (*S*)
6	**8**	(*S*,*S*)-DPEN	120	78	1100	16 (*S*)
7	**9**	en	120	74	400	13 (*S*)
8	**9**	ampy	120	95	1700	17 (*R*)
9	**9**	(±)-*i*Pr-ampy[c]	30	97	6700	17 (*R*)
10	**9**	(*S*,*S*)-DPEN	120	94	700	32 (*R*)
11	**10**	en	120	48	-	13 (*R*)
12	**10**	ampy	120	86	1800	66(*R*)
13	**10**	(*R*,*R*)-DPEN	120	85	800	46 (*S*)
14	**10**	(*S*,*S*)-DPEN	120	46	300	53 (*R*)
15	**11**	en	120	85	3700	-
16	**12**	en	120	46	-	-
17	**13**	en	30	97	6000	18 (*S*)
18	**13**	(±)-*i*Pr-ampy[c]	5	97	19000	24 (*S*)
19	**13**	(*S*,*S*)-DPEN	5	96	12000	19 (*S*)
20	**14**	en	30	91	10000	24 (*R*)
21	**14**	(*R*,*R*)-DPEN	30	97	18000	12 (*R*)
22	**14**	(*S*,*S*)-DPEN	30	92	15000	26 (*R*)

[a] The conversion has been determined by GC analysis. [b] Turnover frequency (moles of ketone converted to alcohol per mole of catalyst per hour) at 50% conversion. [c] 2 eq. with respect to the diphosphine precursors.

Table S2. Further data regarding the catalytic TH of aldehydes and ketones (0.1 M) to alcohols with complexes **1**, **3-5** and **15-16** (S/C 1000) in 2-propanol at 82 °C, and in the presence of 2 mol % NaO*i*Pr.

Entry	Complex	substrate	Time [min]	Conv.[a] [%]
1	**1**	benzaldehyde	10	11
2	**3**	benzaldehyde	10	10
3	**4**	benzaldehyde	30	8
4	**5**	benzaldehyde	60	14
5	**5**	4-bromo-benzaldehyde	60	30
6	**15**	benzaldehyde	60	20
7	**16**	benzaldehyde	60	25

[a]The conversions has been determined by GC analysis.

Table S3. Further data regarding the catalytic HY (30 bar) of ketones (2.0 M) to alcohols with complexes **2**, **15** and KO*t*Bu (2 mol%) as base in EtOH at 70 °C.

Entry	Complex	Substrate	S/C	Time [h]	Conv.[a] [%]
1	**2**	tetralone	10000	16	8
2	**2**	benzoin	10000	16	5
3	**15**	tetralone	10000	16	4
4	**15**	2'-Me-acetophenone	10000	16	28
5	**15**	4'-NO_2-acetophenone	10000	16	1
6	**15**	benzoin	10000	16	9

[a] The conversions has been determined by GC analysis.